

# Massive Star Cluster Formation and Destruction in Luminous Infrared Galaxies in GOALS II: An ACS/WFC3 Survey of Nearby LIRGs

S. T. LINDEN,<sup>1</sup> A. S. EVANS,<sup>2,3</sup> K. LARSON,<sup>4</sup> G. C. PRIVON,<sup>3,5</sup> L. ARMUS,<sup>6</sup> J. RICH,<sup>7</sup> T. DÍAZ-SANTOS,<sup>8</sup> E. J. MURPHY,<sup>3,2</sup> Y. SONG,<sup>2</sup> L. BARCOS-MUÑOZ,<sup>3,2</sup> J. HOWELL,<sup>6</sup> V. CHARMANDARIS,<sup>8,9</sup> H. INAMI,<sup>10</sup> V. U,<sup>11</sup> J. A. SURACE,<sup>12</sup> J. M. MAZZARELLA,<sup>6</sup> AND D. CALZETTI<sup>1</sup>

<sup>1</sup>Department of Astronomy, University of Massachusetts at Amherst, Amherst, MA 01003, USA.

<sup>2</sup>Astronomy Department, University of Virginia, 530 McCormick Road, Charlottesville, VA 22904 USA

<sup>3</sup>National Radio Astronomy Observatory, 520 Edgemont Road, Charlottesville, VA 22903 USA

<sup>4</sup>Space Telescope Science Institute, 3700 San Martin Drive, Baltimore, MD, 21218, USA

<sup>5</sup>Department of Astronomy, University of Florida, 211 Bryant Space Sciences Center, Gainesville, FL 32611

<sup>6</sup>IPAC, California Institute of Technology, MS 100-22, Pasadena, CA 91125 USA

<sup>7</sup>Carnegie Observatories, 813 Santa Barbara St., Pasadena, CA 91101

<sup>8</sup>Department of Physics, University of Crete, GR-71003, Heraklion, Greece

<sup>9</sup>Institute of Astrophysics, FORTH, GR-71110 Heraklion, Greece

<sup>10</sup>Hiroshima Astrophysical Science Center, Hiroshima University, 1-3-1 Kagamiyama, Higashi-Hiroshima, Hiroshima 739-8526, Japan

<sup>11</sup>Department of Physics and Astronomy, University of California, Irvine, 4129 Frederick Reines Hall, Irvine, CA 92697, USA

<sup>12</sup>Eureka Scientific, Inc. 2452 Delmer Street Suite 100 Oakland, CA 94602-3017 USA

(Dated: October 8, 2021)

## ABSTRACT

We present the results of a Hubble Space Telescope WFC3 near-UV and ACS/WFC optical study into the star cluster populations of 10 luminous and ultra-luminous infrared galaxies (U/LIRGs) in the Great Observatories All-Sky LIRG Survey (GOALS). Through integrated broadband photometry we have derived ages, masses, and extinctions for a total of 1027 star clusters in galaxies with  $d_L < 110$  Mpc in order to avoid issues related to cluster blending. The measured cluster age distribution slope of  $dN/d\tau \propto \tau^{-0.5+/-0.2}$  is steeper than what has been observed in lower-luminosity star-forming galaxies. Further, differences in the slope of the observed cluster age distribution between inner- ( $dN/d\tau \propto \tau^{-1.07+/-0.12}$ ) and outer-disk ( $dN/d\tau \propto \tau^{-0.37+/-0.09}$ ) star clusters provides evidence of mass-dependent cluster destruction in the central regions of LIRGs driven primarily by the combined effect of strong tidal shocks and encounters with massive GMCs. Excluding the nuclear ring surrounding the Seyfert 1 nucleus in NGC 7469, the derived cluster mass function (CMF:  $dN/dM \propto M^\alpha$ ) has marginal evidence for a truncation in the power-law (PL) at  $M_t \sim 2 \times 10^6 M_\odot$  for our three most cluster-rich galaxies, which are all classified as early-stage mergers. Finally, we find evidence of a flattening of the CMF slope of  $dN/dM \propto M^{-1.42+0.1}$  for clusters in late-stage mergers relative to early-stage ( $\alpha = -1.65 \pm 0.02$ ), which we attribute to an increase in the formation of massive clusters over the course of the interaction.

*Keywords:* galaxies: star clusters: general - galaxies: starburst - galaxies: ISM - infrared: galaxies

## 1. INTRODUCTION

Imaging surveys of high-redshift star-forming galaxies reveal that these systems tend to display turbulent disks, which host star-forming clumps with stellar masses of  $\sim 10^{7-8} M_\odot$  and sizes of 0.5 – 5 kpc (Elmegreen et al. 2004, 2009; Daddi et al. 2010; Livermore et al. 2015). These extreme clumps are  $\sim 100$ x more massive than the typical giant molecular cloud (GMCs) observed in the local Universe, and give rise to super star clusters

(SSCs) with masses which can reach  $\geq 10^6 M_\odot$ ; i.e., similar to the most massive known globular clusters and 1-2 orders of magnitude more massive than any young cluster or HII region found in nearby normal galaxies like the Milky Way (MW) or M51 (Kobulnicky & Johnson 1999; Whitmore et al. 2014; Cook et al. 2016; Dessauges-Zavadsky & Adamo 2018).

While the total number of massive clusters formed is largely set by the gas density in the interstellar medium

(ISM), high-resolution simulations of cluster formation show that strong stellar (internal) feedback not only changes the efficiency of cluster formation within GMCs, but also alters the dynamical state of the cluster and in some cases may rapidly disrupt the cloud altogether (e.g., Li et al. 2017; Grudić et al. 2020). Star clusters may also lose mass via interaction (external) with their galactic environment (e.g., Lamers et al. 2005; Gieles et al. 2006), resulting in low disruption rates in low pressure environments and high disruption rates in intensely star-forming regions of the ISM. From a theoretical perspective, after their formation clusters lose mass in three phases: (1) stellar evolution and feedback, (2) two-body relaxation-driven evaporation in their host galaxy's tidal field, and (3) tidal shocks resulting primarily from collisions with GMCs and passages of spiral arms (see Krause et al. 2020). During the first phase, expulsion of natal gas by stellar winds and supernovae perturbs the clusters' potential and leaves up to 90% of clusters unbound or destroyed (Lada & Lada 2003). The latter stages of cluster evolution depend both on the clusters' location within the galaxy, and its overall density.

However, there is no consensus for what the relative importance of both internal feedback and the external galactic environment (mass-dependent cluster disruption) have on altering the universality of star cluster properties (see: Portegies Zwart et al. 2010; Whitmore et al. 2010; Bastian et al. 2012; Fall & Chandar 2012; Fouesneau et al. 2012; Chandar et al. 2015; Johnson et al. 2017). Observationally, the shape of both the cluster luminosity function (CLF) and cluster mass function (CMF) as well as the star cluster age distribution have been found to vary between quiescent and starburst galaxies in the local Universe (Gieles 2009; Bastian et al. 2012; Krumholz et al. 2019; Adamo et al. 2020). While Fall et al. (2005) and Whitmore et al. (2007) interpret the age distribution for star clusters in the Antennae galaxies (NGC 4038/39), the nearest example of a massive galaxy merger, as evidence for mass independent cluster disruption (e.g. feedback-driven gas dispersal) up to  $\sim 10^5 M_\odot$ , Lamers et al. (2005) and Silva-Villa et al. (2014) have suggested that strongly varying tidal fields and collisions between GMCs of high surface density can be the dominant physical mechanism which disrupts clusters in such extreme environments. Indeed, simulations of equal-mass galaxy mergers (Kruisjen et al. 2011) find that 80-85% of the cluster disruption seen may be accounted for by tidal shocks.

Luminous and Ultra-luminous infrared galaxies (LIRGs: defined as having IR luminosities  $L_{IR}[8 - 1000\mu m] > 10^{11} L_\odot$ ; ULIRGs:  $L_{IR} > 10^{12} L_\odot$ ) host

the most extreme stellar nurseries in the local Universe, with star-forming clump masses and radii similar to high-redshift galaxies (Larson et al. 2020). The activity in LIRGs is largely interaction triggered, with the progenitors observed to be gas-rich disk galaxies involved in minor interactions (at the low luminosity end) or major merger events (Stierwalt et al. 2013). This framework is supported by simulations of gas-rich mergers which show the inward flow of star-forming gas via tidal and bar-driven dissipation to a nuclear starburst, and the eventual settling into early-type galaxies (Barnes & Hernquist 1992; Barnes 2004; Hopkins et al. 2006). Further, these simulations demonstrate that the chaotic environment of the nuclear region is contrasted against the outer regions of a galaxy merger, where increases in the dense gas and star formation efficiency are comparatively mild (Moreno et al. 2021). Since local LIRGs can be studied at high-resolution across the entirety of their disks, they are ideal laboratories for testing location-dependent cluster formation and disruption in extreme merger-driven environments.

To better understand cluster formation and evolution in LIRGs, we previously combined our *Hubble Space Telescope* (*HST*) F435W (B) and F814W (I) ACS/WFC data with far-UV ACS/SBC F140LP (FUV) data to age-date  $\sim 400$  clusters in a combined sample of 22 LIRGs as part of the Great Observatories All Sky LIRG Survey (GOALS) (Armus et al. 2009; Linden et al. 2017). Overall we found evidence of a steeper decline in the number of clusters per unit time as a function of increasing cluster age ( $dN/d\tau \propto \tau^{-0.9}$  for  $3 < \tau < 300$  Myr) relative to ‘normal’ galaxies, which is a further indication that clusters in massive mergers suffer destruction at a much more rapid rate than normal star-forming galaxies.

However, our 2017 study was limited by three issues: (i) the small field of view (FOV) of the SBC (Solar Blind Channel) observations ( $30'' \times 30''$ ) often limited us to clusters in the central regions of the galaxies in our sample; (ii) the completeness-corrected cluster sample contained only the most massive clusters ( $M \geq 10^5 M_\odot$ ) in each galaxy due to the limited sensitivity achieved with the ACS/SBC; and (iii) age-extinction degeneracies were present for clusters within particular color ranges. Here, we present *HST* WFC3 U- (F336W) band observations of all  $10 L_{IR} > 10^{11.4} L_\odot$  U/LIRGs in GOALS scheduled to be observed by the *James Webb Space Telescope* (*JWST*) as part of the guaranteed time observing (GTO) campaigns and the early release science (ERS) program “A JWST Study of the Starburst-AGN Connection in Merging LIRGs” (PID 1328 - PI Armus). The combination of broad- and narrow-band near-infrared (NIR) and mid-infrared (MIR) imaging

with JWST at comparable resolution as HST will allow us to identify all of the very youngest ( $\sim 1$  Myr) and most highly-embedded SSCs in LIRGs. These sources are often missed in UV-optical studies of cluster formation in nearby galaxies, but are crucial for a complete picture of stellar feedback in the ISM.

Crucially, our new WFC3/UVIS observations provide vast improvements in sensitivity over prior *HST* detectors operating at  $0.3\text{ }\mu\text{m}$ , and combined with our existing *HST* data (ACS/WFC F435W and F814W data), provide high-resolution maps of the distribution of star clusters over the entire extent of each LIRG. Further, the F336W filter provides a much improved lever arm for age-dating clusters relative to the F140LP filter, which allows us to break the reddening-age degeneracy and thus more accurately measure (to within 0.1-0.2 dex in  $\log(\tau)$ ) cluster ages and cluster masses. A fundamental goal of the present paper is to investigate what role the host galaxy environment, and *localized* ISM conditions within individual LIRGs, play in the rapid destruction of SSCs observed in LIRGs.

The paper is organized as follows: In §2, the observations, data reduction, and sample selection are described. Our method for identifying clusters and determining cluster ages, masses, and extinctions is described in §3. In §4 we discuss the completeness limits of our cluster sample. In §5, the age and mass functions are discussed within the context of lower luminosity star-forming galaxies and clusters found in both the inner and outer-disks of our galaxy sample. Finally, we discuss our results in terms of the merger stages (MS) of each system. §6 is a summary of the results.

Throughout this paper, we adopt a WMAP Cosmology of  $H_0 = 69.3\text{ km s}^{-1}\text{ Mpc}^{-1}$ ,  $\Omega_{\text{matter}} = 0.286$ , and  $\Omega_\Lambda = 0.714$  (e.g., see [Hinshaw et al. 2013](#)).

## 2. OBSERVATIONS AND SAMPLE SELECTION

The F336W images of 10 LIRG systems were obtained from August - November 2018 (PI: A. Evans; PID 15472). Table 1 is a summary of the general properties of the sample. Each galaxy was observed with four dithered exposures in ACCUM mode, and when possible, placed at the center of the UVIS2 chip, due to the increased sensitivity at UV wavelengths relative to UVIS1. The approximate integration times for each galaxy is 41 minutes. The data were reduced with the Multidrizzle software provided by STScI to identify and reject cosmic rays and bad pixels, remove geometric distortion, and finally, combine the resulting mosaics with our existing ACS/WFC F435W and F814W observations (see Figure 1). The final pixel scale of our WFC3 images is  $0.0396''/\text{pix}$ . The ACS/WFC and WFC3/UVIS

cameras have comparable fields of view ( $202'' \times 202''$  and  $162'' \times 162''$  respectively), and cover sufficient area to enable single pointing observations of these U/LIRGs.

To understand the impact of combining results from galaxies which span a factor of  $\sim 3$  in distance, we performed simulations of cluster blending: by progressively smoothing *HST* WFC3 archival imaging of the Antennae Galaxies ( $D_L = 22\text{ Mpc}$ : [Whitmore et al. \(2010\)](#)), re-identifying star-clusters, and re-computing the luminosity function, we determined that blending begins to hamper our ability to accurately measure cluster properties (age, mass, extinctions), and thus determine the true slope,  $\alpha$ , of the underlying cluster mass function, at smoothing lengths of  $\geq 5$  pixels (i.e.,  $\Delta\alpha > 0.3$ ). This test demonstrates that clusters can be individually detected and their physical properties can be accurately recovered in galaxies out to a distance of  $\sim 100\text{ Mpc}$ . Therefore we limit our primary cluster analysis in this paper to the 5 nearest systems that have  $D_L \leq 100\text{ Mpc}$ , such that we can be confident our results are not biased towards large, unresolved, complexes of multiple star clusters. However, we run the same cluster identification and photometric analysis on all 10 LIRG systems. We provide photometry and derived physical quantities for all star clusters in the Appendix.

## 3. CLUSTER IDENTIFICATION AND MODEL FITTING

### 3.1. Cluster Identification

Star clusters in all three bands were selected using the program Source Extractor ([Bertin & Arnouts 1996](#)). The identification of clusters and the extraction of photometry is performed after a diffuse background subtraction is applied to each image. This subtraction is described in detail in [Linden et al. \(2017\)](#), and is designed to remove starlight which is unassociated with the compact sources identified in each galaxy. Cluster photometry across all background-subtracted images was then calculated using the IDL package APER. We used an aperture of radius 3.0 pixels, with an annulus from 4-5 pixels to measure the local background surrounding each cluster. Aperture corrections for ACS/WFC and WFC3 were calculated based on the encircled energy values presented in [Sirianni et al. \(2005\)](#) and [Deustua et al. \(2016\)](#) respectively. We additionally applied a correction for foreground Galactic extinction, using the [Schlafly & Finkbeiner \(2011\)](#) dust model combined with the empirical reddening law of [Fitzpatrick \(1999\)](#) available through the NASA Extragalactic Database (NED). We also removed sources with a signal-to-noise ratio  $S/N < 3$  and which are not detected in all three filters.

**Table 1.** Galaxy Sample Properties

Galaxy	RA	Dec	$D_L$ (Mpc)	MS	Log(LIR)	Log( $M_*$ )	SFR ( $M_\odot/\text{yr}$ )	MIR Size (kpc)	b/a (deg)	PA (deg)
IC 1623	01h07m47.180s	-17d30m25.30s	84.40	3	11.71	11.21	94.09	4.60	0.92	302.7
IRAS F08572+3915	09h00m25.390s	+39d03m54.40s	261.13	3	12.16	11.81	254.32	4.70*	0.31	10.8
NGC 3256	10h27m51.270s	-43d54m13.49s	45.66	3	11.64	11.06	76.46	2.10	0.83	25.0
IRAS F12112+0305	12h13m46.00s	+02d48m38.0s	329.38	3	12.36	11.34	402.89	9.83	0.64	9.3
Mrk 231 <sup>a</sup>	12h56m14.234s	+56d52m25.24s	188.57	6	12.50	10.98	380.19	3.34*	0.83	25.0
IRAS 14378-3651	14h40m59.008s	-37d04m31.94s	302.13	6	12.23	—	79.0 <sup>b</sup>	5.78*	0.67	41.7
Arp 220	15h34m57.255s	+23d30m11.30s	81.93	5	12.28	11.06	327.74	1.53*	0.87	286.2
NGC 6240	16h52m58.871s	+02d24m03.33s	108.67	4	11.93	11.59	148.44	2.26	0.45	279.6
IRAS F17207-0014	17h23m21.955s	-00d17m00.94s	189.03	5	12.46	11.18	501.22	3.75*	0.80	30.7
NGC 7469	23h03m15.623s	+08d52m26.39s	66.68	2	11.65	11.38	80.26	1.37	0.53	56.3

NOTE—Infrared luminosity and stellar mass are given in units of  $L/L_\odot$  and  $M/M_\odot$  respectively. RA, Dec, distance, infrared luminosity, stellar mass, and SFR are taken from Howell et al. (2010). Merger stages (MS) are taken from Haan et al. (2013), Kim et al. (2013), and Stierwalt et al. (2013). MIR sizes are taken from Díaz-Santos et al. (2010). The values marked with an asterisk (\*) denotes a galaxy whose central region is unresolved in the Spitzer 2D IRS Spectra. The b/a and PA are taken from Kim et al. (2013).

<sup>a</sup>Data for Mrk 231 is taken from U et al. (2012)

<sup>b</sup>An estimate for the SFR of IRAS 14378-3651 is taken from Sturm et al. (2011)

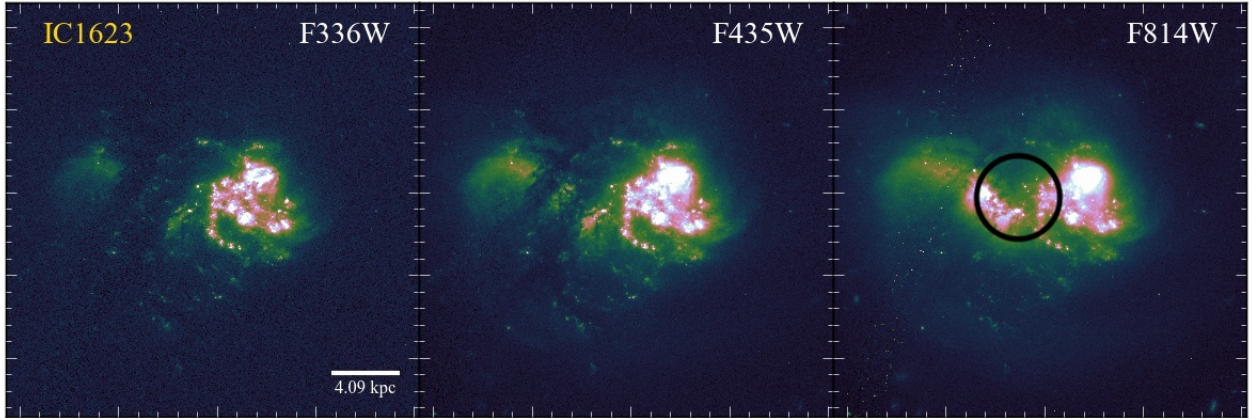


**Figure 1.** A comparison of *HST* WFC3/UVIS F336W image of IC 1623, relative to archival ACS/WFC F814W and F435W images. All three images have a FOV of 30" and are oriented N up E left. A corresponding 10" scale bar is given in the lower-right of the left Panel. The black circle in the right Panel represents the MIR size reported in Table 1 and discussed in Section 3.1. These images demonstrate our ability to detect and characterize star clusters throughout the central regions, disks, and extended tidal features of the galaxies in our sample.

We extracted photometry for 2167 cluster candidates ( $N_{det}$ ) which is given for each galaxy in Table 2. We then used ISHAPE (Larsen 1999) to measure the 2-D FWHM for all remaining sources by de-convolving the *HST* instrumental point spread function with a King profile (King 1966). We find that a cut of 3 pixels FWHM (corresponding to an average cluster size of  $R_{eff} \sim 22$  pc) effectively removes extended sources in both the nearest and farthest galaxies in the sample. This value is consistent with the upper-end of sizes observed for open star clusters in the Milky Way, as well as simulations of

star cluster formation in dwarf starburst galaxies (Lahén et al. 2020). In Figure 2 we show a zoom-in for three regions in IC 1623 with our cluster detections overlaid in blue squares. These regions highlight the structure and variable levels of background emission which surround these clusters. A total of 1027 confirmed clusters across the 5 nearest LIRGs meet the above criteria. We observe a large range of cluster magnitudes ( $M_U = -7 \sim -17$  mag), with a median of  $M_U = -10$  mag, where the brightest clusters are detected in both the central re-

**Table 2.** Cluster Detection Statistics and Overall Properties

Galaxy	$N_{det}$	$N_c$	$m_{U,Outer} 90\%$	$m_{U,Inner} 90\%$	$t_c$	$\sigma_{t_c}$	$M_c$	$\sigma_{M_c}$	$A_V$	$\sigma_{A_V}$
Arp 220	108	46	24.19	23.28	8.33	0.53	5.94	0.91	0.7	0.48
IC 1623	453	180	24.85	23.84	6.97	0.53	5.21	0.89	0.4	0.58
NGC 3256	1082	549	24.51	23.82	7.99	1.06	5.29	1.17	0.6	0.75
NGC 6240	141	87	24.95	23.36	8.24	0.66	5.71	1.16	0.5	0.59
NGC 7469	383	165	24.41	23.71	7.24	0.79	4.82	0.95	0.4	0.55

NOTE— $N_{det}$  is the number of cluster candidates in each galaxy.  $N_c$  is the number of confirmed clusters.  $m_U 90\%$  for both the inner and outer regions in each galaxy are listed in apparent magnitudes. Values for cluster age, mass, and extinction are given in  $\log(t/\text{yr})$ ,  $M/M_\odot$ , and magnitudes respectively. We note that a  $3\sigma$  significance for the PL+truncation model  $N_c/\sigma_{N_c}$  is only reached for the All and Early-stage cluster sub-samples.

gion and outer-disks of these systems. The number of confirmed clusters for each galaxy are given in Table 2.

Finally, in order to make detailed comparisons of clusters at different radii we adopt a similar methodology to Linden et al. (2019), to compute the de-projected galactocentric radius of each cluster ( $r_G$ ) using the axis-ratio ( $b/a$ ) and position angle (PA) of the host galaxy (Jarrett et al. 2000; Paturel et al. 2003; Kim et al. 2013). The  $13.2\mu\text{m}$  mid-infrared size derived from Spitzer/IRS spectra serves as our best estimate (or upper limit) for the size of the central starburst, limited by the resolution of the Spitzer/IRS beam, within each galaxy (Díaz-Santos et al. 2010). By comparing the measured  $r_G$  values to the  $13.2\mu\text{m}$  FWHM determined from a gaussian fit to the 2D spectra, we can place clusters into two categories: those that fall within the MIR size of the galaxy (inner-disk clusters) and those that fall outside of the MIR size (outer-disk clusters). This separation allows us to test whether the cluster properties that we measure with HST are dependent on the current size of the starburst responsible for producing the bulk of the far-infrared emission.

We note that for several galaxies the MIR size is unresolved (FWHM is within 10% of that of the unresolved stellar PSF). Therefore while the  $13.2\mu\text{m}$  MIR size may not represent the true size of the compact starburst in each galaxy, it still serves as our best estimate for where the bulk of the SF activity responsible for heating the dust in each galaxy is. We also stress that for NGC 3256 and IC 1623 (the two galaxies we ultimately examine - See Section 5.1.1) the MIR sizes are resolved. In fact for high-resolution ground-based  $5 - 15\mu\text{m}$  imaging of VV 114 reveal that up to  $\sim 60\%$  of the MIR emission is extended on kpc-scales (Le Floc'h et al. 2002). The values for the  $b/a$ , PA, and MIR size (FWHM) of each system are given in Table 1.

### 3.2. Model Fitting

For all confirmed clusters, the measured 3-band fluxes were compared against a library of simple stellar population (SSP) evolutionary models that were computed using the isochrone synthesis code Starburst99 (Leitherer et al. 1999), hereafter referred to as SB99. This code computes the evolution of an instantaneous burst based on a Kroupa IMF and the stellar evolution models over an age range of 1 Myr to 10 Gyr (e.g., Bertelli et al. 1994). Crucially we add the contribution from nebular emission lines which may contribute up to 40% of the emission observed in the broad-band F814W filter for clusters with ages  $\sim 3 - 5$  Myr (Reines et al. 2010; Zackrisson et al. 2011). We also choose to adopt a solar metallicity, as suggested for LIRGs by Kewley et al. (2010), and the starburst attenuation curve of Calzetti et al. (2000). Although we only consider solar metallicity models in our analysis, Linden et al. (2017) demonstrated that including sub-solar metallicity models does not significantly impact the results. The total attenuation of the stellar continuum,  $R_V = A(V)/E(B-V)_* = 4.05 \pm 0.8$ , is calibrated specifically for starburst galaxies and differs from the typical Milky Way value of  $R_V \sim 3.1$  (Calzetti et al. 2000). It has been shown empirically that clusters and HII regions are more heavily attenuated than the underlying stellar continuum, due to the fact that these objects are often found near dusty regions of ongoing star formation (Calzetti et al. 1994). Our model choices allow us to make consistent comparisons with results from the Legacy Extragalactic UV Survey (LEGUS), which adopt the Yggdrasil nebular+continuum models Zackrisson et al. (2011) to determine cluster ages, masses, and extinctions (e.g., Ryon et al. 2017; Adamo et al. 2017; Cook et al. 2019).

We construct grids for the age, mass, and extinction model parameters and perform a  $\chi^2$ -fit for each point in the grid. We use these to obtain the marginalized pos-

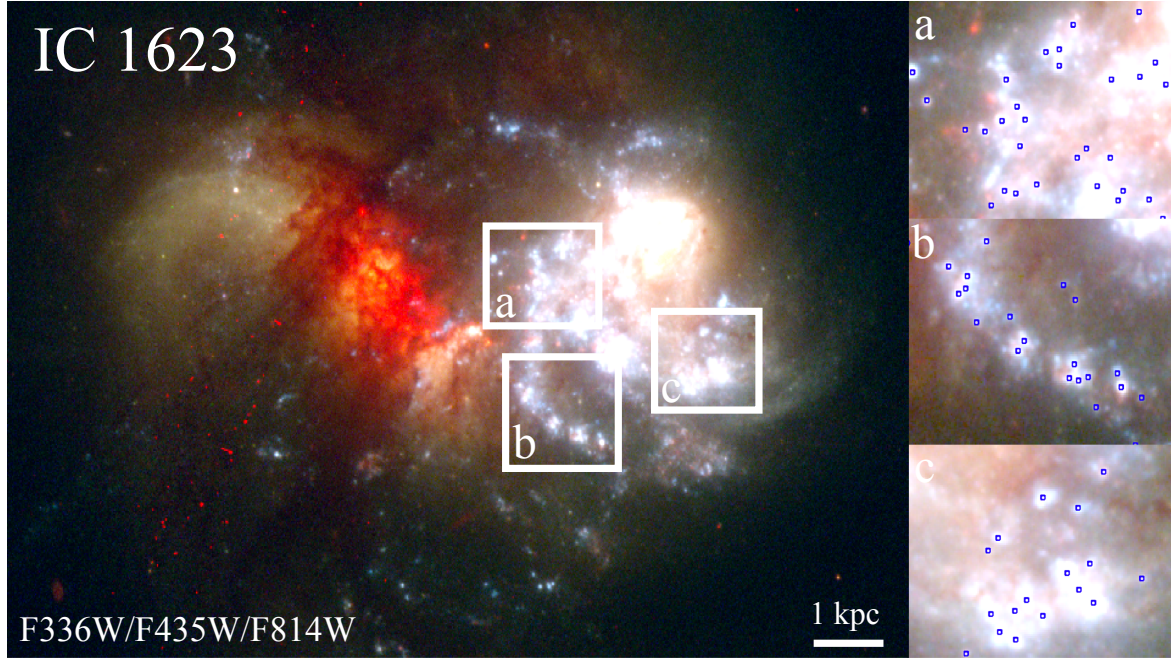


**Figure 2.** A false-color image of IC 1623 constructed with the HST WFC3 F336W and the ACS/WFC F435W and F814W filters in the blue, green, red channels respectively. The 3 regions labeled a, b, c have cluster detections identified in the panels at right. In these panels we overlay cluster detections in blue circles. These cutouts demonstrate that we are able to detect UV-bright compact sources of emission throughout the disk of the eastern galaxy, where the local background shows significant variations and structure. Approximately 200 star clusters are detected.

terior distribution function for all derived parameters, and represent the error in our model fit as the FWHM of each distribution. In the Appendix we give an example of our best-fit model one cluster in NGC 3256, chosen to demonstrate our ability to accurately recover the properties of a young, moderately extinguished ( $A_V = 1.7$ ), massive ( $10^4 M_\odot$ ) cluster. We show both the maximum a posteriori probability (MAP: blue line) as well as the median (pink line) of each parameter along with the corresponding  $1\sigma$  errors. This cluster represents a prototypical degenerate case from our previous F140LP observations, and with the substitution of the F336W filter we are able to recover cluster age, mass, and extinction to within 0.2 dex. This is crucial for accurately recovering the underlying slope of the age and mass distribution functions for each galaxy. The median age, mass, and extinction along with median absolute deviation (MAD) of each distribution are given in Table 2.

#### 4. COMPLETENESS AND THE MASS-AGE DIAGRAM

##### 4.1. Completeness

In order to determine the completeness limit of our cluster sample, we follow a similar prescription to Messa et al. (2018) which utilizes the LEGUS Cluster Completeness Tool. We first create a set of synthetic clusters with the BAOlab software (Larsen 1999) by convolving

the WFC3 F336W PSF with a King profile specified with effective radii of 1, 5, and 10 pc. The resulting sources are then distributed within our original science frames in two ways: (1) 100 clusters with apparent magnitudes of  $18 < m_U < 26$  are randomly placed within the central 300 pixels, which is chosen to match the median MIR size in our 5 sample galaxies, of each F336W science frame, and (2) 500 clusters are randomly placed outside the central 300 pixels of each science frame. In this way we can directly account for significant variations in the depth of our U-band images in the central regions of the LIRGs in our sample. The same procedure described in §3 is then applied to these images and the fraction of simulated clusters recovered in the final catalog is calculated for each effective radius as a function of input cluster magnitude.

For the 5 LIRGs in our cluster sample the total 90% completeness limits for the inner and outer-region are given in Table 2. We find that due to increased dust obscuration and crowding in the central regions we are  $\sim 1$  magnitude less sensitive in the F336W filter, and that we achieve consistent depth ( $m_{U,Inner} 90\%$ ) across the 5 galaxies in our sample given that the range in magnitudes is relatively small. The cluster-weighted median completeness limit for the inner and outer regions of our LIRG sample are  $M_U = -9.3$  and  $M_U = -8.4$  respec-

tively, and are shown as dotted and solid lines in Figure 3.

#### 4.2. The Mass-Age Diagram

Figure 3 shows the derived age and mass of each cluster identified in the sample with outer-disk clusters ( $N_c = 809$ ) plotted in black and inner-disk clusters ( $N_c = 218$ ) plotted in purple. The lack of low-mass ( $\leq 10^4 M_\odot$ ) clusters with ages  $\geq 100$  Myr is due to the fact that clusters dim as they age and eventually become fainter than our UV detection limits. By applying our inner-disk completeness limit to the SB99 model we can define regimes of this mass-age parameter space where we are observationally complete in both the inner- and outer-disks of the LIRGs in our sample. Mass-limited cluster samples have the advantage over luminosity-limited samples because they recover the underlying shape of the age and mass distributions, and are thus not affected by the distance to each galaxy (Renaud 2020).

The two cuts were selected to sample distinct parts of the mass and age distribution for which we maintain completeness. We define Regime 1 to be:

$$5.2 < \log(M/M_\odot) < 8 \quad (1)$$

$$6.6 < \log(\tau) < 8.7 \quad (2)$$

Regime 2 to be:

$$4.5 < \log(M/M_\odot) < 8 \quad (3)$$

$$6.0 < \log(\tau) < 7.5 \quad (4)$$

Regime 1 is chosen to match, as closely as possible, the age and mass limits from Fall et al. (2005); Linden et al. (2017), allowing us to make accurate comparisons to the age distributions of clusters in other nearby galaxies, while also avoiding selecting the very youngest clusters which may actually be unresolved unbound associations (Kruijssen & Bastian 2016). Regime 2 is chosen in order to measure the CMF of the young ( $\tau \leq 10^{7.5}$ ), recently formed clusters that best reflect the current conditions of the ISM in these systems (Adamo et al. 2020). When analyzing Regimes 1 and 2 we exclude the largest mass bin of  $\log(M/M_\odot) = 8.0$ . These very high masses are most likely the result of either an imperfect extinction correction or multiple very compact star clusters in close proximity appearing as a single star cluster at the resolution of these images. We stress that the adopted FWHM cut helps minimize the inclusion of sources which are blends of  $\sim 2 - 3$  clusters. Finally, we note that while clusters of these masses are rare, Bastian et al. (2013) found several clusters in NGC 7252 with masses greater

than  $10^7 M_\odot$ , including one cluster with a total mass of  $\sim 10^8 M_\odot$ . Finally, recent observations of a nearby ( $z = 0.0336$ ) post-starburst galaxy have revealed massive clusters up to  $10^{7.5} M_\odot$  associated with a period of intense SF activity in the galaxy (Chandar et al. 2021).

## 5. DISCUSSION

After determining ages, masses, and extinctions for the entire cluster sample we directly compare these distributions with those of nearby normal and interacting galaxies. We focus on the interpretation of the derived cluster age distribution for both the individual systems and the sample as a whole as well as mass functions for combined samples of galaxies. Further, we will analyze the inner- and outer-cluster distribution functions for each system. Ultimately, we discuss to what degree the differences observed in our cluster populations can be attributed to the extreme star-forming environment unique to LIRGs in the local Universe.

### 5.1. Age Distribution

We consider the age distribution of clusters in our LIRG sample over Regime 1 described in §4. Specifically, we are interested in measuring the power law index  $\gamma$ , where  $dN/d\tau \propto \tau^\gamma$ . In Figure 4 we show the differential number of clusters per time interval,  $\log(dN/d\tau)$ , versus the median cluster age over that interval,  $\log(\tau)$  for all clusters in the mass range given in Equation 1. The data are binned by 0.4 in  $\log(\tau)$  so as to fully encapsulate  $\sim 2\sigma$  times the typical model errors of 0.2 in  $\log(\tau)$  discussed in §3. For clusters in the age-range given in Equation 2 a weighted linear least-squares fit to the age distribution results a power-law index of  $\gamma = -0.54 \pm 0.12$ . The slope of the cluster age distribution reflects a combination of any increase in the formation rate of clusters with  $10^{5.2} M_\odot < M_c < 10^{8.0} M_\odot$  from  $10^{8.7}$  yr to the present day as well as any destruction of star clusters through the methods discussed above over the same age interval. In Section 5.1.2 we attempt to account for this ambiguity directly.

While the observed slope is slightly shallower than both the Antennae age distribution slope and the results from Linden et al. (2017), we see that our combined galaxy slope is consistent with the results for M83 and steeper than what is measured for lower-luminosity star-forming galaxies like the LMC (Adamo & Bastian 2015). When examining the age distribution functions for our three most cluster-rich (i.e.  $N_c > 100$  SSCs) galaxies, we find that the slopes measured for IC 1623, NGC 3256, and the outer-disk of NGC 7469 are all steep with  $\gamma = -0.4$  to -1 (Figures 5, 6, and 7 respectively).

We note that this analysis excludes the 19 clusters identified in the nuclear ring of NGC 7469. The star

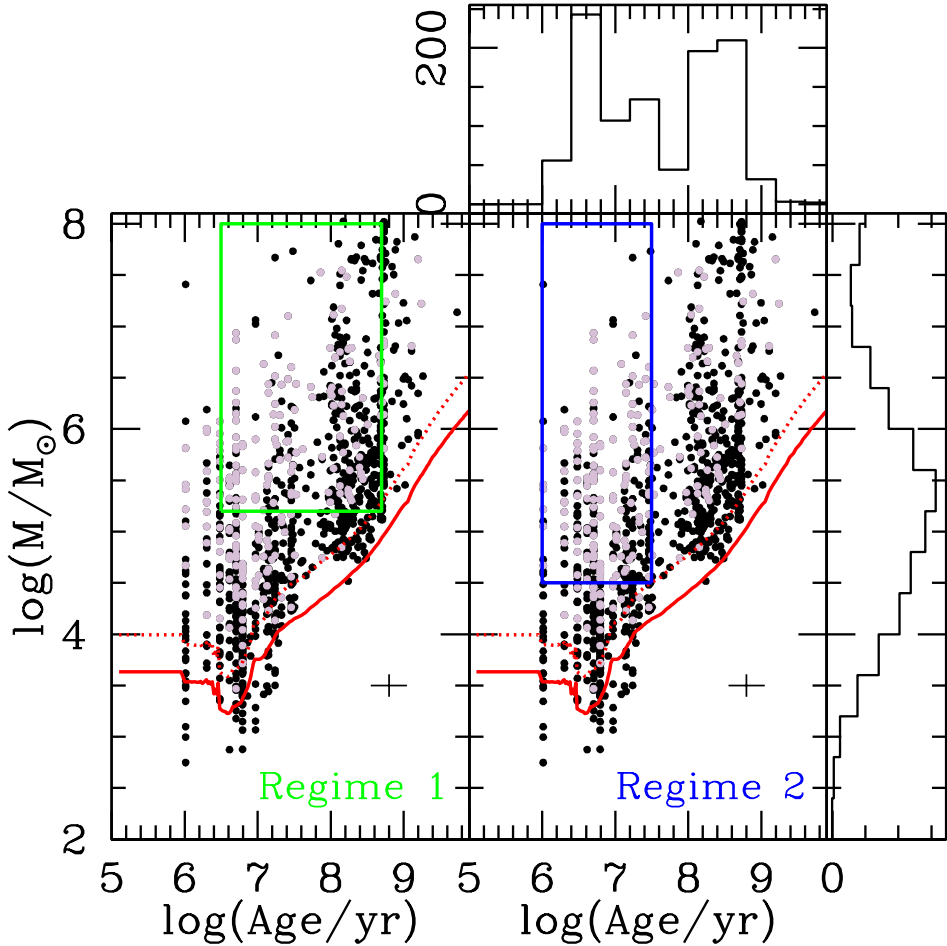


**Figure 3.** The mass, age distribution of all 1027 clusters found in our LIRG sample. Outer- and inner-disk clusters, categorized based on the MIR size of the galaxy, are plotted in black and purple respectively. The solid and dotted red curves represent mass-age tracks produced from the SB99 model with an input of  $M_U = -8.4$  and  $M_U = -9.4$  which correspond to the 90% completeness limits for the inner- and outer-disk respectively. The green box in the left panel represents Regime 1, and is used for the mass-age cuts applied when analyzing the cluster age distribution. The blue box in the right panel represents Regime 2, and is used for the mass-ages cuts applied when analyzing the cluster mass distribution. The histograms show the distribution of cluster ages and masses for the full sample. The cross on the bottom right of each panel represents the median errors in cluster age and mass bootstrapped from our model.

and cluster formation within nuclear rings is likely decoupled from the SFH of their host galaxies due to irregularities in the inflow rate of dense gas (Maoz et al. 2001). Indeed,  $\sim 30\%$  of the nuclear K-band light in NGC 7469 is due to a single source (Davies et al. 2004). Further NGC 7469 is the only nearby galaxy in our sample that contains a bright Seyfert 1 nucleus, which may also affect the temperature and spatial distribution of the gas within the ring itself (Díaz-Santos et al. 2007). Therefore, we are unable to disentangle these effects from variations in the SFH which ultimately complicates any comparison between the age distribution inferred for these clusters the outer-disk clusters in this galaxy. In

the following Section we exclude this galaxy from the inner- and outer-disk comparison.

#### 5.1.1. Inner- and Outer-disk Clusters

All three 'cluster-rich' systems are classified as early-stage mergers (Kim et al. 2013), suggesting that the similar dynamical state (e.g tidal field) within the ISM of these galaxies may set the overall disruption rate seen. Existing wide-field WiFeS IFU observations of IC 1623 and NGC 3256 allow us to connect the cluster properties in both the inner- and outer-disks of these systems to the ionized gas. These two systems both exhibit strong evidence of galaxy-wide shock excitation induced by their ongoing merger activity (Rich et al. 2011). Multi-line Atacama Large Millimeter/submillimeter (ALMA) CO

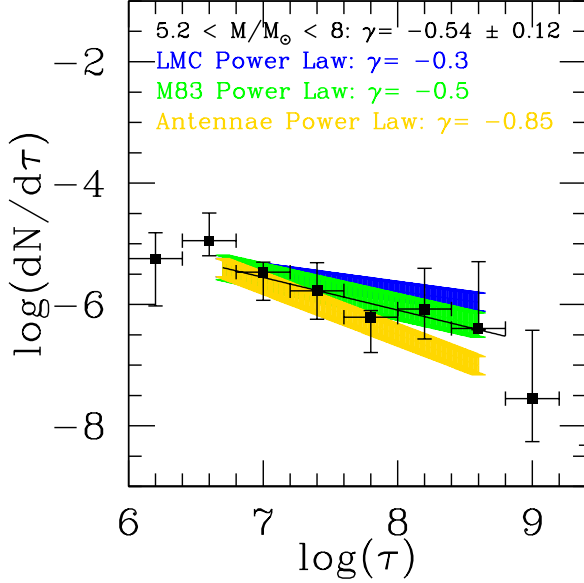


**Figure 4.** The stacked age distribution functions for all 5 galaxies. The black line represent weighted linear least squares fit to the data in Regime 1. The blue, green, and yellow age functions of the LMC, M83, and the Antennae respectively, chosen to span the full range of observed cluster disruption rates, are taken from [Adamo & Bastian \(2015\)](#) and normalized to the total number of clusters in our sample. It is clear LIRGs have elevated levels of cluster disruption relative to lower-luminosity star-forming galaxies like the LMC.

observations of GMCs in IC 1623 and NGC 3256 also suggest they are highly-turbulent ([Saito et al. 2015](#); [Brunetti et al. 2021](#)). With multi-line HCN/HCO+ observations [Saito et al. \(2018\)](#) further attributing this turbulence to galaxy-wide shocks in IC 1623.

By examining the age distribution functions for clusters identified as inner- or outer-disk clusters in NGC 3256 and IC 1623 a striking result emerges. The SSCs classified as inner-disk ( $N_c = 206$ ) show a distribution slope of  $\gamma = -1.1 \pm 0.11$ , whereas SSCs found in the outer-disk ( $N_c = 523$ ) have a distribution slope of  $\gamma = -0.33 \pm 0.12$  (Figure 8). This inner-disk value is consistent with the results from [Linden et al. \(2017\)](#), where the FOV is well-matched to the average MIR size. We stress that NGC 3256 and IC 1623 both individually show increases in the distribution slope between inner and outer-disk clusters, but the samples are combined here such that we achieve better statistics for each region. The outer-disk value is consistent with the results for M83 presented in [Adamo & Bastian \(2015\)](#), which is a prototypical spiral galaxy in the local Universe, and suggests that differences in the observed slope between IC 1623 and M83 in Figure 5 are driven by the inner region of the galaxy.

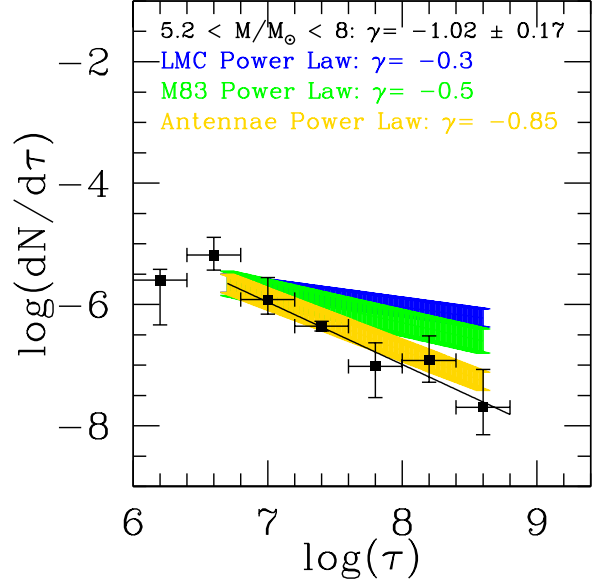


**Figure 5.** The age distribution function for IC 1623 which contains 180 confirmed SSCs. We find that this galaxy shows the steepest slope ( $\gamma = -1.02 \pm 0.17$ ) in our sample, and is steeper than the slopes observed in both M83 or the LMC. This value is consistent with the results presented in [Linden et al. \(2017\)](#) as well as observations of the Antennae galaxy ([Fall et al. 2005](#)).

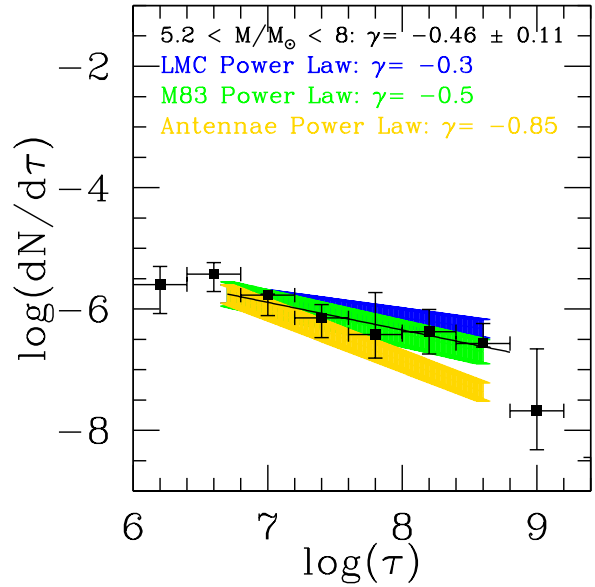


**Figure 6.** The age distribution function for NGC 3256 which contains 549 confirmed SSCs. We find that the distribution slope ( $\gamma = -0.46 \pm 0.11$ ) is consistent with the overall slope measured for the full sample, and importantly, is found to be flatter than what is measured for the Antennae galaxy ([Fall et al. 2005](#)).

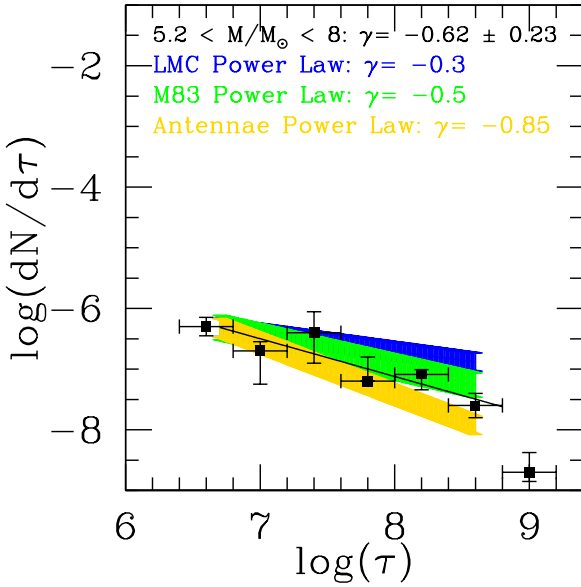


**Figure 7.** The age distribution function for NGC 7469 which contains 146 confirmed SSCs. After excluding clusters in the nuclear ring, we find that the distribution is consistent with the overall slope measured for the full sample, and importantly, is found to be steeper than what is measured for lower-luminosity star-forming galaxies like the LMC.

It was shown in Gieles et al. (2006) that star clusters can be disrupted on  $\sim 1 - 2$  Gyr timescales by tidal shocks that arise from gravitational interactions with passing GMCs. The GMC volume density in the central regions of LIRGs is considerably higher than what is seen in other nearby galaxies or the MW (e.g., Rosolowsky 2005; Hughes et al. 2013; Greve et al. 2009; Papadopoulos et al. 2012). Therefore we might expect more frequent and/or more disruptive shocks, capable of disrupting even the most massive clusters on timescales of  $\leq 100$  Myr, to be prevalent in the youngest and densest star-forming regions of local LIRGs (often referred to as the 'cruel cradle effect': Elmegreen & Hunter 2010). For very short disruption timescales, this scenario predicts that cluster evolution may be strongly dependent on environment (Miholics et al. 2017).

It is likely that both internal feedback and external effects co-exist for the youngest clusters. However, there's a suggestion from simulations that the fraction of clusters which are destroyed by gas expulsion (i.e., 'infant mortality': Lada & Lada 2003) decreases in effectiveness with increasing ambient density of the star-forming region, while at the same time the disruptive effect of tidal shocks increases with ambient gas density (Pfeffer et al. 2018). It may be that 'infant mortality' and the 'cruel cradle effect' each dominate as the main feedback mechanism at the two extremes of the gas density spectrum of

star-forming regions. Their relative strength would then determine the relation between the cluster formation efficiency ( $CFE = CFR/SFR$ ) and the surface density of gas in galaxies (Johnson et al. 2017; Adamo et al. 2020).

Assuming spatially homogeneous distributions of clusters and GMCs, Gieles et al. (2006) found that clusters lose most of their mass in very close encounters with high relative velocities. The derived disruption timescale depends on the cluster mass ( $M_c$ ), the half-mass radius ( $r_h$ ), and the product of the individual mean GMC surface density and the average local GMC density ( $S \propto (\Sigma_{GMC}(M_\odot pc^{-2})\rho_{GMC}(M_\odot pc^{-3}))^{-1}$ ).

In Equation 5 we give the expression for the disruption timescale  $t_{dis}$  for a cluster embedded in a strong external tidal field  $S$  parameterized by the mass density and volume of the ISM in the Solar Neighborhood (Eq. 24 - Gieles et al. 2006):

$$t_{dis} = 2.0 \left( \frac{5.1 M_\odot^2 pc^{-5}}{\Sigma_{ISM} \rho_{ISM}} \right) \left( \frac{M_c}{10^4 M_\odot} \right)^\delta \text{Gyr} \quad (5)$$

where  $\delta = 1 - 3\lambda$  with  $R \propto M^\lambda$ . Simulations of the mass-radius relationship suggest that the appropriate value of  $\delta$  ranges from 0.2 for low-mass clusters to  $\sim 1$  for the highest-mass (weakly-disrupted) clusters (Gieles & Renaud 2016). In the latter case corrections due to adiabatic compression become so important that tidal shocks can destroy clusters in a single encounter (Miholics et al. 2017). Observations of nearby galaxies including M51, M33, and the SMC suggest a weak mass-radius relation ( $\lambda \sim 0.1$  resulting in  $\delta = 0.6 - 0.7$ : Boutloukos & Lamers 2003). However, recent results from LEGUS show that the average  $\lambda$  is 0.24, although the median cluster mass in the LEGUS sample is 1-2 orders of magnitude lower than the clusters studied here (Brown & Gnedin 2021).

Using observations of the molecular gas scale height ( $H = 177$  pc), and GMC surface density ( $\Sigma = 2.5 \times 10^3 M_\odot pc^{-2}$ ) in the central regions of NGC 3256, as well as an average cluster mass of  $10^{5.8} M_\odot$ , we derive a disruption timescale of  $\sim 10$  Myr (Wilson et al. 2019; Brunetti et al. 2021) which is comparable to the timescale over which we expect internal feedback processes to occur ( $\sim 3 - 5$  Myr). The upper-limit represents the point where massive stars begin to die in supernova explosions injecting energy and momentum into their surroundings (Chevance et al. 2020; Barnes et al. 2020). This is contrasted against a disruption timescale for the outer-disk of  $\sim 200 - 300$  Myr, with an order of magnitude lower ISM density and approximately the same median cluster mass ( $10^{5.8} M_\odot$ ).

Gieles & Renaud (2016) presents an updated version of Equation 5 which additionally accounts for internal evolution of the cluster during this disruption phase as

well as the velocity dispersion of the surrounding gas. Depending on the adopted mass-radius relationship this results in an increase in the derived disruption timescale by a factor of  $\sim 3 - 30$ . For the central region of NGC 3256 we derive a disruption timescale of  $\sim 40$  Myr for the inner-disk and  $\sim 400$  Myr of the outer-disk adopting values for the velocity dispersion of the gas of 120 km/s and 40 km/s respectively (Brunetti et al. 2021).

Ultimately, we find that the disruption timescale from tidal shocks can be short enough to affect the age distribution of clusters with  $t < 1$  Gyr in the central regions of LIRGs. Qualitatively, this difference corresponds to an increase in mass-dependent cluster disruption, where long-term cluster evolution in the central regions of LIRGs are primarily influenced by the external tidal field and ISM density within ongoing mergers. Finally, these results are consistent with a similar UV-optical study presented in Adamo et al. (2020) which looked at the cluster populations for a sample of 6 LIRGs, including NGC 3256. While not focusing on the age distribution slope directly, they note a lack of young lower-mass clusters in the inner region relative to their outer-disk cluster sample for this system.

### 5.1.2. Increasing SFR vs. Increasing Cluster Destruction

An important assumption made in the interpretation of these age distributions is that they are the result of cluster disruption, rather than a large increase in the formation of clusters that is a function of distance from the nucleus, or mass. This assumption may not be true in ongoing starbursts like the Antennae or even the central regions of M83. Chandar et al. (2017) used extinction-corrected GALEX FUV and  $24\mu\text{m}$  fluxes to derive SFRs averaged from 10 - 100 and 100 - 400 Myr for several starburst galaxies including NGC 3256, M51, and the Antennae. Combined with published color-magnitude diagram (CMD) analysis for the LMC, SMC, NGC 4214, and NGC 4449, they demonstrate that the SFRs have not varied by more than a factor of  $\sim 2$  for both the dwarf and starburst galaxies in their sample. There also appears to be no systematic trends in the average SFR with age, suggesting that strong variations in the cluster age distribution seen in these systems is likely the result of cluster disruption rather than increased formation. Finally, with complete photometric coverage from the FUV to the FIR Pereira-Santaella et al. (2015) used the SED fitting code MAGPHYs (da Cunha et al. 2008) to derive the SFHs for  $\sim 30$  local LIRGs. They find that, apart from Arp 299, galaxies classified as having a "SF burst" show global enhancements of  $\sim 2 - 4$  in SFR, forming 1 – 2% of the total stellar mass in the galaxy.

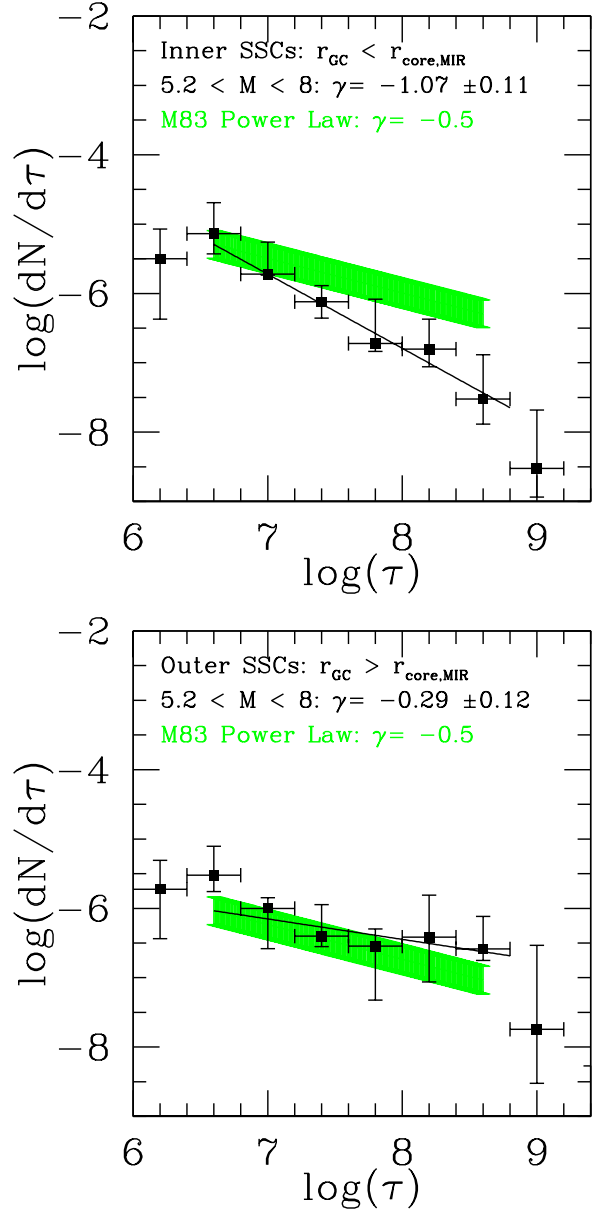


**Figure 8.** The age distribution functions for NGC 3256 and IC 1623 classified as either inner-disk (top) or outer-disk (bottom) clusters relative to the results for the star-forming galaxy M83 shown in green (Adamo & Bastian 2015). We see that the magnitude of the difference  $\gamma$  ( $\sim 0.7$ ) between the inner- and outer-disk clusters is larger than what has been found for nearby normal galaxies (Messa et al. 2018), and remains significant even after accounting for spatial variations in the surface density of young cluster formation (See Section 5.1.2).

If the differences observed between the inner- and outer-disk age distributions in Figure 8 from is due entirely to an increase in the cluster formation rate (CFR) from 1 - 100 Myr, than the increase in  $\gamma$  of 0.7 would correspond to an increase in  $\Delta dN/dt \propto CFR$  of 25

for clusters above the completeness limit ( $10^{5.2} M_{\odot}$ ) of our inner-disk sample. While the CFR/SFR relation may vary in different galactic environments, it has been observed to be approximately linear and thus we take the two quantities proportional to one another (Johnson et al. 2017). The models presented in (Kruijssen 2012) suggest that the CFR/SFR is  $\sim 30 - 40\%$  for regions with  $\Sigma_{\text{gas}} \sim 10^3 M_{\odot} \text{pc}^{-2}$ , and therefore an increase in the CFR of 25 should be considered a lower-limit for the required increase in SFR.

Using the F336W images as a proxy for the recent (10-100 Myr) SF activity we can make estimates of the surface density inside and outside the MIR size of each galaxy. Although the U-band continuum is not tied to the photospheric emission of the youngest stellar populations directly (as is the case for the UV), the errors are minimized for highly star-forming galaxies such as LIRGs (Kennicutt 1998). We find that the increase in F336W-traced SFR surface density is  $6.2 \pm 1.1 M_{\odot} \text{yr}^{-1} \text{kpc}^{-2}$  and  $3.5 \pm 0.4 M_{\odot} \text{yr}^{-1} \text{pc}^{-2}$  for NGC 3256 and IC 1623 respectively. These results are consistent with CALIFA IFU observations of IC 1623 which showed an extinction-corrected enhancement between 30-300 Myr of  $\sim 2 - 3$  in the central half-light radius (Cortijo-Ferrero et al. 2017), which would corresponds to a change in  $\gamma$  of 0.15-0.2.

Given the above, the most plausible explanation is that while the cluster formation rate in the central regions of NGC 3256 and IC 1623 are clearly increasing, the differences in the slope of the age distribution observed for inner- and outer-disk clusters suggests that cluster disruption plays a key role: clusters found in the inner-regions of these LIRGs show greater disruption rates relative to SSCs identified in their outer-disks. The magnitude of this difference is also larger than the differences observed for inner- and outer-disk clusters in other nearby normal galaxies, suggesting that the merging process is crucial for driving such extreme disruption rates (Adamo 2015; Hollyhead et al. 2016).

## 5.2. Mass Function

We consider the mass distribution of clusters in our LIRG sample over Regime 2 described in §4. When modeling the CMF we adopt a maximum-likelihood fitting technique as well as a bootstrap resampling of the posterior distribution functions for both a simple power-law model (PL) and a two component Schechter function of the form  $dN/dM \propto (M/M_t)^{\alpha} e^{-(M/M_t)}$ , where  $M_t$  is the truncation mass and  $\alpha$  is the overall power-law slope. In order to test the hypothesis of a mass truncation, we have fit the cumulative distribution function:

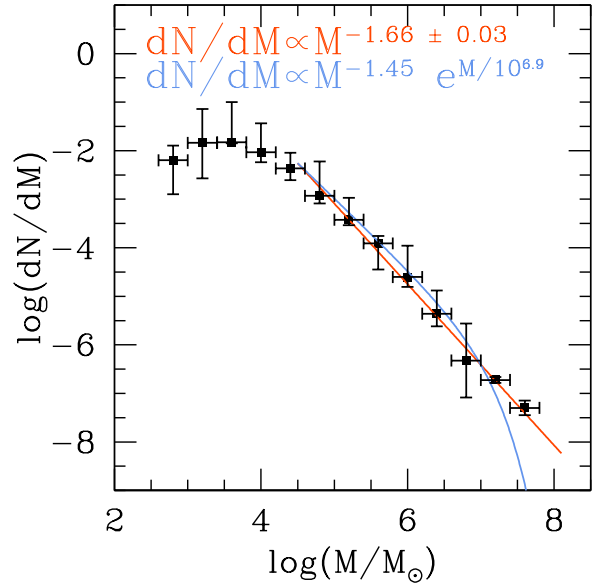


**Figure 9.** The stacked mass distribution function for all 5 galaxies. The red line represents the maximum-likelihood fit to the data for a power-law (PL) only model, with analytic Schechter function (PL+truncation) fit to the empirical distribution overlaid in blue. Although the evidence for a truncation is marginal ( $\sim 3\sigma$ ), the values obtained for the  $M_t$  are larger than what is observed for lower-luminosity star-forming galaxies in the local Universe. These results are consistent with the luminosity function derived from Pa $\beta$  observations of LIRGs in GOALS (Larson et al. 2020), as well as detailed observations of Arp 299 (Randriamanakoto et al. 2019).

$$N(M' > M) = N_t \left[ \left( \frac{M}{M_t} \right)^{\alpha+1} - 1 \right], \quad (6)$$

where  $N_t$  is the number of clusters more massive than  $2^{1/(\alpha+1)} M_t$ . We implement the IDL routine MSPEC-FIT, which has been used previously to study the mass functions of both giant molecular clouds and SSCs in galaxies in the local Universe (Rosolowsky et al. 2007; Messa et al. 2018). A best-fit value for  $N_t$  with a  $\geq 3\sigma$  significance will imply evidence for a truncation in the mass function at the truncation mass  $M_t$ . In Table 3 we list the best-fit values to the cumulative distribution function for all 5 LIRGs, the 3 early-stage systems, the 2 late-stage systems, and finally the inner- and outer-disk cluster samples which are labeled all, early, late, inner, and outer respectively.

In Figure 9 we show the best-fit PL (red) and PL+truncation (blue) models for the full sample. We find that clusters with ages  $t \leq 10^{7.5}$  yr have  $\alpha \sim -1.45 \pm 0.03$  and  $M_t = 10^{6.9} M_{\odot}$ . However at such high values of  $M_t$  our ability to constrain this upper-mass truncation becomes challenging due to the

low number of clusters expected above this limit. Indeed, apart from the All and Early-stage distributions, which each have a  $N_t/\sigma_{N_t} \sim 3$  and  $M_t \geq 10^6$ , we do not find evidence supporting a truncated power-law in any of the remaining sub-samples. Adamo et al. (2020) find evidence, albeit for 1/6 targets that the inclusion of older clusters with ages up to 100 Myr, can increase the significance of the PL+truncation model to  $\geq 3\sigma$ . However we do not find that including older clusters in any of our sub-samples increases the significance of the PL+truncation model such that we favor it over the simple PL model.

Examining the results for inner- and outer-disk clusters we see that the inner-disk clusters drive the trend seen in the larger dataset in support of a truncated power-law model. Given that the inner-disk has been shown to be a highly-disruptive environment for young clusters, it is not unexpected to find stronger evidence of a truncation. Overall, the PL models for the inner- and outer-disk clusters agree within uncertainties. This is consistent with detailed results for another well-studied LIRG, Arp 299, which show differences in the derived  $M_t$  of  $\leq$  a factor of 2 between the two galaxy nuclei and the extended disk (Randriamanakoto et al. 2019).

Finally, our value for the slope of the CMF is consistent with the slope of the luminosity functions derived from Pa $\beta$  observations of LIRGs in GOALS Larson et al. (2020). By comparison,  $\alpha$  is commonly measured to be  $-2$  for lower luminosity star-forming galaxies with an  $M_t \sim 10^{3-4} M_\odot$  (Bastian 2008; Larsen 2010). These results suggest that LIRGs are capable of forming relatively more massive clusters than what is seen in other nearby galaxies.

### 5.2.1. Merger Stage Dependence

Since U/LIRGs in the GOALS sample span the full range of merger stages, we can test if our explanation of cluster formation and destruction depends on the dynamical state of the galaxy. Haan et al. (2013), Kim et al. (2013), and Stierwalt et al. (2013) have classified the merger stage of each U/LIRG in the GOALS sample based on their morphological appearance at multiple wavelengths. These merger classification schemes run from pre-first passage to single coalesced nuclei. In order to search for changes in the cluster age and mass distributions as a function of merger stage, we separated our sample into early (classes 0-3: NGC 3256, IC 1623, NGC 7469) and late-stage (classes 4-6: Arp 220, NGC 6240) mergers. In Figure 10 we show the CMF for Regime 2 for both the early- and late-stage mergers and find that young star clusters in the early-stage show a power-law distribution of  $dN/dM \propto M^{-1.65 \pm 0.04}$  consis-

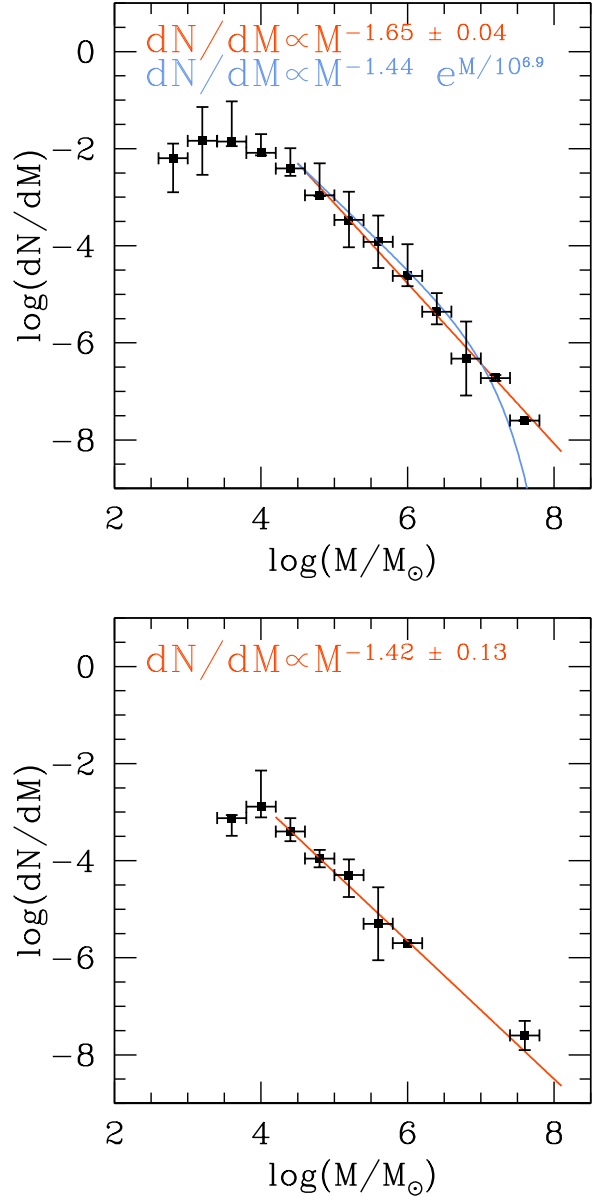


**Figure 10.** The mass distribution function for early- (top Panel) and late-stage (bottom Panel) mergers showing a flattening of the observed CMF. This result is consistent with the idea that the progressive destruction of lower-mass clusters (depending on the exact value of  $\delta$ ) flattens the observed CMF over time such that the late-stage mergers show a statistically flatter slope.

tent with the slope for the full sample. However, when examining the slope for the late-stage mergers we find that it appears flatter ( $\alpha = -1.42 \pm 0.13$ ). For the late-stage mergers we extend Regime 2 down to  $10^{4.2} M_\odot$  given that these systems are not used in the inner- and outer-disk comparison, and that many of the clusters live *outside* the MIR size defined for these systems. This

**Table 3.** Results From MSPECFIT for PL and PL+Truncation

Sample	$N_t$	$\sigma_{N_t}$	$M_t$	$\sigma_{M_t}$	$\alpha$	$\sigma_\alpha$
All	24.22	7.43	8.15e+06	5.74e+06	-1.45	0.03
All-PL	-	-	-	-	-1.66	0.03
Early	23.73	7.61	8.52e+06	2.51e+06	-1.45	0.03
Early-PL	-	-	-	-	-1.65	0.02
Late	0.491	2.02	6.62e+07	1.68e+07	-1.42	0.09
Late-PL	-	-	-	-	-1.42	0.13
Inner	32.83	13.3	6.38e+05	1.71e+06	-1.51	0.17
Inner-PL	-	-	-	-	-1.58	0.08
Outer	3.63	2.65	1.32e+07	1.18e+07	-1.60	0.06
Outer-PL	-	-	-	-	-1.65	0.06

NOTE— $N_t$  is the number of clusters more massive than  $2^{1/(\alpha+1)} M_t$ , where  $M_t$  is the truncation mass in the Schechter function given in  $M/M_\odot$ .  $\alpha$  is the slope of the PL or the PL component of the Schchter function. We note that a  $3\sigma$  significance for the PL+truncation model  $N_t/\sigma_{N_t}$  is only reached for the All and Early-stage cluster sub-samples.

result suggests that late-stage mergers may be able to form massive clusters with an even higher efficiency (increased proportion of higher-mass clusters formed) than what has been observed for LIRGs involved in early-stage mergers. Indeed, the two late-stage mergers are both ULIRGs with a median SFR that is  $\sim 2x$  higher than the early-stage mergers in our sample.

In order to quantify any differences in the age distributions for each merger stage we ran a KS-test comparing the normalized distributions of the early- and late-stage mergers to the total sample (see Figure 11). We find that within our sub-sample of 5 LIRGs there is a  $\sim 3\sigma$  difference in the age distribution of clusters between our early- and late-stage mergers, with the latter showing a much larger fraction of old massive clusters. As we have shown in Figure 8, these clusters are more likely to survive in the outer-disks of early-mergers, where the effect of tidal shocks is less severe compared to the inner-disks. Hence, the fact that we see a higher fraction of older clusters in late-stage mergers, where most clusters are found in the outer-disks, can be directly attributed to the higher survival rates of older clusters in the outer-disks that allow them to accumulate over the course of the merger.

Given the above, the data supports a scenario where the flat CMF for young clusters is due primarily to an increase in the formation of young massive clusters, which results in a flattened mass distribution in Regime 2 relative to the early-stage mergers. However there is a significant population of old massive clusters which have survived the progressive increase in the destruction of

lower-mass clusters (depending on the exact value of  $\delta$ ) throughout the course of the merger. Ultimately, higher SFRs, stronger tidal shocks, and increasing pressures throughout a galaxy merger all play a role in shaping the evolution of the cluster age and mass distributions relative to nearby low-luminosity star-forming galaxies.

## 6. SUMMARY

*Hubble Space Telescope* WFC3/UVIS (F336W) and ACS/WFC optical (F435W and F814W) observations for a sample of 10 LIRGs in the GOALS sample were obtained. These observations have been used to derive the ages, masses, and extinctions of the super star clusters contained within the 5 nearest systems in order to examine the cluster properties in extreme starburst environments relative to those in nearby, lower luminosity star-forming galaxies. The following conclusions are reached:

- (1) We have detected 1027 clusters throughout the disks of these 5 LIRGs. These clusters have  $S/N \geq 3$  in all three filters and de-convolved FWHMs as measured by ISHAPE of  $\leq 3$  pixels, corresponding to a median physical size of  $\sim 22$  pc.
- (2) The derived cluster age distribution implies a disruption rate of  $dN/d\tau \propto \tau^{-0.5+/-0.2}$  over  $10^{6.2} < \tau < 10^{8.7}$  and for cluster masses  $\geq 10^{5.2} M_\odot$ . This is consistent with the general framework that ongoing mergers destroy clusters at a much higher rate due to the high external pressure induced from a strong tidal field. The measured  $\gamma$  is steeper than what has been observed in

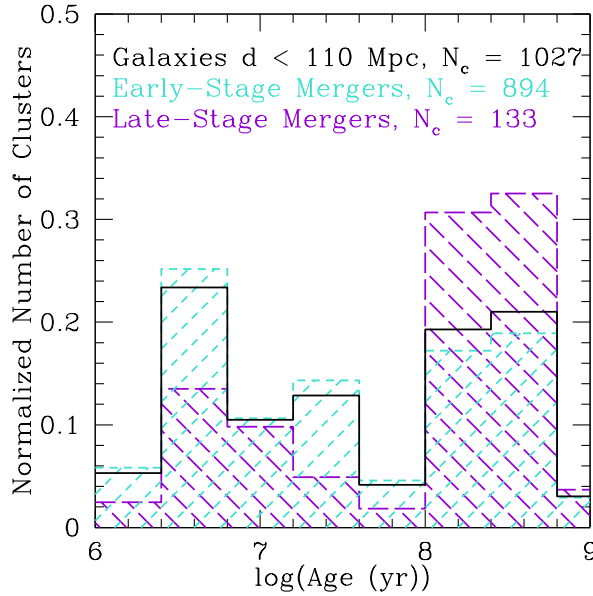


**Figure 11.** The binned cluster ages for early- and late-stage LIRGs normalized to the total number of clusters in each respective sub-sample. A KS-test reveals a  $3\sigma$  difference between the distribution of early- and late-stage cluster ages. This suggests that a significant evolution has taken place within the cluster population of the late-stage mergers.

lower-luminosity star-forming galaxies in the local Universe.

(3) Differences in the slope of the observed cluster age distribution between inner- and outer-disk clusters ( $\Delta\gamma \sim 0.7$ ) provides some of the clearest evidence to date of location-dependent cluster destruction, and that this destruction outweighs the increase in the CFR within the central region. Not only does this effect ap-

pear to be common in LIRGs, but the magnitude of this affect is amplified even relative to strong gradients of cluster disruption observed in normal star-forming galaxies in the local Universe.

(4) The derived cluster masses imply a CMF for our sample galaxies of  $dN/dM = M^{-1.66+/-0.03}$  with marginal evidence for a PL+truncation at  $M_t \sim 2 \times 10^6 M_\odot$  for early-stage mergers, which dominate the full sample. This trend appears to be driven in large part by the inner-disk, where the extreme environment acts to form massive clusters at a rate which exceeds expectations from a  $-2$  power-law at the highest masses.

The authors thank Matteo Messa for useful discussions regarding spatially-variable cluster completeness and assistance in running the LEGUS Cluster Completeness Tool on our dataset.

S.T.L was partially supported thorough NASA grant HST-GO15472. A.S.E. was supported by NSF grant AST 1816838 and by NASA through grants HST-GO10592.01-A, HST-GO11196.01-A, and HST-GO13364 from the Space Telescope Science Institute, which is operated by the Association of Universities for Research in Astronomy, Inc., under NASA contract NAS5- 26555. V.U acknowledges funding support from NASA Astrophysics Data Analysis Program (ADAP) Grant 80NSSC20K0450. HI acknowledges support from JSPS KAKENHI Grant Number JP21H01129. Finally, This research has made use of the NASA/IPAC Extragalactic Database (NED) which is operated by the Jet Propulsion Laboratory, California Institute of Technology, under contract with the National Aeronautics and Space Administration.

## REFERENCES

- Adamo, A. 2015, arXiv e-prints, arXiv:1511.05567
- Adamo, A., & Bastian, N. 2015, arXiv e-prints, arXiv:1511.08212
- Adamo, A., Ryon, J. E., Messa, M., et al. 2017, ApJ, 841, 131
- Adamo, A., Hollyhead, K., Messa, M., et al. 2020, MNRAS, 499, 3267
- Armus, L., Mazzarella, J. M., Evans, A. S., et al. 2009, PASP, 121, 559
- Barnes, A. T., Longmore, S. N., Dale, J. E., et al. 2020, MNRAS, 498, 4906
- Barnes, J. E. 2004, MNRAS, 350, 798
- Barnes, J. E., & Hernquist, L. 1992, ARA&A, 30, 705
- Bastian, N. 2008, MNRAS, 390, 759
- Bastian, N., Schweizer, F., Goudfrooij, P., Larsen, S. S., & Kissler-Patig, M. 2013, MNRAS, 431, 1252
- Bastian, N., Adamo, A., Gieles, M., et al. 2012, MNRAS, 419, 2606
- Bertelli, G., Bressan, A., Chiosi, C., Fagotto, F., & Nasi, E. 1994, A&AS, 106, 275
- Bertin, E., & Arnouts, S. 1996, A&AS, 117, 393
- Boutloukos, S. G., & Lamers, H. J. G. L. M. 2003, MNRAS, 338, 717
- Brown, G., & Gnedin, O. Y. 2021, arXiv e-prints, arXiv:2106.12420
- Brunetti, N., Wilson, C. D., Sliwa, K., et al. 2021, MNRAS, 500, 4730
- Calzetti, D., Armus, L., Bohlin, R. C., et al. 2000, ApJ, 533, 682

- Calzetti, D., Kinney, A. L., & Storchi-Bergmann, T. 1994, ApJ, 429, 582
- Chandar, R., Fall, S. M., & Whitmore, B. C. 2015, ApJ, 810, 1
- Chandar, R., Fall, S. M., Whitmore, B. C., & Mulia, A. J. 2017, ApJ, 849, 128
- Chandar, R., Mok, A., French, K. D., Smercina, A., & Smith, J.-D. T. 2021, arXiv e-prints, arXiv:2106.14883
- Chevance, M., Kruijssen, J. M. D., Krumholz, M. R., et al. 2020, arXiv e-prints, arXiv:2010.13788
- Cook, D. O., Dale, D. A., Lee, J. C., et al. 2016, MNRAS, 462, 3766
- Cook, D. O., Lee, J. C., Adamo, A., et al. 2019, MNRAS, 484, 4897
- Cortijo-Ferrero, C., González Delgado, R. M., Pérez, E., et al. 2017, A&A, 607, A70
- da Cunha, E., Charlot, S., & Elbaz, D. 2008, MNRAS, 388, 1595
- Daddi, E., Elbaz, D., Walter, F., et al. 2010, ApJL, 714, L118
- Davies, R. I., Tacconi, L. J., & Genzel, R. 2004, ApJ, 602, 148
- Dessauges-Zavadsky, M., & Adamo, A. 2018, MNRAS, 479, L118
- Deustua, S. E., Mack, J., Bowers, A. S., et al. 2016, UVIS 2.0 Chip-dependent Inverse Sensitivity Values, Space Telescope WFC Instrument Science Report
- Díaz-Santos, T., Alonso-Herrero, A., Colina, L., Ryder, S. D., & Knapen, J. H. 2007, ApJ, 661, 149
- Díaz-Santos, T., Charmandaris, V., Armus, L., et al. 2010, ApJ, 723, 993
- Elmegreen, B. G., Elmegreen, D. M., & Hirst, A. C. 2004, ApJ, 612, 191
- Elmegreen, B. G., & Hunter, D. A. 2010, ApJ, 712, 604
- Elmegreen, D. M., Elmegreen, B. G., Marcus, M. T., et al. 2009, ApJ, 701, 306
- Fall, S. M., & Chandar, R. 2012, ApJ, 752, 96
- Fall, S. M., Chandar, R., & Whitmore, B. C. 2005, ApJL, 631, L133
- Fitzpatrick, E. L. 1999, PASP, 111, 63
- Fouesneau, M., Lançon, A., Chandar, R., & Whitmore, B. C. 2012, ApJ, 750, 60
- Gieles, M. 2009, Ap&SS, 324, 299
- Gieles, M., Portegies Zwart, S. F., Baumgardt, H., et al. 2006, MNRAS, 371, 793
- Gieles, M., & Renaud, F. 2016, MNRAS, 463, L103
- Greve, T. R., Papadopoulos, P. P., Gao, Y., & Radford, S. J. E. 2009, ApJ, 692, 1432
- Grudić, M. Y., Kruijssen, J. M. D., Faucher-Giguère, C.-A., et al. 2020, arXiv e-prints, arXiv:2008.04453
- Haan, S., Armus, L., Surace, J. A., et al. 2013, MNRAS, 434, 1264
- Hinshaw, G., Larson, D., Komatsu, E., et al. 2013, ApJS, 208, 19
- Hollyhead, K., Adamo, A., Bastian, N., Gieles, M., & Ryon, J. E. 2016, MNRAS, 460, 2087
- Hopkins, P. F., Hernquist, L., Cox, T. J., et al. 2006, ApJS, 163, 1
- Howell, J. H., Armus, L., Mazzarella, J. M., et al. 2010, ApJ, 715, 572
- Hughes, A., Meidt, S. E., Schinnerer, E., et al. 2013, ApJ, 779, 44
- Jarrett, T. H., Chester, T., Cutri, R., et al. 2000, AJ, 119, 2498
- Johnson, L. C., Seth, A. C., Dalcanton, J. J., et al. 2017, ApJ, 839, 78
- Kennicutt, Jr., R. C. 1998, ARA&A, 36, 189
- Kewley, L. J., Rupke, D., Zahid, H. J., Geller, M. J., & Barton, E. J. 2010, ApJL, 721, L48
- Kim, D.-C., Evans, A. S., Vavilkin, T., et al. 2013, ApJ, 768, 102
- King, I. R. 1966, AJ, 71, 64
- Kobulnicky, H. A., & Johnson, K. E. 1999, ApJ, 527, 154
- Krause, M. G. H., Offner, S. S. R., Charbonnel, C., et al. 2020, SSRv, 216, 64
- Kruijssen, J. M. D. 2012, MNRAS, 426, 3008
- Kruijssen, J. M. D., & Bastian, N. 2016, MNRAS, 457, L24
- Kruijssen, J. M. D., Pelupessy, F. I., Lamers, H. J. G. L. M., Portegies Zwart, S. F., & Icke, V. 2011, MNRAS, 414, 1339
- Krumholz, M. R., McKee, C. F., & Bland-Hawthorn, J. 2019, ARA&A, 57, 227
- Lada, C. J., & Lada, E. A. 2003, ARA&A, 41, 57
- Lahén, N., Naab, T., Johansson, P. H., et al. 2020, ApJ, 891, 2
- Lamers, H. J. G. L. M., Gieles, M., & Portegies Zwart, S. F. 2005, A&A, 429, 173
- Larsen, S. S. 1999, A&AS, 139, 393
- . 2010, Philosophical Transactions of the Royal Society of London Series A, 368, 867
- Larson, K. L., Díaz-Santos, T., Armus, L., et al. 2020, ApJ, 888, 92
- Le Floc'h, E., Charmandaris, V., Laurent, O., et al. 2002, A&A, 391, 417
- Leitherer, C., Schaerer, D., Goldader, J. D., et al. 1999, ApJS, 123, 3
- Li, H., Gnedin, O. Y., Gnedin, N. Y., et al. 2017, ApJ, 834, 69
- Linden, S. T., Evans, A. S., Rich, J., et al. 2017, ApJ, 843, 91

- Linden, S. T., Song, Y., Evans, A. S., et al. 2019, ApJ, 881, 70
- Livermore, R. C., Jones, T. A., Richard, J., et al. 2015, MNRAS, 450, 1812
- Maoz, D., Barth, A. J., Ho, L. C., Sternberg, A., & Filippenko, A. V. 2001, AJ, 121, 3048
- Messa, M., Adamo, A., Calzetti, D., et al. 2018, MNRAS, 477, 1683
- Miholics, M., Kruijssen, J. M. D., & Sills, A. 2017, MNRAS, 470, 1421
- Moreno, J., Torrey, P., Ellison, S. L., et al. 2021, MNRAS, 503, 3113
- Papadopoulos, P. P., van der Werf, P. P., Xilouris, E. M., et al. 2012, MNRAS, 426, 2601
- Paturel, G., Petit, C., Prugniel, P., et al. 2003, A&A, 412, 45
- Pereira-Santaella, M., Alonso-Herrero, A., Colina, L., et al. 2015, A&A, 577, A78
- Pfeffer, J., Kruijssen, J. M. D., Crain, R. A., & Bastian, N. 2018, MNRAS, 475, 4309
- Portegies Zwart, S. F., McMillan, S. L. W., & Gieles, M. 2010, ARA&A, 48, 431
- Randriamanakoto, Z., Väistönen, P., Ryder, S. D., & Ranaivomanana, P. 2019, MNRAS, 482, 2530
- Reines, A. E., Nidever, D. L., Whelan, D. G., & Johnson, K. E. 2010, ApJ, 708, 26
- Renaud, F. 2020, in Star Clusters: From the Milky Way to the Early Universe, ed. A. Bragaglia, M. Davies, A. Sills, & E. Vesperini, Vol. 351, 40–46
- Rich, J. A., Kewley, L. J., & Dopita, M. A. 2011, ApJ, 734, 87
- Rosolowsky, E. 2005, PASP, 117, 1403
- Rosolowsky, E., Keto, E., Matsushita, S., & Willner, S. P. 2007, ApJ, 661, 830
- Ryon, J. E., Gallagher, J. S., Smith, L. J., et al. 2017, ApJ, 841, 92
- Saito, T., Iono, D., Yun, M. S., et al. 2015, ApJ, 803, 60
- Saito, T., Iono, D., Espada, D., et al. 2018, ApJ, 863, 129
- Schlafly, E. F., & Finkbeiner, D. P. 2011, ApJ, 737, 103
- Silva-Villa, E., Adamo, A., Bastian, N., Fouesneau, M., & Zackrisson, E. 2014, MNRAS, 440, L116
- Sirianni, M., Jee, M. J., Benítez, N., et al. 2005, PASP, 117, 1049
- Stierwalt, S., Armus, L., Surace, J. A., et al. 2013, arXiv:1302.4477, arXiv:1302.4477
- Sturm, E., González-Alfonso, E., Veilleux, S., et al. 2011, ApJL, 733, L16
- U., V., Sanders, D. B., Mazzarella, J. M., et al. 2012, ApJS, 203, 9
- Whitmore, B. C., Chandar, R., Bowers, A. S., et al. 2014, AJ, 147, 78
- Whitmore, B. C., Chandar, R., & Fall, S. M. 2007, AJ, 133, 1067
- Whitmore, B. C., Chandar, R., Schweizer, F., et al. 2010, AJ, 140, 75
- Wilson, C. D., Elmegreen, B. G., Bemis, A., & Brunetti, N. 2019, ApJ, 882, 5
- Zackrisson, E., Rydberg, C.-E., Schaerer, D., Östlin, G., & Tuli, M. 2011, ApJ, 740, 13

## APPENDIX

**Table 4.** Derived Properties of Individual Star Clusters

ID	R.A.	Decl.	$t_c$	$\sigma_{t_c}$	$M_c$	$\sigma_{M_c}$	$A_V$	$\sigma_{A_V}$
Arp 220								
1	233.746669054	23.480581701	8.73	0.13	9.02	0.05	4.50	0.22
2	233.729549053	23.475817413	8.02	0.38	7.07	0.19	0.80	0.31
3	233.748437605	23.482745482	9.00	0.42	6.49	0.11	0.90	0.65
4	233.751644007	23.484386024	8.26	0.09	6.65	0.05	0.60	0.13
5	233.764694288	23.492547085	8.73	0.15	7.83	0.05	3.40	0.24
6	233.728218353	23.482656154	6.48	0.35	5.16	0.37	3.00	1.02
7	233.732302621	23.484575842	6.97	0.02	5.32	0.05	2.10	0.10
8	233.731859917	23.486152064	8.26	0.27	5.49	0.14	0.80	0.23
9	233.725012898	23.486914452	8.73	0.12	7.92	0.05	3.60	0.21
10	233.728399990	23.488682409	6.97	0.07	4.05	0.00	0.80	0.23
11	233.732310801	23.490791224	6.01	0.10	3.54	0.09	0.20	0.16
12	233.758033822	23.501585925	6.48	0.35	5.25	0.38	2.70	1.02
13	233.743919183	23.499057830	8.69	0.11	5.98	0.04	0.50	0.19
14	233.746843168	23.500644635	8.69	0.11	6.01	0.04	0.40	0.19
15	233.748438076	23.502665246	8.22	0.10	7.06	0.06	0.60	0.12
16	233.739157505	23.500744091	8.17	0.44	4.93	0.28	0.00	0.26
17	233.737237343	23.500609511	7.08	0.45	4.40	0.30	0.60	1.09
18	233.739271698	23.502072103	8.73	0.16	6.44	0.06	1.30	0.28
19	233.744401079	23.503930925	8.73	0.09	6.41	0.04	0.50	0.17
20	233.714860863	23.496138256	8.22	0.37	5.16	0.24	0.40	0.23
21	233.744868069	23.504675138	8.55	0.06	5.77	0.04	0.00	0.11
22	233.740231300	23.503524840	6.79	0.27	4.27	0.33	0.00	0.12
23	233.738994708	23.504212786	8.49	0.23	6.17	0.07	1.20	0.37
24	233.736527312	23.503529566	8.33	0.25	5.89	0.07	0.80	0.34
25	233.759235564	23.510034123	6.30	0.60	6.19	0.38	3.70	1.11
26	233.736907112	23.504055439	8.51	0.06	5.66	0.04	0.00	0.11
27	233.755449114	23.509254099	7.95	0.37	4.81	0.21	0.30	0.28
28	233.736893783	23.504443701	8.35	0.24	6.55	0.06	0.80	0.37
29	233.740410868	23.506510571	8.69	0.11	5.97	0.04	0.30	0.19
30	233.741175276	23.507002973	8.71	0.14	6.16	0.05	0.60	0.24
31	233.737797927	23.507305089	8.28	0.09	6.38	0.05	0.30	0.13
32	233.737246993	23.506877228	6.79	0.35	3.85	0.21	0.90	0.29
33	233.736771854	23.506976292	8.37	0.07	5.65	0.04	0.10	0.11
34	233.739774525	23.507955558	8.69	0.12	5.99	0.04	0.30	0.21
35	233.740905432	23.508247391	8.57	0.12	5.44	0.05	0.10	0.16
36	233.739595349	23.510001954	8.40	0.08	6.13	0.04	0.10	0.12
37	233.739758003	23.510207087	8.28	0.08	5.64	0.04	0.10	0.10
38	233.739091396	23.510010435	8.46	0.06	5.64	0.04	0.00	0.12
39	233.743268929	23.511439049	8.69	0.16	6.66	0.05	1.50	0.27

*Table 4 continued*

**Table 4** (*continued*)

ID	R.A.	Decl.	$t_c$	$\sigma_{t_c}$	$M_c$	$\sigma_{M_c}$	$A_V$	$\sigma_{A_V}$
40	233.727476088	23.507374383	7.24	0.31	5.32	0.19	2.20	0.31
41	233.741596461	23.512409998	8.35	0.35	6.37	0.09	1.90	0.56
42	233.712641673	23.510708076	6.01	0.91	3.48	0.03	0.00	0.24
43	233.715786536	23.512925158	6.61	0.55	4.10	0.29	1.60	0.78
44	233.712782544	23.510291460	7.15	0.34	4.21	0.23	0.70	0.35
45	233.723315397	23.517722087	8.11	0.22	7.80	0.13	0.90	0.17
46	233.729693112	23.518352156	8.37	0.33	5.94	0.08	1.40	0.51
IC 1623								
1	16.956330436	-17.512001234	7.13	0.54	4.57	0.20	0.40	1.06
2	16.952532574	-17.506213564	7.15	0.31	4.27	0.18	0.20	0.35
3	16.952056299	-17.506413601	8.69	0.11	5.80	0.05	0.10	0.18
4	16.950488627	-17.503461826	7.46	0.27	4.88	0.13	0.40	0.28
5	16.951049126	-17.504863361	7.13	0.53	4.59	0.25	0.30	1.06
6	16.950682091	-17.503408300	6.97	0.02	4.18	0.06	0.30	0.13
7	16.950863906	-17.505510101	8.13	0.17	6.74	0.10	0.30	0.15
8	16.951187415	-17.504873247	8.06	0.39	4.82	0.25	0.00	0.25
9	16.951016387	-17.504706370	7.15	0.35	4.05	0.34	0.10	0.39
10	16.950953107	-17.505277867	6.79	0.28	3.88	0.34	0.10	0.08
11	16.950933284	-17.505083708	6.79	0.27	3.99	0.33	0.00	0.01
12	16.951712337	-17.506958854	8.26	0.13	5.53	0.08	0.20	0.13
13	16.950656373	-17.506143697	8.69	0.17	5.92	0.06	0.60	0.30
14	16.950439886	-17.505528995	8.26	0.34	5.57	0.21	0.40	0.26
15	16.951137759	-17.506609878	8.22	0.48	5.05	0.33	0.00	0.07
16	16.951057446	-17.506948375	6.48	0.16	5.15	0.10	1.90	0.36
17	16.950684474	-17.505765956	8.28	0.41	5.45	0.25	0.40	0.33
18	16.951081971	-17.506765096	6.01	0.47	3.83	0.28	1.10	0.45
19	16.950331622	-17.505568794	7.13	0.58	4.28	0.45	0.50	0.65
20	16.950383338	-17.505899273	6.79	0.31	3.83	0.30	0.20	0.14
21	16.950139217	-17.505923913	8.08	0.39	5.63	0.20	0.40	0.28
22	16.950317584	-17.506007153	8.55	0.05	5.71	0.04	0.00	0.06
23	16.950673781	-17.506899767	8.31	0.33	5.12	0.24	0.00	0.00
24	16.950229093	-17.505925623	8.40	0.14	5.34	0.12	0.00	0.03
25	16.950195881	-17.509102603	6.70	0.11	5.56	0.09	0.70	0.27
26	16.950391225	-17.509086287	8.35	0.43	5.21	0.31	0.00	0.04
27	16.950163349	-17.508897779	7.24	0.26	4.40	0.28	0.00	0.05
28	16.949651745	-17.507838234	6.01	0.70	4.49	0.15	1.80	0.91
29	16.948344739	-17.505423525	8.08	0.27	5.61	0.17	0.30	0.20
30	16.948445615	-17.506098875	7.02	0.08	5.00	0.14	0.40	0.22
31	16.948484736	-17.506534316	7.28	1.13	6.72	0.61	3.60	1.17
32	16.948102147	-17.505207847	6.61	0.12	4.26	0.12	0.70	0.32
33	16.949389027	-17.507903630	7.24	0.27	4.37	0.12	0.20	0.13
34	16.949829329	-17.508651885	6.70	0.41	3.72	0.26	0.50	0.39
35	16.948317672	-17.505563534	7.37	0.48	4.53	0.42	1.00	0.42
36	16.947889794	-17.507043198	6.97	0.02	7.02	0.06	4.50	0.11
37	16.947965298	-17.506198813	6.79	0.26	4.22	0.31	0.00	0.64

*Table 4 continued*

**Table 4** (*continued*)

ID	R.A.	Decl.	$t_c$	$\sigma_{t_c}$	$M_c$	$\sigma_{M_c}$	$A_V$	$\sigma_{A_V}$
38	16.947752490	-17.507483910	8.28	0.70	7.65	0.36	3.80	0.86
39	16.947385263	-17.505449009	6.61	0.10	4.52	0.10	0.90	0.13
40	16.946678280	-17.504533764	7.22	0.08	5.08	0.06	0.30	0.14
41	16.947975960	-17.507050693	6.61	0.45	5.04	0.22	1.70	0.88
42	16.946567042	-17.504677056	6.61	0.12	5.30	0.09	1.00	0.30
43	16.947791506	-17.507128658	6.97	0.04	6.12	0.91	4.00	0.24
44	16.946996936	-17.507414550	7.42	0.27	7.10	0.13	0.80	0.27
45	16.947713167	-17.508250172	8.28	0.41	5.49	0.27	0.20	0.36
46	16.947014010	-17.505451289	7.51	0.27	4.77	0.14	0.20	0.27
47	16.949012988	-17.511146341	7.42	0.27	5.36	0.13	0.70	0.27
48	16.946722658	-17.507154505	6.70	0.09	5.24	0.10	0.60	0.12
49	16.946652113	-17.506442294	6.70	0.08	5.83	0.07	0.20	0.09
50	16.944873609	-17.505209805	6.30	0.26	5.28	0.04	1.70	0.09
51	16.948484203	-17.509902320	6.79	0.29	4.04	0.29	0.40	0.18
52	16.945688780	-17.503468736	6.79	0.03	3.77	0.03	0.00	0.27
53	16.948655346	-17.510695392	6.70	0.08	4.11	0.08	0.20	0.10
54	16.947880191	-17.508878486	6.79	0.26	4.00	0.19	0.60	0.20
55	16.946114235	-17.505040886	6.61	0.15	4.06	0.10	0.90	0.33
56	16.945860762	-17.504741111	6.79	0.03	3.89	0.09	0.00	0.04
57	16.946733243	-17.507569505	8.71	0.10	8.20	0.05	3.70	0.18
58	16.946536243	-17.506641279	6.61	0.15	5.50	0.09	1.20	0.32
59	16.945716058	-17.505028645	6.70	0.13	4.36	0.11	0.90	0.33
60	16.946422010	-17.506539383	6.97	0.56	4.25	0.83	0.60	0.98
61	16.946094439	-17.506846826	6.70	0.12	5.52	0.09	1.00	0.29
62	16.948518639	-17.511750047	8.02	0.37	5.82	0.18	0.10	0.32
63	16.946953432	-17.507883215	7.48	0.93	5.65	0.40	1.90	0.94
64	16.945965265	-17.505289185	7.46	0.53	4.56	0.18	1.00	0.44
65	16.945540057	-17.505167563	7.22	0.37	5.28	0.23	2.00	0.31
66	16.948142799	-17.510880461	6.48	0.14	5.03	0.09	1.30	0.31
67	16.946493149	-17.506889534	7.24	0.40	4.13	0.26	0.10	0.37
68	16.948062477	-17.511049327	7.24	0.03	4.82	0.05	0.10	0.02
69	16.946682984	-17.508136495	6.01	0.58	5.05	0.28	3.10	0.98
70	16.945234499	-17.505439446	6.61	0.36	4.77	0.11	1.30	0.78
71	16.945969821	-17.506759715	6.70	0.10	5.92	0.09	1.00	0.14
72	16.947901658	-17.510545063	7.24	0.25	4.34	0.31	0.00	0.10
73	16.946530267	-17.508011460	6.48	0.46	5.50	0.36	3.20	1.05
74	16.946643097	-17.507983442	7.13	0.51	4.47	0.25	0.10	1.01
75	16.944692419	-17.504623460	7.33	0.21	5.09	0.10	0.40	0.18
76	16.946320608	-17.508471490	6.30	0.58	5.19	0.35	2.40	1.09
77	16.947062861	-17.509181492	6.79	0.35	4.22	0.21	0.80	0.23
78	16.945398036	-17.506120962	7.73	0.27	6.41	0.13	0.60	0.27
79	16.944434232	-17.506128945	7.42	0.27	6.49	0.13	0.40	0.27
80	16.944936624	-17.505436674	8.73	0.11	6.82	0.04	0.00	0.15
81	16.945624964	-17.506315582	6.70	0.08	5.31	0.07	0.00	0.15
82	16.946032944	-17.507331770	7.02	0.45	4.96	0.25	0.10	0.99
83	16.946058840	-17.507798293	7.46	0.49	5.38	0.58	1.10	0.43
84	16.945808445	-17.506932406	6.01	0.50	5.46	0.22	2.00	1.00

Table 4 continued

**Table 4** (*continued*)

ID	R.A.	Decl.	$t_c$	$\sigma_{t_c}$	$M_c$	$\sigma_{M_c}$	$A_V$	$\sigma_{A_V}$
85	16.945360563	-17.506399314	6.48	0.32	5.04	0.11	1.50	0.38
86	16.945514157	-17.506409280	7.24	0.26	5.90	0.28	0.00	0.38
87	16.945939568	-17.507243124	7.26	0.15	5.84	0.08	0.50	0.17
88	16.946139734	-17.508346754	6.48	0.23	5.86	0.06	1.40	0.18
89	16.945122304	-17.506508861	6.48	0.15	5.86	0.08	1.10	0.31
90	16.945855697	-17.507263000	6.70	0.33	5.53	0.11	1.20	0.55
91	16.944892946	-17.506046744	6.61	0.33	5.32	0.10	1.20	0.42
92	16.945022553	-17.505606732	6.70	0.07	4.75	0.08	0.30	0.11
93	16.947831523	-17.512134698	8.20	0.50	5.20	0.37	0.00	0.14
94	16.944425198	-17.504560418	6.70	0.40	4.87	0.33	2.40	0.39
95	16.944753197	-17.506384457	6.79	0.03	5.31	0.04	0.00	0.20
96	16.947549999	-17.511920170	8.00	0.36	5.33	0.18	0.10	0.31
97	16.944749356	-17.506748533	8.44	0.15	6.30	0.08	0.20	0.20
98	16.944415486	-17.504935321	6.61	0.14	4.54	0.09	0.50	0.31
99	16.945682285	-17.508713991	7.15	0.47	5.66	0.18	0.00	0.64
100	16.946192902	-17.508672591	8.06	0.46	5.17	0.65	0.40	0.41
101	16.944848869	-17.506457859	6.48	0.14	5.79	0.09	0.90	0.31
102	16.943471002	-17.505395744	6.97	0.04	4.74	0.07	0.60	0.10
103	16.944580305	-17.506042845	6.48	0.57	5.95	0.33	2.50	0.83
104	16.945235468	-17.507243388	6.30	0.26	6.00	0.05	1.50	0.11
105	16.944710276	-17.506542753	6.30	0.26	5.97	0.05	1.20	0.10
106	16.944844406	-17.507312092	6.79	0.26	5.15	0.31	0.00	0.16
107	16.945296523	-17.506960602	7.02	0.08	4.92	0.11	0.00	0.02
108	16.946047398	-17.508618200	8.44	0.08	5.51	0.07	0.00	0.10
109	16.944501877	-17.505892939	7.15	0.49	5.54	0.21	0.10	0.50
110	16.945074374	-17.507305903	6.01	0.62	5.41	0.12	1.30	0.19
111	16.944467245	-17.506601687	7.51	0.26	6.19	0.12	0.50	0.27
112	16.946774065	-17.510866373	6.61	0.10	4.39	0.10	0.80	0.13
113	16.943929110	-17.504871749	6.01	0.39	5.22	0.04	1.50	0.09
114	16.944291472	-17.506016274	6.48	0.53	5.69	0.15	1.80	0.84
115	16.944198148	-17.507259813	7.15	0.28	6.35	0.17	1.00	0.35
116	16.944767385	-17.507737361	7.08	0.18	6.63	0.13	0.00	1.74
117	16.946010694	-17.509611770	8.42	0.17	5.55	0.09	0.20	0.15
118	16.945032031	-17.507254109	7.08	0.84	5.21	0.15	0.00	0.78
119	16.943871004	-17.505334561	8.17	0.13	5.77	0.11	0.00	0.44
120	16.945326160	-17.508278668	6.48	0.15	4.45	0.10	0.90	0.34
121	16.943687458	-17.505791646	6.70	0.48	5.80	0.19	1.40	0.63
122	16.944623235	-17.506899815	6.70	0.48	6.26	0.18	1.40	0.63
123	16.944737164	-17.507514185	6.97	0.04	5.34	0.09	0.10	0.09
124	16.943009665	-17.506280105	8.73	0.18	6.14	0.06	0.50	0.29
125	16.944699230	-17.507424096	6.01	0.46	5.81	0.08	1.80	0.17
126	16.945240974	-17.508384781	8.33	0.10	5.99	0.05	0.30	0.15
127	16.945078484	-17.509080892	6.79	0.28	4.29	0.33	0.10	0.05
128	16.944550912	-17.506899307	7.53	0.25	6.44	0.11	0.20	0.27
129	16.943699249	-17.504821909	6.79	0.30	3.72	0.40	0.40	0.22
130	16.943485251	-17.504766311	6.70	0.53	4.46	0.21	1.30	0.58
131	16.943702074	-17.505030635	6.61	0.15	4.74	0.10	1.30	0.33

*Table 4 continued*

**Table 4** (*continued*)

ID	R.A.	Decl.	$t_c$	$\sigma_{t_c}$	$M_c$	$\sigma_{M_c}$	$A_V$	$\sigma_{A_V}$
132	16.943916325	-17.506141272	6.79	0.26	5.83	0.32	0.00	0.02
133	16.944482053	-17.506867448	8.06	0.38	6.70	0.21	0.70	0.29
134	16.943252755	-17.504826992	8.51	0.28	6.04	0.08	1.00	0.43
135	16.944059029	-17.506634288	8.13	0.45	6.75	0.24	1.00	0.38
136	16.945999240	-17.510729997	6.70	0.13	4.67	0.09	0.50	0.30
137	16.943626127	-17.505234155	6.79	0.21	4.14	0.20	0.50	0.18
138	16.943578710	-17.504686369	6.79	0.29	3.71	0.17	0.10	0.13
139	16.944882397	-17.508939808	7.22	0.11	6.14	0.05	0.40	0.16
140	16.946261540	-17.511191572	6.79	0.26	3.63	0.31	0.00	0.07
141	16.945888173	-17.510898407	6.61	0.10	4.80	0.08	0.50	0.13
142	16.945148530	-17.510137217	6.70	0.31	5.30	0.37	1.70	0.79
143	16.944775647	-17.509316346	6.97	0.02	4.47	0.06	0.70	0.13
144	16.945398735	-17.509884292	8.13	0.22	5.37	0.14	0.00	0.02
145	16.943802331	-17.507003457	6.48	0.35	6.07	0.38	2.30	1.02
146	16.943217574	-17.506867444	8.69	0.13	6.13	0.05	0.30	0.23
147	16.943650953	-17.506660386	7.22	0.20	5.28	0.13	0.50	0.18
148	16.945681364	-17.510859147	7.26	0.03	5.11	0.05	0.00	0.04
149	16.944146393	-17.507657768	7.02	0.87	4.57	0.16	0.00	0.77
150	16.944736845	-17.509010897	6.70	0.37	4.67	0.14	0.90	0.52
151	16.945048246	-17.509489327	6.70	0.43	3.47	0.31	0.20	0.36
152	16.944838317	-17.509998763	7.88	0.33	4.74	0.22	0.00	0.26
153	16.944691762	-17.509672621	6.70	0.10	4.39	0.11	0.80	0.15
154	16.942905487	-17.507047512	6.70	0.09	6.15	0.07	0.10	0.07
155	16.943705718	-17.508325068	7.53	0.20	5.36	0.09	0.00	0.18
156	16.944097663	-17.509111084	6.70	0.50	4.77	0.23	1.60	0.73
157	16.944035899	-17.508439526	6.70	0.12	4.45	0.10	0.30	0.31
158	16.942886937	-17.508040845	6.70	0.08	6.57	0.07	0.20	0.09
159	16.943567475	-17.507738466	7.24	0.32	4.77	0.24	0.00	0.25
160	16.943638596	-17.508676774	8.04	0.41	5.62	0.24	0.70	0.32
161	16.943309351	-17.508043026	6.70	0.10	5.64	0.09	0.50	0.01
162	16.943509235	-17.508245022	6.48	0.06	4.80	0.05	0.10	0.06
163	16.943487445	-17.508182486	6.70	0.09	4.96	0.09	0.00	0.01
164	16.942628052	-17.506668043	8.73	0.12	5.81	0.05	0.10	0.21
165	16.943070594	-17.507890030	6.79	0.26	5.60	0.30	0.00	1.50
166	16.943507240	-17.509586501	6.48	0.21	4.91	0.08	1.60	0.29
167	16.943218679	-17.508114808	6.79	0.26	4.65	0.30	0.00	0.24
168	16.943625620	-17.509217601	7.33	0.21	4.36	0.22	0.10	0.21
169	16.942244586	-17.506579230	8.00	0.37	5.29	0.20	0.00	0.22
170	16.942573217	-17.507897826	6.61	0.17	5.01	0.10	1.20	0.36
171	16.943492065	-17.509226702	7.97	0.48	5.38	0.36	0.90	0.39
172	16.942853625	-17.509161495	7.46	0.26	5.58	0.12	0.80	0.27
173	16.941825546	-17.506694949	6.79	0.72	4.04	0.54	0.60	0.30
174	16.942144905	-17.507960677	7.15	0.50	4.64	0.37	1.10	0.47
175	16.942311938	-17.508462330	7.46	0.52	4.26	0.51	0.00	0.39
176	16.941812747	-17.507915887	8.15	0.45	4.85	0.33	0.00	0.23
177	16.941798439	-17.508212173	8.28	0.12	5.30	0.10	0.00	0.03
178	16.937643223	-17.502271807	7.24	0.31	4.48	0.12	0.20	0.41

*Table 4 continued*

**Table 4** (*continued*)

ID	R.A.	Decl.	$t_c$	$\sigma_{t_c}$	$M_c$	$\sigma_{M_c}$	$A_V$	$\sigma_{A_V}$
179	16.937748789	-17.502161950	7.33	0.09	4.08	0.14	0.00	0.12
180	16.939126424	-17.507439554	6.30	0.58	5.49	0.20	2.40	1.07
IRAS14378-3651								
1	220.245188574	-37.079012817	8.73	0.11	9.36	0.05	3.90	0.19
2	220.245601058	-37.076101935	8.17	0.07	6.80	0.06	0.00	0.15
3	220.245991264	-37.075613240	7.15	0.24	8.82	0.29	4.30	0.20
4	220.253339337	-37.068994414	8.71	0.10	9.91	0.04	2.70	0.17
5	220.252564206	-37.065958219	8.75	0.14	9.01	0.05	1.80	0.23
6	220.251577818	-37.065198208	7.53	0.25	6.24	0.12	0.40	0.26
7	220.251021993	-37.064251976	6.61	0.31	5.96	0.37	1.80	0.79
8	220.251849954	-37.063106953	6.70	0.34	6.38	0.17	0.70	0.26
9	220.252769577	-37.062017270	6.79	0.36	7.67	0.19	2.00	0.31
10	220.247466409	-37.064321421	8.26	0.09	9.29	0.05	0.60	0.12
11	220.234749361	-37.069964277	8.98	0.36	8.55	0.09	1.20	0.55
IRASF08572+3915								
1	135.104376272	39.065192661	8.15	0.26	6.09	0.17	0.20	0.18
2	135.105338178	39.064726566	6.30	0.48	5.66	0.30	2.20	1.03
3	135.107809889	39.062810319	6.70	0.34	5.39	0.17	0.70	0.29
4	135.107890839	39.062914247	6.79	0.29	4.89	0.33	0.30	0.17
5	135.107963073	39.062689830	6.48	0.25	5.20	0.07	1.50	0.25
6	135.109960161	39.063250810	7.30	0.24	5.80	0.12	0.50	0.20
7	135.109564681	39.063170540	6.61	0.14	5.41	0.09	1.00	0.31
8	135.110918073	39.063011108	6.48	0.23	4.84	0.14	1.20	0.40
IRASF12112+0305								
1	183.444389005	2.808148590	7.97	0.37	7.71	0.19	0.80	0.31
2	183.442171690	2.809289987	6.48	0.39	6.48	0.36	2.40	1.04
3	183.443025620	2.809631292	7.08	1.07	5.18	0.16	0.00	0.79
4	183.441938663	2.809256343	7.75	0.26	5.97	0.13	0.00	0.23
5	183.441748544	2.809609326	6.01	0.23	6.15	0.03	1.70	0.10
6	183.441794866	2.809499470	8.06	0.39	6.47	0.21	0.20	0.34
7	183.442343064	2.810497195	6.61	0.13	5.75	0.09	1.00	0.30
8	183.440951228	2.809444908	6.48	0.26	5.13	0.14	0.90	0.37
9	183.442252824	2.810559867	6.61	0.46	5.78	0.40	1.80	0.79
10	183.442462829	2.811423844	8.46	0.07	7.39	0.04	0.00	0.04
11	183.442227065	2.811234192	6.48	0.35	6.86	0.36	3.00	1.03
12	183.440905977	2.810949464	7.53	0.28	6.40	0.14	1.00	0.27
13	183.442451914	2.811659334	8.08	0.39	6.98	0.21	0.60	0.29
14	183.439770379	2.810306124	6.70	0.10	5.66	0.11	1.10	0.17
15	183.442932505	2.811755486	6.86	0.32	5.41	0.36	0.60	0.81
16	183.442623709	2.812045792	8.15	0.10	6.84	0.07	0.10	0.05
17	183.442276125	2.811961758	7.26	0.08	5.73	0.07	0.30	0.13
18	183.441649964	2.811871181	7.24	0.09	5.89	0.07	0.40	0.15

*Table 4 continued*

**Table 4** (*continued*)

ID	R.A.	Decl.	$t_c$	$\sigma_{t_c}$	$M_c$	$\sigma_{M_c}$	$A_V$	$\sigma_{A_V}$
19	183.442957512	2.812775989	7.22	0.23	6.08	0.12	0.60	0.21
20	183.439372320	2.811241919	6.01	0.48	5.33	0.13	1.60	0.85
21	183.443162665	2.813415484	8.22	0.09	6.34	0.06	0.00	0.18
22	183.443092592	2.813436515	6.79	0.30	5.26	0.27	0.50	0.20
23	183.443106795	2.813654752	7.53	0.19	6.39	0.08	0.00	0.17
24	183.443220359	2.813746669	7.13	0.57	5.58	0.18	0.10	1.03
25	183.439802170	2.813516804	6.79	0.28	4.71	0.33	0.10	0.04
IRASF17207-0014								
1	260.837198269	-0.287979491	8.13	0.56	8.54	0.19	1.40	0.72
2	260.842028703	-0.283223436	8.69	0.13	6.99	0.07	0.20	0.24
3	260.842545441	-0.284283076	8.28	0.10	6.94	0.05	0.60	0.14
4	260.842200429	-0.282861509	8.28	0.09	7.71	0.05	0.70	0.13
5	260.841597178	-0.283210990	8.17	0.78	8.32	0.39	3.10	0.91
6	260.841699543	-0.283259702	8.02	0.37	7.42	0.19	0.60	0.32
7	260.841837898	-0.283231376	8.24	0.45	7.77	0.13	1.30	0.65
8	260.841058401	-0.283173502	8.37	0.31	7.61	0.07	1.70	0.48
9	260.836341192	-0.281360948	8.17	0.45	8.86	0.13	1.20	0.60
Mrk 231 - Center								
1	194.059834915	56.874131763	8.60	0.09	7.59	0.04	0.1	0.12
2	194.059833841	56.873642959	7.15	0.49	6.91	0.18	1.0	0.62
Mrk 231 - Extended Galaxy								
1	194.062618168	56.875447094	8.73	0.10	6.41	0.04	0.00	0.14
2	194.059362818	56.875227717	8.73	0.09	7.89	0.04	2.10	0.15
3	194.062816723	56.874502731	8.31	0.11	6.17	0.06	0.30	0.14
4	194.050987104	56.876546488	7.59	0.29	5.94	0.16	1.20	0.28
5	194.058132336	56.874168111	8.69	0.11	7.84	0.04	1.70	0.19
6	194.060359373	56.873286213	7.39	0.33	6.24	0.20	1.10	0.33
7	194.055163293	56.873972517	8.49	0.14	6.93	0.04	0.40	0.22
8	194.060152531	56.872853822	8.11	0.26	7.49	0.16	0.40	0.19
9	194.054717691	56.873982656	8.71	0.11	6.40	0.05	0.00	0.16
10	194.060334669	56.872920241	6.86	0.52	5.14	0.23	0.00	0.83
11	194.059504658	56.872859932	8.69	0.24	7.02	0.07	0.80	0.39
12	194.059790383	56.872658683	8.06	0.25	6.75	0.15	0.20	0.18
13	194.060201324	56.872544918	8.13	0.43	6.09	0.31	0.20	0.37
14	194.058896215	56.872460715	8.51	0.06	6.73	0.05	0.00	0.04
15	194.058929716	56.872678827	8.04	0.38	7.36	0.19	0.20	0.29
16	194.059507661	56.872436584	6.97	0.09	5.66	0.16	0.50	0.16
17	194.059782501	56.872528884	6.61	0.55	4.94	0.27	0.70	0.60
18	194.056184871	56.872672378	8.71	0.13	6.80	0.05	0.10	0.21
19	194.051681795	56.873287796	6.97	0.50	4.18	0.98	0.00	0.99
20	194.058323461	56.872196389	6.79	0.28	3.98	0.33	0.00	0.10
21	194.056634064	56.872152713	8.73	0.11	6.55	0.05	0.30	0.20

*Table 4 continued*

**Table 4** (*continued*)

ID	R.A.	Decl.	$t_c$	$\sigma_{t_c}$	$M_c$	$\sigma_{M_c}$	$A_V$	$\sigma_{A_V}$
22	194.058427778	56.870652081	8.35	0.10	7.19	0.04	0.30	0.15
23	194.057168387	56.870623558	8.44	0.06	6.55	0.01	0.00	0.03
24	194.053721360	56.871088503	8.53	0.08	6.69	0.04	0.10	0.10
25	194.053865501	56.870639610	8.33	0.12	6.92	0.05	0.50	0.18
26	194.054559180	56.870334239	6.61	0.58	4.71	0.24	1.40	0.68
27	194.053851480	56.869025517	8.40	0.09	7.32	0.04	0.20	0.14
28	194.050822057	56.867598372	6.48	0.50	5.27	0.30	2.60	0.97
NGC 3256								
1	156.938847659	-43.920972207	8.22	0.09	6.22	0.05	0.70	0.12
2	156.937446200	-43.917401271	8.71	0.10	8.42	0.04	1.40	0.17
3	156.957457643	-43.926641923	8.73	0.11	8.29	0.04	3.40	0.19
4	156.953743483	-43.924400772	8.71	0.16	7.57	0.05	1.60	0.26
5	156.960454492	-43.926141908	8.08	0.38	6.98	0.19	0.70	0.28
6	156.957522591	-43.922692436	8.73	0.11	8.26	0.04	3.60	0.18
7	156.975540763	-43.929940669	8.44	0.07	7.54	0.04	0.00	0.04
8	156.976180843	-43.930211531	9.11	0.45	6.42	0.13	0.00	0.64
9	156.951006734	-43.918937971	8.73	0.17	8.22	0.05	4.10	0.27
10	156.941274253	-43.913136873	8.69	0.12	7.68	0.04	1.10	0.21
11	156.947146751	-43.916398824	8.73	0.07	8.18	0.05	4.80	0.12
12	156.969133450	-43.926195523	7.24	0.29	3.65	0.11	0.20	0.19
13	156.934232358	-43.910484466	8.69	0.13	7.67	0.05	1.80	0.22
14	156.978953832	-43.929530068	8.73	0.13	7.97	0.05	2.00	0.22
15	156.972192682	-43.926971948	6.01	-0.28	3.77	0.04	1.30	0.13
16	156.938411006	-43.911223207	8.13	0.13	6.89	0.08	1.20	0.15
17	156.953085895	-43.917519337	9.11	0.48	6.76	0.13	0.20	0.70
18	156.961177901	-43.919181476	8.66	0.07	7.32	0.04	0.00	0.05
19	156.934842777	-43.908153361	8.71	0.12	8.23	0.04	4.60	0.19
20	156.933409124	-43.906790552	8.57	0.18	7.61	0.05	0.90	0.29
21	156.954905210	-43.916107035	8.17	0.11	6.84	0.07	1.00	0.12
22	156.967620549	-43.921105889	8.71	0.09	8.00	0.04	2.40	0.15
23	156.943175045	-43.910562994	8.84	0.21	7.58	0.06	1.50	0.33
24	156.947636840	-43.911595838	8.06	0.91	6.15	0.46	2.70	1.03
25	156.947663413	-43.908459000	8.26	0.48	8.19	0.13	1.60	0.72
26	156.936365470	-43.905141536	8.69	0.08	5.29	0.04	0.00	0.08
27	156.946899705	-43.907988212	8.53	0.18	8.35	0.05	4.00	0.29
28	156.931227420	-43.902400664	7.15	0.28	3.80	0.16	0.50	0.32
29	156.953425523	-43.911555290	8.71	0.11	5.32	0.04	0.20	0.20
30	156.961788530	-43.915101580	7.91	0.33	4.98	0.17	0.90	0.30
31	156.933535569	-43.902180171	6.97	0.07	4.11	0.12	1.20	0.13
32	156.946148173	-43.907201601	8.71	0.11	7.46	0.04	2.50	0.18
33	156.973924613	-43.919265812	8.15	0.71	6.30	0.37	1.80	0.85
34	156.933574505	-43.901973654	7.46	0.25	4.23	0.12	0.50	0.27
35	156.960374620	-43.913018658	8.49	0.10	5.06	0.04	0.20	0.13
36	156.954365756	-43.910045670	8.95	0.32	8.13	0.08	0.10	0.50
37	156.971677577	-43.917552504	6.01	0.25	3.62	0.14	1.20	0.25

*Table 4 continued*

**Table 4** (*continued*)

ID	R.A.	Decl.	$t_c$	$\sigma_{t_c}$	$M_c$	$\sigma_{M_c}$	$A_V$	$\sigma_{A_V}$
38	156.957924474	-43.911597032	8.37	0.10	4.92	0.05	0.20	0.14
39	156.959465854	-43.911976787	8.26	0.13	4.90	0.07	0.50	0.14
40	156.959654875	-43.911901799	7.93	0.31	5.03	0.16	0.00	0.25
41	156.954943420	-43.909491213	8.17	0.11	4.76	0.07	0.10	0.08
42	156.964932400	-43.912538428	6.97	0.02	7.06	0.04	1.30	0.12
43	156.957011995	-43.910484188	6.48	0.15	3.37	0.11	1.00	0.36
44	156.955339665	-43.909379987	7.33	0.33	4.26	0.17	0.80	0.30
45	156.959063971	-43.910986676	8.35	0.10	4.94	0.05	0.20	0.14
46	156.955491309	-43.909190278	6.79	0.03	3.39	0.02	0.00	0.40
47	156.954115513	-43.908614519	8.71	0.09	5.11	0.04	0.00	0.11
48	156.959160782	-43.910773809	6.61	0.16	2.87	0.14	0.20	0.38
49	156.956716871	-43.909719000	6.30	0.25	3.88	0.06	1.80	0.12
50	156.953817730	-43.908000671	8.55	0.08	5.34	0.04	0.00	0.07
51	156.955823530	-43.909210608	7.28	0.32	3.91	0.20	0.70	0.29
52	156.956035377	-43.908950528	6.79	0.30	3.75	0.28	0.50	0.20
53	156.956535206	-43.909240475	8.53	0.12	5.35	0.04	0.30	0.19
54	156.960319423	-43.910703313	7.46	0.24	4.53	0.11	0.20	0.27
55	156.956062448	-43.909092456	8.15	0.16	4.87	0.10	0.10	0.14
56	156.959449515	-43.910429753	8.15	0.10	5.23	0.06	0.50	0.12
57	156.948292671	-43.902586623	7.24	0.25	7.67	0.12	1.40	0.26
58	156.956851859	-43.908911927	6.01	0.34	4.61	0.03	1.50	0.09
59	156.953347549	-43.907089812	8.69	0.10	5.66	0.04	0.10	0.15
60	156.954447709	-43.907854424	6.48	0.17	3.97	0.09	1.60	0.30
61	156.953338961	-43.906846003	6.61	0.13	4.09	0.09	1.10	0.30
62	156.957056386	-43.908914571	6.48	0.37	4.61	0.15	2.00	0.98
63	156.957391037	-43.909029071	7.15	0.38	3.68	0.28	0.60	0.40
64	156.957346182	-43.909126978	6.70	0.37	3.57	0.16	0.90	0.47
65	156.953383491	-43.907231309	7.33	0.32	4.19	0.17	0.70	0.30
66	156.956105199	-43.908521181	6.01	0.45	3.10	0.13	0.70	0.23
67	156.954563902	-43.907847881	6.79	0.30	3.45	0.31	0.50	0.20
68	156.953639889	-43.907192274	6.30	0.29	3.72	0.06	1.60	0.12
69	156.959136393	-43.909518476	7.24	0.07	4.01	0.08	0.30	0.15
70	156.956899657	-43.908688492	6.70	0.12	3.18	0.12	0.10	0.26
71	156.982535296	-43.919045697	8.73	0.10	7.47	0.04	2.30	0.17
72	156.969226509	-43.913679510	8.73	0.09	5.48	0.04	0.10	0.17
73	156.955628696	-43.907702577	6.70	0.13	3.94	0.09	0.30	0.30
74	156.955333103	-43.907783859	6.70	0.07	3.25	0.09	0.10	0.08
75	156.957373231	-43.908570241	6.01	0.01	3.75	0.09	1.40	0.01
76	156.958162043	-43.908640587	6.79	0.27	2.88	0.33	0.00	0.03
77	156.95783889	-43.908559297	6.01	0.02	2.75	0.05	0.00	0.01
78	156.956115962	-43.907569839	6.48	0.22	4.32	0.08	0.60	0.27
79	156.959644004	-43.906493783	7.15	0.47	3.83	0.25	0.10	0.44
80	156.955295936	-43.907206344	6.48	0.55	3.57	0.17	1.70	0.78
81	156.955403649	-43.907105855	6.90	0.50	3.97	0.17	1.50	1.10
82	156.954701206	-43.906423978	8.69	0.10	5.48	0.04	0.30	0.18
83	156.971288772	-43.913761250	8.62	0.10	5.28	0.04	0.00	0.13
84	156.975543511	-43.914545708	8.75	0.12	7.63	0.05	3.80	0.21

Table 4 continued

**Table 4** (*continued*)

ID	R.A.	Decl.	$t_c$	$\sigma_{t_c}$	$M_c$	$\sigma_{M_c}$	$A_V$	$\sigma_{A_V}$
85	156.954092990	-43.906425732	8.73	0.09	5.45	0.04	0.30	0.17
86	156.955336689	-43.906626282	8.69	0.09	6.37	0.04	0.00	0.11
87	156.953335297	-43.905446708	8.62	0.07	6.30	0.04	0.00	0.08
88	156.971535450	-43.913706378	8.53	0.06	5.25	0.04	0.00	0.02
89	156.955922001	-43.907021449	8.55	0.08	5.26	0.04	0.00	0.09
90	156.954955769	-43.906597173	8.73	0.09	5.52	0.04	0.00	0.11
91	156.953187609	-43.905728299	8.55	0.05	5.02	0.03	0.00	0.01
92	156.954805451	-43.906565986	8.37	0.06	4.85	0.02	0.00	0.22
93	156.956833784	-43.907178870	6.30	0.65	4.69	0.39	2.30	1.10
94	156.966131608	-43.911108813	8.13	0.14	5.09	0.09	0.00	0.04
95	156.955662848	-43.906724758	8.55	0.05	5.51	0.03	0.00	0.01
96	156.954028963	-43.905665047	8.69	0.08	5.92	0.04	0.00	0.10
97	156.955905677	-43.906883727	7.22	0.13	4.01	0.07	0.40	0.17
98	156.976986592	-43.915783221	8.69	0.08	5.25	0.04	0.00	0.09
99	156.955634213	-43.906573079	8.60	0.08	5.30	0.04	0.10	0.07
100	156.956218953	-43.906627049	8.31	0.07	5.26	0.04	0.00	0.06
101	156.960624256	-43.907893973	9.20	0.74	5.96	0.38	0.50	0.88
102	156.956042937	-43.905923459	8.11	0.33	5.29	0.18	0.90	0.21
103	156.956132700	-43.906569362	8.69	0.08	5.74	0.04	0.00	0.09
104	156.974551450	-43.913649026	8.57	0.06	5.46	0.03	0.00	0.04
105	156.955738702	-43.906380890	8.69	0.13	5.51	0.04	0.30	0.23
106	156.960009465	-43.907527710	8.69	0.10	7.66	0.04	2.00	0.18
107	156.956508610	-43.905418934	8.06	0.38	6.92	0.19	0.60	0.30
108	156.956044894	-43.905489184	8.15	0.11	6.15	0.08	0.00	0.04
109	156.955320072	-43.906290132	6.30	0.64	3.67	0.48	2.00	0.96
110	156.941110968	-43.898787718	8.42	0.25	7.79	0.06	1.20	0.40
111	156.954814721	-43.905996785	8.31	0.12	5.17	0.06	0.50	0.16
112	156.956795271	-43.906805867	8.24	0.39	4.52	0.25	0.00	0.19
113	156.957092814	-43.906491680	6.48	0.38	4.44	0.36	2.50	1.02
114	156.957169965	-43.905641362	8.20	0.09	5.50	0.04	0.30	0.12
115	156.946530829	-43.901753391	8.11	0.16	6.15	0.09	0.60	0.16
116	156.964895560	-43.909789517	8.71	0.08	5.21	0.04	0.00	0.09
117	156.955639274	-43.905946176	8.37	0.06	5.33	0.02	0.00	0.07
118	156.959756948	-43.906127892	7.46	0.35	6.06	0.21	3.30	0.32
119	156.955092282	-43.905735605	8.49	0.08	4.74	0.06	0.00	0.02
120	156.954631107	-43.905205758	8.28	0.12	4.91	0.06	0.30	0.14
121	156.955145926	-43.905321609	8.60	0.09	5.42	0.04	0.10	0.11
122	156.966289721	-43.910192938	8.69	0.10	5.37	0.04	0.30	0.19
123	156.961885408	-43.908296720	7.59	0.31	4.99	0.16	0.70	0.29
124	156.958297710	-43.905470611	8.51	0.13	6.75	0.04	0.30	0.21
125	156.957783123	-43.905464132	9.00	0.44	6.24	0.12	0.40	0.65
126	156.963048646	-43.908203490	8.35	0.36	5.98	0.09	2.10	0.56
127	156.958372436	-43.906358656	9.26	0.97	6.52	0.51	1.00	1.03
128	156.959692386	-43.906287106	8.71	0.11	6.06	0.04	1.10	0.20
129	156.959772153	-43.906646244	8.69	0.15	6.79	0.05	1.50	0.25
130	156.960885889	-43.907119374	6.86	0.55	3.92	0.37	1.40	0.75
131	156.955999268	-43.905367222	8.08	0.23	5.29	0.16	0.00	0.14

*Table 4 continued*

**Table 4** (*continued*)

ID	R.A.	Decl.	$t_c$	$\sigma_{t_c}$	$M_c$	$\sigma_{M_c}$	$A_V$	$\sigma_{A_V}$
132	156.958478216	-43.905744839	6.30	0.54	5.67	0.55	4.00	1.10
133	156.956221772	-43.905330086	7.62	0.22	4.72	0.12	0.00	0.20
134	156.956596865	-43.905207405	8.73	0.13	5.91	0.04	0.10	0.22
135	156.960330325	-43.906203856	7.91	0.34	6.32	0.17	0.70	0.30
136	156.963180474	-43.907763024	7.15	0.48	4.33	0.22	0.90	0.66
137	156.960229603	-43.906665413	8.15	0.16	4.88	0.12	0.00	0.05
138	156.957695841	-43.905679019	8.42	0.06	5.09	0.05	0.00	0.23
139	156.958611067	-43.905987202	7.15	0.47	5.13	0.23	0.90	0.70
140	156.956506836	-43.904561391	8.71	0.16	6.36	0.05	1.00	0.26
141	156.978723906	-43.914256634	8.69	0.11	5.12	0.04	0.00	0.14
142	156.958103096	-43.905632499	7.15	0.31	5.23	0.37	1.00	0.78
143	156.964428285	-43.908290784	8.24	0.11	4.83	0.07	0.20	0.12
144	156.960661928	-43.906632018	6.48	0.55	4.65	0.27	2.80	0.96
145	156.975940296	-43.913124252	8.73	0.14	5.45	0.05	0.20	0.24
146	156.967323010	-43.909442925	8.53	0.05	4.96	0.04	0.00	0.05
147	156.956592839	-43.904751258	9.06	0.47	6.48	0.13	0.70	0.71
148	156.960562349	-43.906039006	6.48	0.39	5.63	0.23	3.40	1.05
149	156.963326585	-43.906356648	6.79	0.29	4.68	0.28	0.40	0.19
150	156.956630759	-43.904886688	8.40	0.08	5.01	0.06	0.00	0.02
151	156.964737894	-43.908397509	6.97	0.06	3.15	0.09	0.00	0.02
152	156.962515338	-43.907087314	8.98	0.37	5.84	0.09	0.70	0.57
153	156.966133873	-43.908434700	7.75	0.29	4.65	0.14	0.30	0.28
154	156.956464734	-43.904750923	6.01	0.60	4.03	0.27	2.00	0.95
155	156.956662367	-43.904839417	8.71	0.16	5.51	0.05	0.40	0.26
156	156.954943887	-43.903590564	8.71	0.09	6.46	0.04	2.00	0.16
157	156.962336473	-43.906602974	8.73	0.14	5.55	0.06	0.10	0.23
158	156.965336301	-43.908167373	7.15	0.28	4.76	0.14	0.40	0.32
159	156.965164203	-43.908298456	6.61	0.14	3.78	0.10	0.60	0.33
160	156.957317496	-43.904789884	8.89	0.24	6.81	0.06	1.30	0.39
161	156.959716307	-43.905780983	8.11	0.13	6.41	0.08	0.80	0.14
162	156.961666630	-43.906652272	7.15	0.28	4.63	0.16	1.00	0.33
163	156.965149016	-43.908175302	6.79	0.26	3.15	0.30	0.00	0.17
164	156.962530532	-43.906871971	9.73	0.89	7.14	0.44	0.40	1.02
165	156.960804770	-43.906267765	7.35	0.31	4.89	0.16	0.80	0.30
166	156.964957259	-43.907963076	8.15	0.15	5.17	0.10	0.80	0.14
167	156.959945266	-43.905483439	8.57	0.18	7.32	0.05	1.90	0.29
168	156.968239503	-43.909333595	8.62	0.08	5.55	0.04	0.00	0.09
169	156.978514428	-43.913711736	8.62	0.06	5.46	0.04	0.00	0.06
170	156.954868923	-43.903323399	8.69	0.09	6.23	0.04	0.70	0.17
171	156.960697711	-43.905296591	8.00	0.37	6.42	0.20	1.40	0.31
172	156.942411381	-43.896880334	8.73	0.09	8.31	0.04	2.70	0.16
173	156.960737774	-43.905482312	8.04	1.01	7.19	0.52	2.90	1.09
174	156.965481687	-43.907755087	7.68	0.28	5.10	0.14	1.10	0.28
175	156.965892608	-43.908082753	7.51	0.26	4.26	0.13	0.40	0.28
176	156.980321801	-43.913768834	8.33	0.36	7.64	0.09	1.30	0.55
177	156.960956691	-43.906079841	7.86	0.27	5.07	0.14	0.00	0.25
178	156.961869188	-43.906551086	8.55	0.08	4.92	0.08	0.00	0.04

Table 4 *continued*

**Table 4** (*continued*)

ID	R.A.	Decl.	$t_c$	$\sigma_{t_c}$	$M_c$	$\sigma_{M_c}$	$A_V$	$\sigma_{A_V}$
179	156.962197285	-43.906644609	8.08	0.24	5.35	0.15	1.20	0.22
180	156.968340121	-43.909167646	8.73	0.10	5.65	0.04	0.00	0.14
181	156.965525340	-43.907986978	6.79	0.15	3.32	0.20	0.30	0.15
182	156.972460379	-43.910930236	6.79	0.37	3.63	0.20	1.10	0.29
183	156.965727561	-43.907972761	8.69	0.10	5.18	0.05	0.10	0.17
184	156.962632847	-43.906158693	8.71	0.13	7.11	0.05	3.00	0.21
185	156.952392158	-43.902052926	8.71	0.10	5.65	0.04	0.10	0.18
186	156.964814126	-43.907405478	8.57	0.09	5.15	0.04	0.10	0.11
187	156.958250904	-43.904217082	8.73	0.12	6.18	0.05	1.50	0.21
188	156.967184477	-43.907623013	7.46	0.26	5.77	0.12	0.50	0.26
189	156.963919733	-43.906901193	7.48	0.25	4.50	0.12	0.20	0.25
190	156.967223793	-43.908388036	8.69	0.11	5.14	0.05	0.10	0.18
191	156.966317623	-43.907618042	8.13	0.18	5.82	0.10	0.80	0.15
192	156.963363633	-43.905993411	6.70	0.28	6.08	0.16	3.40	0.32
193	156.965741622	-43.907634000	6.79	0.03	3.23	0.02	0.00	0.61
194	156.966787202	-43.907618564	8.60	0.08	5.65	0.03	0.10	0.08
195	156.964211095	-43.906747729	8.17	0.32	4.75	0.19	0.00	0.21
196	156.977776898	-43.912650484	6.01	0.61	3.00	0.13	0.50	0.26
197	156.971777619	-43.909556212	8.26	0.09	5.55	0.04	0.20	0.12
198	156.964268892	-43.906229732	6.61	0.32	5.03	0.35	2.50	0.81
199	156.961669535	-43.904245082	8.71	0.26	6.26	0.10	1.80	0.45
200	156.960935624	-43.904295665	9.98	0.86	8.38	0.43	1.70	0.99
201	156.955560579	-43.902378190	8.42	0.21	5.75	0.06	0.70	0.33
202	156.965676035	-43.905381342	9.24	0.81	7.22	0.40	0.90	0.95
203	156.939733126	-43.895635221	7.97	0.34	5.07	0.17	0.60	0.31
204	156.983800121	-43.914476692	8.55	0.05	5.29	0.03	0.00	0.01
205	156.945598559	-43.898077791	8.93	0.30	6.35	0.07	0.70	0.48
206	156.958444148	-43.903389226	8.15	0.62	5.13	0.28	1.20	0.56
207	156.943113703	-43.896557439	7.30	0.31	5.79	0.16	1.50	0.29
208	156.979711983	-43.912606178	6.79	0.35	3.85	0.18	1.50	0.30
209	156.964007615	-43.905785563	8.69	0.11	6.65	0.04	1.50	0.19
210	156.965086626	-43.906054358	6.79	0.35	4.40	0.18	1.70	0.31
211	156.961302557	-43.904525012	7.42	0.26	5.88	0.13	1.40	0.27
212	156.970570186	-43.908447767	8.62	0.07	5.25	0.04	0.00	0.07
213	156.984143540	-43.914099167	8.57	0.07	5.71	0.04	0.00	0.05
214	156.970855793	-43.908514803	8.00	0.37	5.03	0.20	0.90	0.30
215	156.962128386	-43.904428089	8.28	0.43	6.79	0.11	1.40	0.63
216	156.960319232	-43.903540686	7.91	1.06	6.56	0.55	2.00	1.10
217	156.965858010	-43.905934029	7.51	0.26	5.52	0.13	0.50	0.31
218	156.960559918	-43.903658432	8.69	0.12	6.49	0.04	1.00	0.21
219	156.958740618	-43.902987593	8.73	0.14	7.22	0.05	3.20	0.23
220	156.964175023	-43.904942605	8.15	0.81	7.17	0.41	3.90	0.95
221	156.962363552	-43.903771538	8.73	0.13	6.44	0.04	1.20	0.22
222	156.960091881	-43.903321683	7.46	0.25	5.44	0.12	1.50	0.26
223	156.960725535	-43.901721133	8.17	0.44	5.84	0.13	1.20	0.59
224	156.959877956	-43.901899575	8.00	1.06	6.42	0.55	2.60	1.11
225	156.959711173	-43.902679106	8.84	0.20	6.27	0.05	0.70	0.32

*Table 4 continued*

**Table 4** (*continued*)

ID	R.A.	Decl.	$t_c$	$\sigma_{t_c}$	$M_c$	$\sigma_{M_c}$	$A_V$	$\sigma_{A_V}$
226	156.964308979	-43.904878395	8.26	0.63	6.66	0.34	2.00	0.79
227	156.960011434	-43.902560800	8.22	0.09	5.36	0.05	0.20	0.12
228	156.952100713	-43.899999877	7.15	0.35	3.44	0.22	0.30	0.38
229	156.965973202	-43.904301350	7.75	0.27	6.31	0.13	0.60	0.27
230	156.965556020	-43.905549498	6.70	0.46	4.83	0.23	1.80	0.75
231	156.965781411	-43.905631015	6.48	0.27	4.15	0.16	1.50	0.44
232	156.966269997	-43.905879780	8.40	0.21	5.29	0.06	0.70	0.32
233	156.959216467	-43.902728576	8.73	0.16	6.12	0.05	1.10	0.27
234	156.964071037	-43.904235535	7.46	0.25	6.60	0.11	0.50	0.28
235	156.966168527	-43.905672200	8.17	0.12	5.40	0.08	0.80	0.18
236	156.964359273	-43.904476808	8.13	0.13	5.93	0.11	0.00	0.21
237	156.966103836	-43.905567569	7.15	0.42	4.23	0.17	0.20	0.37
238	156.960198593	-43.902496671	8.73	0.12	7.49	0.05	3.20	0.20
239	156.962823509	-43.904011048	8.73	0.11	6.85	0.06	2.40	0.20
240	156.964455320	-43.904170491	8.04	0.38	6.23	0.18	0.50	0.31
241	156.962345091	-43.903067586	9.11	0.74	6.81	0.38	0.90	0.87
242	156.964227026	-43.904555564	8.40	0.13	5.73	0.11	0.00	0.07
243	156.962176002	-43.903711156	7.13	0.48	4.91	0.39	1.80	1.10
244	156.964792451	-43.904572082	8.00	0.35	6.37	0.20	1.50	0.31
245	156.961085475	-43.902938332	8.26	0.10	5.60	0.08	0.50	0.22
246	156.964886233	-43.904471658	7.13	0.51	5.45	0.21	1.10	1.06
247	156.984785876	-43.912853017	8.60	0.06	5.55	0.04	0.00	0.05
248	156.966869989	-43.904995471	9.20	0.70	5.94	0.39	0.20	0.85
249	156.964327737	-43.904131753	7.15	0.34	5.53	0.22	0.70	0.38
250	156.965495850	-43.904536336	7.24	0.25	6.24	0.12	1.40	0.26
251	156.960047616	-43.901978679	8.35	0.36	6.44	0.09	2.50	0.55
252	156.966951796	-43.903856930	7.19	0.30	6.45	0.15	1.20	0.29
253	156.958198260	-43.900580331	8.49	0.17	7.63	0.05	0.50	0.28
254	156.961308552	-43.902206257	6.30	0.26	5.59	0.04	1.70	0.09
255	156.963973746	-43.903498956	9.20	0.66	7.65	0.32	0.00	0.75
256	156.966445872	-43.904236555	6.48	0.16	5.35	0.10	1.70	0.30
257	156.965075204	-43.903627934	7.24	0.05	6.02	0.06	0.20	0.08
258	156.965409584	-43.903818930	7.42	0.10	5.72	0.06	0.00	0.16
259	156.966787911	-43.904720055	7.88	0.31	5.70	0.17	1.40	0.28
260	156.964054635	-43.903398018	7.15	0.47	6.44	0.21	0.90	0.71
261	156.965646656	-43.903642290	7.24	0.05	6.91	0.06	0.20	0.08
262	156.988913485	-43.913755236	8.08	0.27	6.31	0.17	1.10	0.19
263	156.974162624	-43.907391806	8.69	0.10	5.25	0.04	0.20	0.18
264	156.963202140	-43.902709459	7.15	0.47	5.51	0.22	0.30	0.72
265	156.962344503	-43.902694418	7.46	0.29	5.17	0.19	0.40	0.31
266	156.964489138	-43.903679485	8.02	0.36	6.33	0.19	0.00	0.26
267	156.963497594	-43.902846745	8.24	0.09	6.78	0.06	0.40	0.12
268	156.953220835	-43.898608110	8.69	0.09	5.88	0.04	0.50	0.17
269	156.958990724	-43.901057953	8.69	0.09	5.50	0.04	0.40	0.16
270	156.963717343	-43.903115581	6.61	0.33	5.53	0.38	2.20	0.97
271	156.966192919	-43.903975046	6.70	0.09	5.49	0.10	0.50	0.09
272	156.963779668	-43.902887614	6.79	0.53	4.62	0.41	0.60	0.24

Table 4 *continued*

**Table 4** (*continued*)

ID	R.A.	Decl.	$t_c$	$\sigma_{t_c}$	$M_c$	$\sigma_{M_c}$	$A_V$	$\sigma_{A_V}$
273	156.965318553	-43.903353424	6.97	0.03	5.31	0.07	1.40	0.10
274	156.964494786	-43.903014622	8.17	0.10	6.13	0.06	0.90	0.12
275	156.965667952	-43.903859265	6.61	0.13	5.45	0.09	0.30	0.30
276	156.965227530	-43.903720348	6.79	0.03	4.54	0.04	0.00	0.29
277	156.962507246	-43.902297092	8.13	0.38	5.45	0.20	0.00	0.23
278	156.962134167	-43.901908149	8.75	0.14	7.24	0.05	1.10	0.24
279	156.964225614	-43.902996278	7.53	0.25	5.77	0.12	1.20	0.26
280	156.963120801	-43.901988256	6.97	0.40	5.05	0.50	1.90	1.06
281	156.965766303	-43.903843305	6.70	0.10	5.56	0.10	0.50	0.22
282	156.962309195	-43.902184506	7.13	0.51	4.61	0.19	0.10	1.03
283	156.963898925	-43.902584811	8.00	0.36	6.79	0.18	0.90	0.31
284	156.963920687	-43.902756957	6.70	0.46	5.08	0.16	1.30	0.64
285	156.961582456	-43.901844756	7.30	0.30	6.14	0.16	1.70	0.28
286	156.963400720	-43.902607473	7.88	0.30	5.73	0.15	0.40	0.29
287	156.964425668	-43.902836585	8.02	0.37	6.41	0.21	1.30	0.30
288	156.961811235	-43.901929911	6.30	0.26	4.89	0.04	1.20	0.09
289	156.959409722	-43.900873428	8.73	0.10	5.60	0.04	0.40	0.18
290	156.968532510	-43.904794794	8.17	0.10	4.99	0.06	0.20	0.12
291	156.963064609	-43.902306987	6.01	0.61	4.67	0.24	2.00	0.96
292	156.967011449	-43.903709698	6.79	0.30	4.13	0.30	0.00	0.10
293	156.959946260	-43.900483616	8.73	0.11	6.24	0.04	1.20	0.19
294	156.965319088	-43.902775291	6.79	0.28	4.69	0.29	0.20	0.07
295	156.964537155	-43.902411108	7.33	0.30	6.43	0.15	1.10	0.28
296	156.965952481	-43.903212799	7.24	0.25	6.51	0.12	1.40	0.26
297	156.962842232	-43.902227000	6.30	0.26	5.05	0.04	0.80	0.10
298	156.963763810	-43.902408656	7.15	0.25	4.85	0.15	0.00	0.32
299	156.962730898	-43.901678486	8.42	0.09	5.57	0.05	0.20	0.13
300	156.963937473	-43.902427415	7.62	0.27	5.80	0.13	0.40	0.27
301	156.986753720	-43.912399448	8.53	0.07	4.93	0.04	0.00	0.03
302	156.961730128	-43.901480653	6.70	0.09	5.33	0.09	0.40	0.11
303	156.963318796	-43.902228490	7.37	0.10	5.00	0.08	0.10	0.16
304	156.976821808	-43.908159650	6.79	0.66	3.50	0.47	0.70	0.02
305	156.966796135	-43.903533468	8.37	0.14	5.71	0.10	0.00	0.06
306	156.964897705	-43.902803641	7.02	0.05	5.04	0.10	0.00	0.01
307	156.964076677	-43.902589964	8.35	0.10	5.84	0.08	0.00	0.02
308	156.966844903	-43.903724815	7.02	0.43	4.98	0.38	1.20	1.06
309	156.962074947	-43.901707725	6.30	0.25	4.19	0.07	0.00	0.02
310	156.965994623	-43.902963808	8.15	0.10	6.37	0.06	0.80	0.12
311	156.962151416	-43.901225329	8.33	0.11	5.63	0.09	0.00	0.06
312	156.961643853	-43.900776267	6.70	0.48	5.76	0.22	2.40	0.69
313	156.958807786	-43.899767657	8.69	0.11	6.24	0.04	0.50	0.19
314	156.960614259	-43.900557152	8.71	0.12	5.89	0.04	0.20	0.21
315	156.967494475	-43.902362645	8.33	0.05	6.36	0.02	0.00	3.49
316	156.965954530	-43.902765801	6.30	0.60	5.29	0.16	1.90	0.96
317	156.965127829	-43.902626596	7.30	0.33	5.70	0.17	0.90	0.30
318	156.964660918	-43.902599556	6.79	0.12	4.59	0.14	0.40	0.17
319	156.963512523	-43.902077355	6.79	0.50	4.38	0.37	0.70	0.24

*Table 4 continued*

**Table 4** (*continued*)

ID	R.A.	Decl.	$t_c$	$\sigma_{t_c}$	$M_c$	$\sigma_{M_c}$	$A_V$	$\sigma_{A_V}$
320	156.977419079	-43.907037664	8.91	0.29	7.82	0.07	0.10	0.45
321	156.961476046	-43.901016122	7.48	0.25	5.65	0.13	1.50	0.26
322	156.965422715	-43.902485006	8.04	0.38	7.11	0.19	0.10	0.31
323	156.962012838	-43.901492249	7.08	0.63	4.34	0.15	0.00	0.71
324	156.968059119	-43.903750564	6.48	0.14	4.48	0.09	1.60	0.31
325	156.966970031	-43.903176728	8.04	0.38	5.72	0.19	0.10	0.32
326	156.965334496	-43.902658548	6.48	0.19	4.58	0.10	0.20	0.15
327	156.970291745	-43.904461794	8.89	0.24	7.75	0.06	3.30	0.38
328	156.961895460	-43.901312022	6.30	0.34	4.40	0.16	1.30	0.38
329	156.965768213	-43.901926746	6.61	0.11	5.49	0.09	1.20	0.16
330	156.965281210	-43.902254444	6.97	0.04	4.52	0.08	0.20	0.10
331	156.956648633	-43.898626881	7.48	0.16	4.24	0.06	0.00	0.16
332	156.980057560	-43.908446006	8.75	0.09	8.00	0.04	3.90	0.14
333	156.963641798	-43.901408987	7.46	0.26	5.36	0.12	0.40	0.30
334	156.968806685	-43.903866828	8.51	0.05	5.14	0.04	0.00	0.08
335	156.965699926	-43.902499616	7.39	0.20	5.88	0.10	0.20	0.18
336	156.964899471	-43.902404491	6.79	0.27	4.28	0.19	0.60	0.23
337	156.966709515	-43.903146351	6.01	0.35	5.10	0.08	1.00	0.12
338	156.969149739	-43.904289087	6.48	0.14	3.95	0.09	0.90	0.31
339	156.968462533	-43.903865609	6.01	0.50	3.62	0.22	1.30	0.41
340	156.961362776	-43.900535601	8.02	1.05	6.24	0.57	3.10	1.05
341	156.957993346	-43.898628430	8.69	0.10	6.03	0.04	0.70	0.17
342	156.957489900	-43.898818713	8.73	0.12	5.70	0.05	0.80	0.21
343	156.967839036	-43.903382588	6.61	0.31	4.98	0.36	2.60	0.80
344	156.962307412	-43.901038256	7.08	0.69	4.60	0.18	0.00	0.88
345	156.963817206	-43.901644948	8.24	0.07	5.37	0.05	0.00	0.15
346	156.963557111	-43.901170442	8.08	0.24	6.37	0.14	0.90	0.18
347	156.965517980	-43.902556127	8.66	0.08	6.71	0.04	0.00	0.09
348	156.969019446	-43.903831782	6.48	0.16	4.57	0.10	1.90	0.34
349	156.964590467	-43.902193878	8.26	0.08	5.34	0.07	0.00	0.03
350	156.960189543	-43.899616246	8.26	0.09	6.08	0.04	0.20	0.12
351	156.961898356	-43.900809850	7.86	0.30	5.18	0.15	0.40	0.29
352	156.963327706	-43.901449366	8.24	0.18	5.41	0.11	0.60	0.27
353	156.968707950	-43.903003912	6.48	0.35	5.37	0.36	2.40	1.01
354	156.965906089	-43.902410205	7.08	1.24	4.76	0.16	0.00	0.56
355	156.968899972	-43.903760948	6.79	0.22	3.52	0.21	0.50	0.19
356	156.966055015	-43.902224589	6.79	0.23	4.33	0.16	0.60	0.21
357	156.968322474	-43.903582969	8.24	0.14	5.11	0.13	0.00	0.03
358	156.968377429	-43.902739356	7.46	0.25	5.78	0.11	0.90	0.26
359	156.967935531	-43.903164864	6.01	0.48	4.73	0.40	3.10	1.08
360	156.964545850	-43.901650576	7.19	0.31	4.73	0.16	1.30	0.29
361	156.969317382	-43.903777578	7.15	0.49	4.03	0.21	0.20	0.68
362	156.963866174	-43.901421129	7.33	0.30	5.14	0.15	1.00	0.29
363	156.962953416	-43.900893088	6.01	0.38	4.38	0.07	1.20	0.13
364	156.965837751	-43.902283675	8.40	0.05	5.63	0.02	0.00	1.12
365	156.962126462	-43.900396301	8.00	0.36	5.59	0.19	1.20	0.31
366	156.963031972	-43.900972431	6.79	0.29	3.97	0.31	0.20	0.11

Table 4 *continued*

**Table 4** (*continued*)

ID	R.A.	Decl.	$t_c$	$\sigma_{t_c}$	$M_c$	$\sigma_{M_c}$	$A_V$	$\sigma_{A_V}$
367	156.963848596	-43.901061051	7.15	0.45	4.72	0.22	1.10	0.75
368	156.969636235	-43.903472107	8.44	0.22	5.01	0.10	0.60	0.32
369	156.967128254	-43.902430799	6.61	0.10	5.65	0.08	0.50	0.24
370	156.987238721	-43.910352254	8.73	0.12	7.85	0.04	0.40	0.21
371	156.968011028	-43.902671067	7.15	0.48	5.63	0.22	0.20	0.70
372	156.969937094	-43.903765184	7.13	0.60	3.49	0.69	0.30	1.01
373	156.965104155	-43.901505818	7.39	0.36	4.70	0.25	1.50	0.33
374	156.966248328	-43.902161162	8.40	0.17	5.34	0.06	0.50	0.24
375	156.964497184	-43.901309080	7.91	0.32	5.10	0.16	0.30	0.29
376	156.970487854	-43.903223684	6.70	0.34	6.20	0.17	0.60	0.26
377	156.966483297	-43.902122427	7.48	0.25	4.97	0.12	0.20	0.25
378	156.966351435	-43.901927199	7.19	0.32	5.07	0.16	1.30	0.29
379	156.941834804	-43.889899748	7.73	0.27	7.45	0.13	0.60	0.27
380	156.963484856	-43.900677380	7.59	0.22	4.70	0.11	0.00	0.19
381	156.970886290	-43.903863380	7.24	0.29	3.62	0.12	0.20	0.16
382	156.969024235	-43.903009865	7.48	0.25	4.91	0.12	0.80	0.26
383	156.963744326	-43.900803142	7.24	0.26	5.71	0.12	1.40	0.26
384	156.962876934	-43.900644356	6.70	0.54	3.62	0.54	1.30	0.57
385	156.966201215	-43.901880587	7.13	0.56	4.02	0.17	0.00	0.99
386	156.964645581	-43.900804826	8.69	0.14	5.84	0.05	1.10	0.24
387	156.968537698	-43.902489631	6.97	0.04	4.88	0.07	2.10	0.11
388	156.966919585	-43.902063852	6.48	0.15	4.54	0.09	1.40	0.31
389	156.968394122	-43.902568795	6.70	0.31	5.00	0.36	2.50	0.80
390	156.963976657	-43.900835184	7.22	0.18	4.30	0.15	0.40	0.17
391	156.966616570	-43.901666983	8.13	0.12	5.09	0.07	0.20	0.13
392	156.968046699	-43.902172805	6.61	0.31	4.61	0.38	2.20	0.80
393	156.963340656	-43.900449242	6.61	0.15	3.78	0.12	1.20	0.43
394	156.969147835	-43.902815739	8.31	0.08	5.07	0.06	0.00	0.02
395	156.969923411	-43.903285897	8.22	0.10	5.41	0.06	0.70	0.12
396	156.965533027	-43.900574814	7.66	0.26	5.42	0.13	0.10	0.25
397	156.962911178	-43.900260349	6.61	0.54	3.94	0.28	1.80	0.75
398	156.963764148	-43.900268930	6.48	0.15	3.96	0.13	1.40	0.38
399	156.969311747	-43.902826488	8.31	0.46	4.76	0.34	0.00	0.30
400	156.973873636	-43.904626017	9.02	0.41	6.51	0.11	0.30	0.61
401	156.967621022	-43.902138819	6.01	0.37	4.37	0.10	1.40	0.18
402	156.989028758	-43.910869355	8.20	0.13	6.64	0.09	1.10	0.17
403	156.968878499	-43.902488655	7.26	0.25	4.56	0.30	0.00	0.06
404	156.963368049	-43.899699886	6.79	0.27	4.35	0.21	0.70	0.23
405	156.967004864	-43.901639344	6.79	0.32	3.71	0.20	0.70	0.25
406	156.963347122	-43.900129876	6.30	0.58	4.48	0.29	3.20	1.04
407	156.969888700	-43.902722287	7.15	0.23	4.33	0.11	0.00	0.25
408	156.968099052	-43.902010049	8.44	0.19	5.66	0.05	0.60	0.31
409	156.965728370	-43.901127203	6.48	0.32	3.35	0.19	1.00	0.43
410	156.966245326	-43.900637422	7.13	0.49	4.61	0.19	0.20	1.05
411	156.964642774	-43.900531268	6.48	0.30	4.49	0.10	1.60	0.34
412	156.965408750	-43.900967067	6.79	0.09	3.75	0.12	0.30	0.11
413	156.963052323	-43.899519268	7.15	0.46	4.99	0.22	1.00	0.73

*Table 4 continued*

**Table 4** (*continued*)

ID	R.A.	Decl.	$t_c$	$\sigma_{t_c}$	$M_c$	$\sigma_{M_c}$	$A_V$	$\sigma_{A_V}$
414	156.967693049	-43.901704945	8.02	0.98	5.41	0.47	1.60	0.96
415	156.963610244	-43.899509452	7.33	0.32	6.27	0.16	0.70	0.30
416	156.965857470	-43.900876963	6.97	0.05	3.98	0.09	0.90	0.12
417	156.968489549	-43.902143377	6.48	0.54	3.93	0.17	1.90	0.92
418	156.964198395	-43.900277812	7.13	0.58	3.79	0.94	0.50	0.90
419	156.970297697	-43.902729057	8.44	0.08	4.86	0.06	0.00	0.10
420	156.968499770	-43.901613016	6.70	0.46	5.50	0.22	2.00	0.72
421	156.963435124	-43.899321073	7.84	0.37	6.31	0.22	2.10	0.34
422	156.967497374	-43.901585583	6.48	0.58	3.81	0.25	2.00	0.85
423	156.968963655	-43.901817077	6.61	0.47	4.23	0.19	1.50	0.80
424	156.965891221	-43.900630403	6.70	0.51	4.28	0.22	1.60	0.79
425	156.970092985	-43.902382107	8.20	0.08	5.03	0.07	0.00	0.77
426	156.968532281	-43.901325633	8.71	0.21	5.13	0.11	0.10	0.32
427	156.969271799	-43.901978438	7.46	0.26	5.03	0.13	1.20	0.27
428	156.968074521	-43.901614137	7.46	0.25	4.79	0.12	1.00	0.27
429	156.969928238	-43.902433046	6.79	0.03	3.68	0.01	0.00	4.98
430	156.969695215	-43.902035246	7.79	0.31	4.88	0.17	0.60	0.31
431	156.975275381	-43.904103647	8.75	0.10	8.17	0.04	3.40	0.16
432	156.959630255	-43.897959136	9.02	0.40	5.45	0.12	0.10	0.55
433	156.970694807	-43.902709260	6.01	0.46	4.06	0.23	1.40	0.47
434	156.969409681	-43.901997519	6.48	0.23	4.58	0.06	1.60	0.27
435	156.969215012	-43.901582447	7.15	0.43	5.19	0.19	0.10	0.41
436	156.967823960	-43.901130165	8.22	0.09	5.49	0.06	0.70	0.12
437	156.965121647	-43.899917258	8.71	0.15	5.13	0.10	0.10	0.26
438	156.9665556718	-43.900862612	8.17	0.09	4.90	0.06	0.10	0.08
439	156.968817206	-43.901489749	8.06	0.37	4.87	0.19	0.00	0.30
440	156.964241026	-43.899767670	8.91	0.27	5.42	0.08	0.00	0.37
441	156.969543200	-43.902270841	6.97	0.10	3.51	0.23	0.20	0.32
442	156.965791794	-43.900617885	6.70	0.41	3.86	0.19	0.90	0.66
443	156.966707191	-43.900822343	7.15	0.47	4.22	0.22	0.40	0.73
444	156.969552029	-43.902035136	7.15	0.27	4.03	0.17	0.10	0.32
445	156.964868504	-43.899896927	8.13	0.52	5.89	0.17	1.40	0.69
446	156.968182136	-43.901367773	8.49	0.22	5.60	0.06	1.00	0.36
447	156.966040994	-43.900684246	7.46	0.37	4.23	0.38	0.70	0.43
448	156.970905938	-43.902776366	6.61	0.13	4.57	0.10	1.00	0.31
449	156.964346993	-43.899004793	7.13	0.51	5.31	0.19	1.30	1.06
450	156.963576429	-43.899139113	7.66	0.26	4.57	0.14	0.10	0.25
451	156.970465814	-43.901824008	7.15	0.52	4.07	0.24	0.40	0.75
452	156.966095465	-43.900606569	6.01	-0.07	4.20	0.06	1.50	0.12
453	156.965469584	-43.900133624	8.11	0.17	5.24	0.10	0.80	0.19
454	156.967234574	-43.901004020	8.46	0.06	4.80	0.05	0.00	0.15
455	156.968115890	-43.901296123	8.51	0.13	5.38	0.05	0.30	0.21
456	156.964409558	-43.899694434	9.06	0.55	5.90	0.19	0.60	0.78
457	156.963922503	-43.899321687	7.82	0.29	5.87	0.14	0.50	0.28
458	156.956027971	-43.894742990	6.01	0.66	7.41	0.40	4.70	1.16
459	156.970516303	-43.902282291	6.97	0.10	4.18	0.18	0.30	0.18
460	156.970465210	-43.902120531	6.48	0.38	5.07	0.14	2.00	0.97

Table 4 continued

**Table 4** (*continued*)

ID	R.A.	Decl.	$t_c$	$\sigma_{t_c}$	$M_c$	$\sigma_{M_c}$	$A_V$	$\sigma_{A_V}$
461	156.966993464	-43.900535335	6.61	0.10	4.60	0.07	0.90	0.13
462	156.969583573	-43.901881919	6.48	0.52	3.70	0.24	1.60	0.74
463	156.967472227	-43.900397674	7.15	0.47	5.23	0.22	0.40	0.72
464	156.968870536	-43.900787570	6.70	0.47	5.05	0.21	1.50	0.71
465	156.967488344	-43.900892976	6.86	0.56	3.40	0.27	0.40	0.86
466	156.993626556	-43.911548923	8.17	0.10	6.77	0.06	0.60	0.12
467	156.963392614	-43.899151707	8.15	0.43	4.80	0.25	0.50	0.33
468	156.966279121	-43.900293657	7.24	0.25	4.09	0.31	0.00	0.09
469	156.968260159	-43.901026776	7.15	0.31	4.79	0.36	0.30	0.79
470	156.967106469	-43.900174476	7.97	0.35	5.93	0.18	0.80	0.31
471	156.971965293	-43.901880815	8.22	0.46	6.89	0.13	1.30	0.64
472	156.968215128	-43.900872333	7.88	0.32	4.85	0.17	0.70	0.29
473	156.968666504	-43.900554882	6.30	0.24	5.38	0.05	1.00	0.13
474	156.971166021	-43.902028269	7.06	0.39	4.45	0.44	1.50	1.04
475	156.971506772	-43.902218636	7.24	0.33	4.55	0.15	0.00	0.15
476	156.967016449	-43.900399441	6.79	0.28	3.41	0.34	0.00	0.03
477	156.976861967	-43.904273910	8.71	0.10	5.86	0.04	0.50	0.17
478	156.967852761	-43.900555412	7.24	0.83	4.81	0.46	2.30	0.75
479	156.959465954	-43.897017232	6.79	0.36	3.66	0.20	1.20	0.29
480	156.970472609	-43.901624022	6.70	0.47	5.22	0.17	1.30	0.60
481	156.967813644	-43.900214804	7.08	0.46	4.47	0.35	0.90	1.07
482	156.970220600	-43.901540997	7.22	0.26	4.74	0.13	1.00	0.26
483	156.970296038	-43.901472144	6.70	0.27	4.62	0.15	1.40	0.32
484	156.968013132	-43.900467046	7.44	0.15	4.35	0.13	0.00	0.16
485	156.968482623	-43.900429171	6.30	0.26	4.93	0.05	1.80	0.09
486	156.969291387	-43.901016753	6.01	1.01	3.98	0.10	0.90	0.17
487	156.968124723	-43.900518528	7.46	0.36	4.48	0.24	0.80	0.36
488	156.973390704	-43.902559274	7.46	0.25	4.29	0.13	0.30	0.27
489	156.973220843	-43.902429456	7.46	0.16	4.73	0.09	0.00	0.20
490	156.969297794	-43.900854594	7.51	0.31	4.56	0.20	0.90	0.31
491	156.970629111	-43.901543596	6.70	0.50	3.32	0.30	0.90	0.50
492	156.970357571	-43.901298214	8.02	0.43	4.84	0.27	1.10	0.31
493	156.964556089	-43.898992758	8.71	0.14	5.24	0.05	0.20	0.23
494	156.969490692	-43.900618290	6.70	0.11	4.54	0.10	1.10	0.29
495	156.967418706	-43.900132659	6.79	0.29	3.39	0.29	0.40	0.16
496	156.968641361	-43.900445773	7.15	0.28	4.48	0.14	0.20	0.33
497	156.972850431	-43.901991444	8.69	0.10	5.82	0.04	0.10	0.16
498	156.960317420	-43.896402698	8.93	0.33	7.03	0.08	2.70	0.52
499	156.954690490	-43.894217751	8.69	0.09	5.35	0.04	0.00	0.10
500	156.960929567	-43.896933933	8.69	0.11	5.55	0.04	0.40	0.19
501	156.961631310	-43.897298605	6.97	0.06	3.07	0.11	0.00	0.02
502	156.969311798	-43.900504432	6.70	0.13	3.49	0.15	0.60	0.40
503	156.963715929	-43.897503492	8.69	0.09	5.23	0.04	0.00	0.11
504	156.967013699	-43.898457627	8.82	0.19	5.56	0.05	0.10	0.30
505	156.966749670	-43.898417298	8.31	0.12	5.54	0.05	0.80	0.17
506	156.964082305	-43.896075544	8.71	0.10	5.72	0.04	0.90	0.18
507	156.971558399	-43.898971630	8.11	0.15	6.82	0.09	0.80	0.15

*Table 4 continued*

**Table 4** (*continued*)

ID	R.A.	Decl.	$t_c$	$\sigma_{t_c}$	$M_c$	$\sigma_{M_c}$	$A_V$	$\sigma_{A_V}$
508	156.989172961	-43.906342383	8.13	0.11	6.71	0.07	0.80	0.12
509	156.973274279	-43.899903453	6.79	0.26	3.42	0.31	0.00	0.06
510	156.977963284	-43.901446161	8.69	0.11	6.08	0.04	0.10	0.17
511	156.962992887	-43.895257491	8.28	0.17	4.90	0.07	0.60	0.19
512	156.965555865	-43.895691851	8.73	0.12	7.71	0.04	3.00	0.20
513	156.967927133	-43.896800192	7.24	0.36	3.50	0.18	0.30	0.28
514	156.958004687	-43.891758846	8.08	0.18	6.79	0.10	1.00	0.16
515	156.969328860	-43.895926920	8.69	0.11	5.84	0.04	0.20	0.20
516	156.966656515	-43.894426130	8.04	0.96	6.09	0.49	2.20	1.05
517	156.980355167	-43.899043040	8.37	0.13	4.72	0.07	0.20	0.14
518	156.956382439	-43.888116734	9.00	0.40	7.23	0.10	0.40	0.60
519	156.955733186	-43.887719892	8.69	0.15	7.84	0.05	1.60	0.25
520	156.986919376	-43.899697627	8.71	0.12	7.75	0.04	0.70	0.21
521	156.980811866	-43.897552193	8.73	0.13	8.58	0.05	4.50	0.21
522	156.980995524	-43.897223818	8.71	0.10	8.64	0.04	1.30	0.17
523	156.966657093	-43.891636812	8.40	0.27	6.23	0.07	1.50	0.43
524	156.956790109	-43.887206627	8.73	0.13	6.95	0.04	1.90	0.22
525	156.982832483	-43.897244471	8.46	0.21	7.66	0.06	1.70	0.33
526	156.962254569	-43.889634097	8.15	0.13	5.07	0.09	0.90	0.13
527	156.993567107	-43.901502715	8.73	0.12	7.95	0.05	1.70	0.20
528	156.980242847	-43.893242423	8.73	0.10	8.02	0.04	1.20	0.17
529	156.966727887	-43.888816715	6.79	0.30	3.06	0.34	0.40	0.21
530	156.966942801	-43.888393846	6.48	0.06	3.69	0.01	0.00	7.11
531	156.981700499	-43.894324338	8.86	0.23	7.50	0.06	1.30	0.36
532	156.966699136	-43.887782177	6.79	0.03	3.31	0.04	0.30	0.10
533	156.986112495	-43.894668773	8.22	0.48	6.76	0.14	1.40	0.68
534	156.979114992	-43.890783923	8.75	0.16	7.03	0.05	1.70	0.26
535	156.948235816	-43.877326786	8.71	0.09	8.57	0.04	3.20	0.15
536	156.984591778	-43.893631793	6.48	0.38	3.83	0.16	2.00	0.98
537	156.948978535	-43.877024557	8.17	0.10	8.02	0.06	1.00	0.12
538	156.968247275	-43.885767497	8.35	0.37	7.67	0.09	1.40	0.56
539	156.979617821	-43.889977176	8.73	0.14	7.98	0.04	0.70	0.24
540	156.981021074	-43.890744019	8.73	0.14	7.85	0.05	1.60	0.23
541	156.998122997	-43.896622068	8.71	0.12	8.32	0.04	3.60	0.19
542	156.973281044	-43.886394621	8.69	0.10	5.30	0.04	0.10	0.15
543	156.975829175	-43.887633927	6.48	0.16	3.37	0.10	1.30	0.33
544	156.984006672	-43.890441016	8.46	0.23	6.62	0.06	2.00	0.36
545	156.981131422	-43.886561545	7.08	-0.10	3.41	0.11	0.00	0.26
546	156.956147514	-43.876020451	8.73	0.15	7.61	0.05	0.60	0.25
547	156.973115601	-43.883928026	8.73	0.11	7.92	0.04	1.40	0.19
548	156.965032410	-43.879979577	8.62	0.17	7.84	0.05	1.60	0.28
549	157.002316135	-43.898129594	6.97	0.03	3.28	-0.58	0.20	0.14

## NGC 6240

1	253.245151301	2.385341817	6.70	0.09	4.17	0.10	0.50	0.17
2	253.240476147	2.385195675	6.79	0.36	4.21	0.21	0.70	0.19

*Table 4 continued*

**Table 4** (*continued*)

ID	R.A.	Decl.	$t_c$	$\sigma_{t_c}$	$M_c$	$\sigma_{M_c}$	$A_V$	$\sigma_{A_V}$
3	253.233335488	2.385569137	6.97	0.05	4.78	0.10	1.00	0.12
4	253.235648695	2.386861539	7.15	0.45	4.47	0.20	0.10	0.42
5	253.256689255	2.390426093	8.13	0.73	7.51	0.39	1.80	0.86
6	253.235597099	2.389104110	8.75	0.16	8.65	0.05	1.40	0.26
7	253.248123273	2.392081469	9.15	0.51	7.87	0.15	0.00	0.72
8	253.258165578	2.393571304	8.71	0.09	8.78	0.04	3.90	0.15
9	253.250820715	2.392368899	8.08	0.32	6.02	0.18	0.90	0.22
10	253.236703120	2.391623448	8.28	0.45	7.66	0.12	1.50	0.68
11	253.257281505	2.396666846	8.13	0.12	8.33	0.07	0.90	0.13
12	253.254707133	2.396941003	8.20	0.10	8.23	0.06	0.80	0.12
13	253.249015863	2.394923363	8.53	0.06	5.86	0.04	0.00	0.01
14	253.242341496	2.393931430	8.26	0.18	5.49	0.12	0.20	0.14
15	253.249637806	2.395750504	8.20	0.15	5.86	0.10	0.80	0.14
16	253.254921289	2.397132350	7.55	0.30	5.16	0.15	0.70	0.28
17	253.243147832	2.395653155	8.46	0.06	5.99	0.04	0.00	0.01
18	253.242519685	2.395423430	6.79	0.35	4.48	0.18	1.20	0.31
19	253.252436540	2.397291421	9.04	0.48	7.06	0.13	0.40	0.72
20	253.244368992	2.396311372	8.33	0.18	6.20	0.05	0.70	0.28
21	253.243075362	2.396399998	7.15	0.51	4.73	0.22	0.60	0.59
22	253.243227067	2.396379353	8.28	0.12	5.50	0.10	0.10	0.15
23	253.243124319	2.396963250	7.73	0.28	5.55	0.14	0.20	0.28
24	253.242997190	2.396703917	8.33	0.30	5.90	0.11	0.80	0.36
25	253.243299863	2.396913538	8.24	0.07	5.76	0.05	0.00	0.08
26	253.242624709	2.396881557	7.02	0.09	4.84	0.16	0.80	0.19
27	253.241743351	2.396806099	8.20	0.10	5.84	0.07	0.40	0.12
28	253.243362265	2.397125081	7.44	0.12	5.36	0.05	0.00	0.15
29	253.243376376	2.397207908	7.15	0.52	4.64	0.24	0.40	0.67
30	253.247577063	2.397991952	8.71	0.10	6.22	0.04	0.10	0.18
31	253.248138049	2.398332174	8.69	0.11	6.23	0.04	0.20	0.19
32	253.246897177	2.397885485	8.49	0.06	5.70	0.04	0.00	0.12
33	253.242374464	2.397319279	8.42	0.18	5.52	0.16	0.00	0.07
34	253.242592456	2.397617117	6.70	0.07	4.82	0.10	0.40	0.14
35	253.242272341	2.397557089	6.70	0.48	5.64	0.21	1.60	0.70
36	253.242579131	2.397733169	7.73	0.28	5.67	0.14	0.50	0.28
37	253.243170864	2.398110564	7.57	0.27	5.62	0.13	0.60	0.27
38	253.249076438	2.398929117	6.97	0.09	4.26	0.83	0.60	0.29
39	253.242502516	2.398433398	8.35	0.12	6.40	0.05	0.50	0.18
40	253.241593692	2.398132362	6.48	0.48	4.48	0.13	1.80	0.63
41	253.242718514	2.398287283	8.17	0.39	5.57	0.21	0.00	0.29
42	253.246581717	2.399531760	8.60	0.18	6.10	0.05	0.50	0.29
43	253.242669533	2.398232841	8.49	0.12	5.72	0.09	0.00	0.08
44	253.241537262	2.398246390	8.62	0.10	5.67	0.05	0.00	0.11
45	253.242670302	2.398646382	8.46	0.19	6.11	0.06	0.60	0.30
46	253.245273324	2.399861965	8.73	0.10	6.50	0.08	0.40	0.21
47	253.247646124	2.399936318	8.51	0.10	5.91	0.05	0.10	0.12
48	253.242487672	2.399281715	8.08	0.41	5.17	0.27	0.00	0.20
49	253.245625048	2.401380005	9.51	0.90	9.36	0.46	1.80	1.03

*Table 4 continued*

**Table 4** (*continued*)

ID	R.A.	Decl.	$t_c$	$\sigma_{t_c}$	$M_c$	$\sigma_{M_c}$	$A_V$	$\sigma_{A_V}$
50	253.242300520	2.400082154	8.26	0.09	5.55	0.06	0.00	0.00
51	253.247814584	2.401035511	7.15	0.37	4.24	0.36	0.40	0.43
52	253.242403649	2.400046367	6.70	0.10	4.03	0.18	0.40	0.29
53	253.246512681	2.401571412	8.02	1.00	6.23	0.56	1.90	1.01
54	253.241982293	2.400299091	6.79	0.41	4.23	0.24	1.10	0.28
55	253.241617320	2.400700246	8.28	0.08	5.98	0.04	0.10	0.08
56	253.245390286	2.401945551	8.02	1.00	6.62	0.54	2.00	1.10
57	253.245331882	2.401452436	8.89	0.27	7.32	0.13	1.70	0.45
58	253.241325120	2.401040504	8.06	0.40	5.37	0.22	0.30	0.26
59	253.243092395	2.401470764	8.20	0.21	5.70	0.14	0.60	0.15
60	253.246884584	2.402088261	8.69	0.13	6.45	0.05	0.70	0.22
61	253.244188945	2.402373150	8.46	0.09	5.62	0.07	0.00	0.01
62	253.249443823	2.403818420	8.44	0.25	9.05	0.06	4.60	0.38
63	253.245321888	2.403457249	8.86	0.24	6.77	0.06	0.90	0.38
64	253.246186138	2.403553613	8.60	0.07	5.80	0.04	0.00	0.04
65	253.245792981	2.403727200	6.70	0.07	4.52	0.07	0.00	0.04
66	253.245845333	2.404062263	8.49	0.09	6.88	0.04	0.10	0.11
67	253.247268748	2.404058367	8.73	0.16	6.15	0.05	0.30	0.26
68	253.242143023	2.403665666	7.24	0.25	4.39	0.10	0.10	0.06
69	253.242972001	2.404239477	8.26	0.15	5.52	0.09	0.30	0.14
70	253.247679536	2.406161662	7.48	0.25	7.73	0.11	1.30	0.29
71	253.246338598	2.405268175	8.55	0.27	6.54	0.07	1.60	0.44
72	253.246916849	2.405877434	8.33	0.54	5.20	0.44	0.00	0.06
73	253.247315034	2.406354336	8.60	0.08	6.29	0.04	0.10	0.10
74	253.247733950	2.407170359	8.40	0.14	5.40	0.09	0.00	0.06
75	253.245061372	2.406528953	6.79	0.27	3.64	0.32	0.00	0.06
76	253.245497866	2.406880021	6.79	0.29	3.88	0.36	0.20	0.13
77	253.242154454	2.407563375	8.71	0.15	8.34	0.05	2.50	0.24
78	253.250073988	2.409126104	6.70	0.31	4.81	0.20	1.80	0.35
79	253.247921386	2.409238853	8.08	0.37	5.61	0.19	0.30	0.24
80	253.248968940	2.414310701	8.06	0.38	8.15	0.20	1.00	0.30
81	253.237699219	2.412622719	8.75	0.14	7.71	0.05	2.90	0.24
82	253.233434586	2.412364706	7.13	0.54	5.40	0.28	1.50	1.07
83	253.235273753	2.412667808	8.42	0.27	7.45	0.07	2.10	0.43
84	253.244029290	2.415295186	8.89	0.06	9.34	0.05	5.00	0.08
85	253.253047150	2.419620687	8.33	0.37	8.34	0.09	1.70	0.56
86	253.247310386	2.420393656	6.01	0.59	4.59	0.05	1.70	0.11
87	253.232192931	2.414740323	6.70	0.36	4.21	0.16	0.80	0.43

## NGC 7469 - Center

1	345.816394351	8.874674009	8.73	0.11	6.06	0.04	0.40	0.20
2	345.815126935	8.871716691	6.70	0.08	5.17	0.10	0.50	0.09
3	345.815894330	8.873206478	8.15	0.11	6.24	0.07	0.10	0.09
4	345.815266216	8.871845945	6.70	0.13	4.36	0.16	0.50	0.36
5	345.815802806	8.873600887	6.97	0.04	5.58	0.07	1.00	0.10
6	345.815557282	8.874816390	8.69	0.12	6.33	0.05	0.90	0.22

*Table 4 continued*

**Table 4** (*continued*)

ID	R.A.	Decl.	$t_c$	$\sigma_{t_c}$	$M_c$	$\sigma_{M_c}$	$A_V$	$\sigma_{A_V}$
7	345.815625808	8.873844245	8.22	0.10	7.48	0.06	0.50	0.12
8	345.814496650	8.872920692	7.37	0.08	5.38	0.07	0.00	0.14
9	345.815297761	8.874815993	8.04	0.37	6.09	0.19	0.60	0.32
10	345.815420526	8.874223200	7.86	0.30	7.53	0.15	0.20	0.28
11	345.815290289	8.874120031	6.97	0.03	5.90	0.09	0.30	0.15
12	345.815217422	8.873600801	6.70	0.44	6.37	0.16	1.10	0.69
13	345.815013974	8.873415349	6.70	0.45	6.87	0.14	1.20	0.54
14	345.815406198	8.873808790	6.79	0.28	5.85	0.32	0.10	0.05
15	345.814258264	8.872610553	6.79	0.29	3.97	0.32	0.30	0.17
16	345.814659356	8.873876872	6.70	0.31	6.94	0.15	1.50	0.76
17	345.814031500	8.872533496	6.79	0.28	3.82	0.36	0.10	0.09
18	345.814978168	8.874293404	8.15	0.14	7.54	0.09	1.20	0.17
19	345.813232223	8.872904107	6.79	0.27	4.07	0.17	0.70	0.23
NGC 7469 - Extended Galaxy and Companion								
1	345.821279745	8.861853007	6.30	0.27	3.99	0.03	1.30	0.11
2	345.824580588	8.872132633	8.13	0.74	6.18	0.39	1.80	0.87
3	345.821362773	8.871531687	8.08	0.40	4.75	0.24	0.00	0.22
4	345.820713131	8.871284929	6.79	0.03	4.14	0.02	0.00	0.83
5	345.819853475	8.870399206	8.06	0.39	5.00	0.21	0.00	0.16
6	345.818999800	8.868943264	6.70	0.42	4.52	0.11	1.20	0.49
7	345.816058885	8.864634713	8.35	0.34	6.22	0.08	1.50	0.53
8	345.822632550	8.875992178	6.79	0.66	3.99	0.50	0.70	0.11
9	345.820590021	8.873419106	8.71	0.17	5.65	0.05	0.20	0.27
10	345.830947575	8.891575037	7.46	0.25	4.92	0.11	0.70	0.28
11	345.817918795	8.872921049	7.08	0.42	4.64	0.00	1.20	1.08
12	345.818340830	8.872728189	8.28	0.40	5.12	0.26	0.30	0.35
13	345.817468958	8.871884290	6.70	0.47	4.71	0.17	1.30	0.60
14	345.817970838	8.871952126	8.20	0.14	5.02	0.11	0.00	0.22
15	345.817901920	8.872136632	6.48	0.21	4.63	0.08	1.50	0.28
16	345.817824211	8.872401317	7.46	0.25	5.30	0.11	0.20	0.29
17	345.816584385	8.871434483	7.24	0.04	5.10	0.06	0.10	0.06
18	345.817632093	8.872447694	7.24	0.32	5.03	0.18	0.00	0.38
19	345.817840460	8.872167802	7.51	0.27	4.36	0.22	0.00	0.27
20	345.817487316	8.872574582	6.48	0.15	4.95	0.09	1.60	0.31
21	345.817992000	8.873158709	7.97	0.34	5.33	0.17	0.20	0.31
22	345.818242512	8.873434953	7.15	0.50	4.07	0.20	0.10	0.65
23	345.817562577	8.872561983	7.24	0.04	4.88	0.05	0.10	0.02
24	345.816161871	8.870666403	6.79	0.36	4.03	0.20	0.90	0.28
25	345.815616679	8.870362327	6.70	0.10	4.98	0.11	0.70	0.16
26	345.821511705	8.879199906	7.35	0.31	5.05	0.17	1.40	0.29
27	345.816632482	8.871927746	6.79	0.44	4.48	0.31	0.60	0.23
28	345.816052909	8.871531562	7.26	0.07	5.50	0.07	0.30	0.12
29	345.816244524	8.871155863	6.79	0.29	3.47	0.33	0.20	0.11
30	345.815916478	8.871236707	8.31	0.19	5.50	0.07	0.60	0.22
31	345.817797861	8.874785980	8.13	0.12	7.40	0.07	0.60	0.13

*Table 4 continued*

**Table 4** (*continued*)

ID	R.A.	Decl.	$t_c$	$\sigma_{t_c}$	$M_c$	$\sigma_{M_c}$	$A_V$	$\sigma_{A_V}$
32	345.813895424	8.868027321	6.70	0.35	4.26	0.12	1.10	0.38
33	345.818189304	8.874801984	6.70	0.36	4.04	0.13	0.90	0.44
34	345.815424890	8.871463171	8.46	0.04	5.49	0.03	0.00	0.27
35	345.817205489	8.874397613	7.33	0.10	4.53	0.12	0.10	0.13
36	345.814515730	8.870599498	8.13	0.11	5.49	0.07	0.20	0.13
37	345.820321235	8.879466834	6.79	0.28	4.11	0.29	0.20	0.07
38	345.814900598	8.871774657	7.30	0.16	5.75	0.07	0.40	0.18
39	345.828044433	8.891748297	7.46	0.44	4.72	0.31	1.20	0.35
40	345.816688659	8.874715204	6.79	0.38	4.41	0.23	1.60	0.30
41	345.827884238	8.892363744	7.46	0.26	5.50	0.13	0.90	0.27
42	345.816633147	8.875438197	8.42	0.05	5.41	0.04	0.00	1.06
43	345.816370169	8.875790398	8.44	0.20	5.89	0.06	0.60	0.30
44	345.828688234	8.895161365	8.73	0.11	8.23	0.04	2.60	0.18
45	345.816273615	8.875295552	6.01	-0.39	3.50	0.06	0.00	0.07
46	345.819663503	8.880677173	6.61	0.54	3.80	0.30	1.30	0.46
47	345.813375781	8.871220466	8.15	0.21	5.03	0.15	0.00	0.02
48	345.819220024	8.880455326	8.00	0.37	5.07	0.21	0.10	0.30
49	345.826915516	8.892704187	9.20	0.75	6.35	0.40	0.30	0.89
50	345.816061959	8.875700775	6.48	0.55	3.79	0.30	1.30	0.63
51	345.813978448	8.872394185	6.01	-0.26	3.35	0.04	0.00	0.09
52	345.813583375	8.872585223	7.46	0.25	4.99	0.12	0.50	0.27
53	345.812175092	8.870176943	6.79	0.28	3.70	0.28	0.30	0.10
54	345.818414310	8.880360929	8.22	0.17	4.90	0.12	0.00	0.16
55	345.812772686	8.872609104	8.02	0.36	5.34	0.18	0.10	0.32
56	345.813041485	8.872814169	6.90	0.52	3.79	0.36	0.10	1.10
57	345.825839661	8.893197068	9.04	0.46	6.10	0.16	0.10	0.63
58	345.826065281	8.893383888	7.24	0.40	5.32	0.34	1.90	0.41
59	345.812675682	8.872818978	6.01	0.45	4.13	0.13	1.70	0.39
60	345.825899875	8.893346655	7.79	0.29	5.35	0.17	0.40	0.31
61	345.825763804	8.893671677	6.61	0.14	5.46	0.09	1.30	0.32
62	345.812542696	8.874103463	8.26	0.09	6.52	0.06	0.60	0.12
63	345.812669399	8.873872696	8.40	0.06	5.65	0.02	0.00	0.08
64	345.812977571	8.874416916	8.11	0.43	5.16	0.25	0.60	0.35
65	345.816862094	8.880460632	8.15	0.22	5.08	0.15	0.30	0.16
66	345.816648700	8.880378669	8.46	0.05	5.64	0.04	0.00	0.14
67	345.824982315	8.893791396	7.42	0.26	5.94	0.13	1.20	0.27
68	345.812126463	8.873938802	8.62	0.08	5.74	0.04	0.00	0.09
69	345.820139390	8.886027517	7.24	0.05	4.17	0.07	0.10	0.07
70	345.825321669	8.893927349	8.55	0.04	5.69	0.05	0.00	0.09
71	345.812625928	8.874697270	7.46	0.25	5.04	0.11	0.30	0.26
72	345.812391872	8.874693785	6.79	0.33	3.75	0.24	0.70	0.23
73	345.812628753	8.875279681	6.79	0.30	4.08	0.28	0.40	0.17
74	345.812114655	8.875357333	8.26	0.09	5.67	0.04	0.20	0.12
75	345.812653056	8.875595305	7.46	0.29	4.82	0.16	0.60	0.32
76	345.812225254	8.874827859	8.11	0.42	4.90	0.27	0.00	0.19
77	345.824792319	8.895227735	7.33	0.32	5.45	0.16	1.30	0.30
78	345.823867904	8.893648148	8.73	0.25	6.46	0.11	1.70	0.44

*Table 4 continued*

**Table 4** (*continued*)

ID	R.A.	Decl.	$t_c$	$\sigma_{t_c}$	$M_c$	$\sigma_{M_c}$	$A_V$	$\sigma_{A_V}$
79	345.812040797	8.875680825	8.00	0.37	5.05	0.20	0.30	0.30
80	345.812123434	8.875742494	7.15	0.27	4.52	0.16	0.10	0.34
81	345.824073457	8.894508613	7.51	0.25	6.01	0.11	0.60	0.28
82	345.813710169	8.878434560	8.17	0.08	5.46	0.06	0.00	0.23
83	345.811873738	8.875716630	7.13	0.47	4.76	0.42	1.20	1.06
84	345.812071080	8.876111634	8.69	0.10	5.77	0.04	0.00	0.13
85	345.813318836	8.878553905	7.48	0.26	5.17	0.13	0.50	0.27
86	345.813102141	8.877583682	6.79	0.26	3.91	0.31	0.00	1.19
87	345.812207394	8.876098969	6.70	0.49	4.23	0.55	1.70	0.48
88	345.824438800	8.895189044	7.97	0.39	5.34	0.23	1.10	0.30
89	345.813847762	8.878931023	6.79	0.19	3.61	0.21	0.50	0.19
90	345.813319734	8.878330373	6.70	0.06	4.08	0.08	0.30	0.09
91	345.812754059	8.877622128	7.15	0.28	4.42	0.16	0.10	0.34
92	345.812005991	8.876460995	8.28	0.09	5.30	0.06	0.00	0.02
93	345.811884951	8.876475277	7.46	0.25	4.53	0.13	0.20	0.25
94	345.823286878	8.894006939	7.48	0.25	6.21	0.14	2.30	0.30
95	345.813919361	8.879569565	6.79	0.30	3.67	0.30	0.50	0.21
96	345.823118866	8.894084550	7.48	0.24	5.10	0.13	0.20	0.24
97	345.823539862	8.894830448	6.48	0.55	5.73	0.40	4.50	0.95
98	345.823518656	8.895777361	8.69	0.11	5.85	0.04	0.30	0.20
99	345.814510405	8.881625777	8.22	0.46	4.80	0.31	0.10	0.27
100	345.814860227	8.882064016	6.01	0.01	3.95	0.08	1.50	0.15
101	345.822464193	8.894955265	8.13	0.71	6.52	0.38	1.70	0.84
102	345.814400536	8.881610582	6.48	0.49	4.06	0.14	1.70	0.72
103	345.821439578	8.893413569	6.70	0.35	4.49	0.11	1.30	0.88
104	345.813527100	8.881678257	8.31	0.15	5.12	0.09	0.20	0.13
105	345.811418574	8.878806049	6.79	0.59	4.06	0.46	0.60	0.17
106	345.821118295	8.893793074	6.79	0.16	4.20	0.11	0.60	0.21
107	345.811648863	8.879540132	6.79	0.28	3.67	0.31	0.20	0.06
108	345.811179714	8.878872044	7.33	0.22	4.57	0.11	0.40	0.19
109	345.821890550	8.895707386	7.46	0.25	6.22	0.11	1.00	0.30
110	345.821013494	8.893886827	6.79	0.11	3.85	0.11	0.50	0.18
111	345.811730934	8.879924852	7.26	0.07	4.20	0.09	0.10	0.05
112	345.821820915	8.895663487	7.33	0.30	6.01	0.15	1.50	0.28
113	345.821926794	8.895869006	6.97	0.42	4.30	0.04	0.50	1.03
114	345.812280676	8.881538161	6.61	0.12	4.26	0.08	0.30	0.30
115	345.821546440	8.895766050	8.64	0.11	5.91	0.06	0.00	0.17
116	345.811722467	8.880493117	8.13	0.19	5.01	0.13	0.10	0.07
117	345.812042129	8.881347406	7.42	0.19	4.64	0.10	0.10	0.18
118	345.814753053	8.885228576	7.24	0.10	4.17	0.10	0.30	0.18
119	345.821716861	8.896196039	6.30	0.32	4.84	0.08	1.40	0.14
120	345.821526733	8.896178380	6.48	0.15	5.18	0.08	1.70	0.31
121	345.812009314	8.881905706	7.13	0.50	4.19	0.39	0.50	1.02
122	345.821564176	8.896252514	6.90	0.52	4.22	0.35	0.40	1.10
123	345.820270368	8.894469422	7.24	0.04	4.59	0.06	0.10	0.05
124	345.817422923	8.891120147	6.01	-0.45	6.08	0.05	1.20	0.09
125	345.811370076	8.882297753	7.24	0.27	5.23	0.30	0.00	0.73

*Table 4 continued*

**Table 4** (*continued*)

ID	R.A.	Decl.	$t_c$	$\sigma_{t_c}$	$M_c$	$\sigma_{M_c}$	$A_V$	$\sigma_{A_V}$
126	345.811839504	8.882471595	6.79	0.35	4.23	0.19	0.80	0.23
127	345.810932394	8.881775344	7.24	0.25	4.54	0.26	0.00	0.23
128	345.807364165	8.877017305	6.48	0.35	5.03	0.37	2.30	1.01
129	345.807313254	8.876636741	7.33	0.33	4.75	0.18	1.00	0.29
130	345.809750427	8.880250516	6.70	0.08	3.90	0.07	0.00	0.19
131	345.807491967	8.877112328	6.61	0.14	3.55	0.11	0.00	0.21
132	345.807330301	8.876905970	7.24	0.37	3.98	0.20	0.10	0.39
133	345.807068383	8.876848577	7.95	0.36	5.20	0.20	0.80	0.28
134	345.807108992	8.877506472	6.61	0.56	4.35	0.36	2.00	0.74
135	345.818437165	8.895120763	6.70	0.07	3.45	0.10	0.00	0.08
136	345.807814589	8.879177506	6.70	0.52	3.91	0.20	1.20	0.47
137	345.810870779	8.884172499	6.79	0.09	3.79	0.11	0.30	0.10
138	345.817836540	8.895893269	6.48	0.14	4.31	0.09	1.60	0.31
139	345.809769976	8.884208889	8.73	0.10	7.48	0.04	3.10	0.18
140	345.804864030	8.877937757	7.24	0.05	4.44	0.06	0.20	0.10
141	345.816828787	8.897096150	6.48	0.15	4.07	0.10	0.70	0.31
142	345.816135162	8.897500268	6.70	0.09	4.29	0.07	0.10	0.12
143	345.816230835	8.897514875	6.70	0.37	4.18	0.13	1.00	0.49
144	345.815796879	8.897830279	6.79	0.31	3.81	0.29	0.60	0.23
145	345.811433488	8.892652604	7.15	0.45	4.56	0.23	0.80	0.75
146	345.814247888	8.899668916	6.30	0.26	3.90	0.04	0.90	0.10

NOTE—All values for age, mass, and extinction are given in  $\log(t/\text{yr})$ ,  $\log(M/M_\odot)$ , and magnitudes respectively

**Table 5.** Observational Properties of Individual Star Clusters

ID	R.A.	Decl.	$f_{336}$	$\sigma_{f_{336}}$	$f_{435}$	$\sigma_{f_{435}}$	$f_{814}$	$\sigma_{f_{814}}$
Arp 220								
1	233.746669054	23.480581701	1.07E-18	3.20E-20	9.25E-18	1.51E-20	5.17E-17	7.53E-20
2	233.729549053	23.475817413	1.70E-17	9.12E-20	2.64E-17	1.95E-20	1.25E-17	2.07E-20
3	233.748437605	23.482745482	2.94E-19	2.42E-20	8.17E-19	9.83E-21	7.72E-19	4.42E-21
4	233.751644007	23.484386024	4.57E-18	5.31E-20	8.37E-18	1.33E-20	3.47E-18	7.76E-21
5	233.764694288	23.492547085	3.30E-19	2.67E-20	2.08E-18	1.10E-20	6.02E-18	9.32E-21
6	233.728218353	23.482656154	5.77E-19	3.30E-20	6.28E-19	1.44E-20	4.25E-19	9.87E-21
7	233.732302621	23.484575842	5.76E-19	2.97E-20	4.69E-19	1.18E-20	1.21E-18	7.63E-21
8	233.731859917	23.486152064	2.39E-19	2.96E-20	4.50E-19	1.32E-20	2.18E-19	7.02E-21
9	233.725012898	23.486914452	2.61E-19	3.09E-20	2.14E-18	1.27E-20	6.63E-18	1.30E-20
10	233.728399990	23.488682409	2.25E-19	3.55E-20	1.19E-19	1.24E-20	1.25E-19	6.18E-21
11	233.732310801	23.490791224	6.96E-19	3.48E-20	2.87E-19	1.73E-20	4.97E-20	7.30E-21
12	233.758033822	23.501585925	1.07E-18	3.50E-20	1.09E-18	1.57E-20	6.39E-19	8.78E-21
13	233.743919183	23.499057830	2.92E-19	3.00E-20	1.05E-18	1.41E-20	4.47E-19	7.51E-21
14	233.746843168	23.500644635	3.79E-19	3.29E-20	1.27E-18	1.56E-20	5.08E-19	7.13E-21

*Table 5 continued*

**Table 5** (*continued*)

ID	R.A.	Decl.	$f_{336}$	$\sigma_{f_{336}}$	$f_{435}$	$\sigma_{f_{435}}$	$f_{814}$	$\sigma_{f_{814}}$
15	233.748438076	23.502665246	1.33E-17	8.67E-20	2.30E-17	2.19E-20	9.76E-18	1.86E-20
16	233.739157505	23.500744091	2.66E-19	3.70E-20	3.85E-19	2.94E-20	1.02E-19	1.43E-20
17	233.737237343	23.500609511	3.77E-19	4.24E-20	2.80E-19	2.58E-20	1.91E-19	1.49E-20
18	233.739271698	23.502072103	2.30E-19	4.17E-20	9.97E-19	7.18E-20	7.81E-19	5.18E-20
19	233.744401079	23.503930925	7.65E-19	3.74E-20	2.89E-18	2.20E-20	1.12E-18	1.11E-20
20	233.714860863	23.496138256	2.23E-19	4.29E-20	3.71E-19	2.06E-20	1.34E-19	1.13E-20
21	233.744868069	23.504675138	6.28E-19	3.55E-20	1.46E-18	2.08E-20	4.33E-19	9.54E-21
22	233.740231300	23.503524840	2.14E-18	5.88E-20	2.10E-18	5.49E-20	3.68E-19	5.73E-20
23	233.738994708	23.504212786	3.50E-19	4.23E-20	9.74E-19	4.37E-20	6.22E-19	3.63E-20
24	233.736527312	23.503529566	5.02E-19	3.95E-20	1.05E-18	3.34E-20	4.89E-19	1.21E-20
25	233.759235564	23.510034123	2.00E-18	3.92E-20	2.32E-18	1.67E-20	2.91E-18	2.62E-20
26	233.736907112	23.504055439	5.51E-19	4.21E-20	1.23E-18	3.47E-20	3.59E-19	1.58E-20
27	233.755449114	23.509254099	2.26E-19	3.31E-20	2.89E-19	1.33E-20	1.01E-19	4.62E-21
28	233.736893783	23.504443701	2.17E-18	5.46E-20	4.66E-18	3.78E-20	2.17E-18	1.52E-20
29	233.740410868	23.506510571	4.00E-19	3.54E-20	1.30E-18	1.76E-20	4.95E-19	8.00E-21
30	233.741175276	23.507002973	4.09E-19	3.66E-20	1.23E-18	1.67E-20	6.33E-19	9.52E-21
31	233.737797927	23.507305089	3.58E-18	5.24E-20	6.19E-18	2.38E-20	2.10E-18	9.21E-21
32	233.737246993	23.506877228	2.23E-19	2.83E-20	2.70E-19	1.59E-20	8.23E-20	6.74E-21
33	233.736771854	23.506976292	7.07E-19	3.71E-20	1.29E-18	1.86E-20	3.92E-19	8.28E-21
34	233.739774525	23.507955558	4.43E-19	3.56E-20	1.27E-18	1.69E-20	5.15E-19	7.13E-21
35	233.740905432	23.508247391	2.34E-19	3.56E-20	5.47E-19	1.92E-20	1.88E-19	7.78E-21
36	233.739595349	23.510001954	2.03E-18	4.03E-20	3.71E-18	1.99E-20	1.17E-18	8.22E-21
37	233.739758003	23.510207087	8.62E-19	3.58E-20	1.43E-18	1.85E-20	4.32E-19	5.67E-21
38	233.739091396	23.510010435	6.22E-19	3.55E-20	1.28E-18	1.36E-20	3.55E-19	6.22E-21
39	233.743268929	23.511439049	3.91E-19	3.77E-20	1.41E-18	1.35E-20	1.26E-18	5.68E-21
40	233.727476088	23.507374383	2.97E-19	3.59E-20	4.30E-19	1.72E-20	3.37E-19	1.72E-20
41	233.741596461	23.512409998	2.91E-19	3.11E-20	8.49E-19	1.24E-20	7.95E-19	5.69E-21
42	233.712641673	23.510708076	2.90E-18	4.78E-20	2.29E-19	2.04E-20	6.35E-20	1.60E-20
43	233.715786536	23.512925158	2.44E-19	2.84E-20	2.16E-19	1.01E-20	8.59E-20	4.63E-21
44	233.712782544	23.510291460	1.81E-19	2.80E-20	2.07E-19	1.03E-20	1.06E-19	4.62E-21
45	233.723315397	23.517722087	6.42E-17	1.93E-19	1.10E-16	4.98E-20	5.62E-17	9.39E-20
46	233.729693112	23.518352156	2.10E-19	2.70E-20	5.40E-19	1.04E-20	3.71E-19	5.17E-21

## IC 1623

1	16.956330436	-17.512001234	5.61E-19	3.42E-20	4.71E-19	1.15E-20	2.43E-19	4.81E-21
2	16.952532574	-17.506213564	3.65E-19	3.17E-20	3.61E-19	2.84E-20	1.28E-19	1.15E-20
3	16.952056299	-17.506413601	2.86E-19	3.55E-20	8.34E-19	2.65E-20	3.05E-19	8.42E-21
4	16.950488627	-17.503461826	5.59E-19	3.92E-20	6.14E-19	3.12E-20	2.14E-19	1.32E-20
5	16.951049126	-17.504863361	6.58E-19	4.94E-20	5.48E-19	3.92E-20	2.82E-19	1.37E-20
6	16.950682091	-17.503408300	7.31E-19	3.80E-20	8.73E-20	1.85E-20	2.04E-19	8.42E-21
7	16.950863906	-17.505510101	1.01E-17	7.72E-20	1.49E-17	8.86E-20	5.28E-18	2.98E-20
8	16.951187415	-17.504873247	2.28E-19	3.42E-20	3.03E-19	3.44E-20	8.16E-20	8.56E-21
9	16.951016387	-17.504706370	2.49E-19	4.18E-20	2.40E-19	3.06E-20	8.01E-20	1.35E-20
10	16.950953107	-17.505277867	4.78E-19	6.46E-20	7.79E-19	5.96E-20	8.24E-20	1.97E-20
11	16.950933284	-17.505083708	8.62E-19	8.48E-20	9.17E-19	7.14E-20	1.46E-19	1.94E-20
12	16.951712337	-17.506958854	5.04E-19	4.68E-20	8.22E-19	1.98E-20	2.72E-19	9.34E-21

Table 5 continued

**Table 5** (*continued*)

ID	R.A.	Decl.	$f_{336}$	$\sigma_{f_{336}}$	$f_{435}$	$\sigma_{f_{435}}$	$f_{814}$	$\sigma_{f_{814}}$
13	16.950656373	-17.506143697	1.56E-19	4.68E-20	6.19E-19	4.49E-20	3.06E-19	1.59E-20
14	16.950439886	-17.505528995	4.09E-19	6.33E-20	7.02E-19	5.67E-20	2.63E-19	2.02E-20
15	16.951137759	-17.506609878	2.47E-19	4.05E-20	4.02E-19	2.68E-20	8.44E-20	1.47E-20
16	16.951057446	-17.506948375	2.27E-18	3.67E-20	1.83E-18	2.96E-20	6.31E-19	1.27E-20
17	16.950684474	-17.505765956	2.96E-19	5.06E-20	5.26E-19	5.96E-20	1.93E-19	2.12E-20
18	16.951081971	-17.506765096	3.09E-19	3.55E-20	1.41E-19	2.61E-20	4.83E-20	1.21E-20
19	16.950331622	-17.505568794	2.47E-19	6.33E-20	2.16E-19	4.30E-20	1.23E-19	2.17E-20
20	16.950383338	-17.505899273	4.21E-19	6.84E-20	5.79E-19	7.52E-20	7.94E-20	2.22E-20
21	16.950139217	-17.505923913	7.63E-19	4.94E-20	1.13E-18	7.36E-20	4.21E-19	2.60E-20
22	16.950317584	-17.506007153	2.77E-19	5.06E-20	1.22E-18	6.12E-20	2.69E-19	2.29E-20
23	16.950673781	-17.506899767	2.36E-19	4.05E-20	4.13E-19	3.00E-20	9.35E-20	1.13E-20
24	16.950229093	-17.505925623	2.54E-19	5.82E-20	8.62E-19	9.12E-20	1.00E-19	2.53E-20
25	16.950195881	-17.509102603	1.51E-17	6.33E-20	1.12E-17	5.07E-20	2.55E-18	1.43E-20
26	16.950391225	-17.509086287	2.45E-19	6.20E-20	5.28E-19	5.13E-20	1.09E-19	1.32E-20
27	16.950163349	-17.508897779	6.69E-19	5.44E-20	5.89E-19	2.74E-20	1.12E-19	6.16E-21
28	16.949651745	-17.507838234	4.91E-19	5.19E-20	3.20E-19	2.74E-20	1.28E-19	8.92E-21
29	16.948344739	-17.505423525	8.32E-19	4.30E-20	1.19E-18	3.25E-20	4.16E-19	1.84E-20
30	16.948445615	-17.506098875	1.98E-18	4.05E-20	1.34E-18	3.98E-20	9.09E-19	1.56E-19
31	16.948484736	-17.506534316	6.58E-19	5.82E-20	1.65E-18	2.19E-19	3.06E-18	3.57E-19
32	16.948102147	-17.505207847	1.02E-18	4.81E-20	7.40E-19	3.28E-20	1.62E-19	1.68E-20
33	16.949389027	-17.507903630	4.82E-19	5.19E-20	4.29E-19	1.63E-20	9.35E-20	1.05E-20
34	16.949829329	-17.508651885	2.75E-19	4.94E-20	2.06E-19	1.47E-20	3.87E-20	5.80E-21
35	16.948317672	-17.505563534	1.36E-19	3.80E-20	1.79E-19	1.91E-20	7.80E-20	1.37E-20
36	16.947889794	-17.507043198	1.17E-18	4.81E-20	1.02E-18	3.28E-20	1.54E-17	3.63E-19
37	16.947965298	-17.506198813	1.67E-18	4.18E-20	1.50E-18	3.38E-20	1.94E-19	2.67E-20
38	16.947752490	-17.507483910	3.43E-19	4.81E-20	1.55E-18	1.16E-19	4.65E-18	2.15E-19
39	16.947385263	-17.505449009	1.41E-18	4.56E-20	1.11E-18	2.55E-20	2.67E-19	1.17E-20
40	16.946678280	-17.504533764	2.11E-18	6.71E-20	2.08E-18	3.16E-20	4.96E-19	1.07E-20
41	16.947975960	-17.507050693	1.46E-18	4.94E-20	1.36E-18	3.19E-20	5.56E-19	1.19E-19
42	16.946567042	-17.504677056	7.35E-18	1.10E-19	5.70E-18	9.43E-20	1.53E-18	2.49E-20
43	16.947791506	-17.507128658	3.74E-19	4.05E-20	1.81E-19	3.28E-20	2.24E-18	1.64E-19
44	16.946996936	-17.507414550	5.95E-17	3.62E-19	7.35E-17	3.64E-19	3.07E-17	5.15E-19
45	16.947713167	-17.508250172	4.33E-19	5.06E-20	7.26E-19	8.86E-20	2.34E-19	4.32E-20
46	16.947014010	-17.505451289	5.19E-19	4.18E-20	5.57E-19	1.98E-20	1.74E-19	5.59E-21
47	16.949012988	-17.511146341	1.25E-18	5.95E-20	1.50E-18	4.30E-20	5.90E-19	1.72E-20
48	16.946722658	-17.507154505	8.13E-18	8.10E-20	6.20E-18	1.02E-19	1.23E-18	4.63E-20
49	16.946652113	-17.506442294	5.54E-17	2.75E-19	3.98E-17	1.38E-19	6.01E-18	4.33E-20
50	16.944873609	-17.505209805	3.70E-18	1.03E-19	2.52E-18	1.26E-19	8.78E-19	2.82E-20
51	16.948484203	-17.509902320	5.24E-19	3.17E-20	6.78E-19	1.53E-20	1.37E-19	6.09E-21
52	16.945688780	-17.503468736	5.42E-19	4.18E-20	5.81E-19	2.33E-20	7.30E-20	8.63E-21
53	16.948655346	-17.510695392	1.06E-18	3.80E-20	7.72E-19	1.85E-20	1.14E-19	6.79E-21
54	16.947880191	-17.508878486	3.81E-19	3.80E-20	4.57E-19	3.09E-20	1.10E-19	1.23E-20
55	16.946114235	-17.505040886	4.94E-19	3.29E-20	3.71E-19	2.36E-20	9.59E-20	7.08E-21
56	16.945860762	-17.504741111	5.90E-19	4.81E-20	8.43E-19	4.24E-20	9.27E-20	1.56E-20
57	16.946733243	-17.507569505	2.72E-19	5.06E-20	3.34E-18	1.02E-19	9.80E-18	8.90E-20
58	16.946536243	-17.506641279	8.85E-18	8.23E-20	7.00E-18	5.51E-20	2.21E-18	1.57E-20
59	16.945716058	-17.505028645	7.08E-19	4.56E-20	5.51E-19	3.35E-20	1.41E-19	9.77E-21

Table 5 continued

**Table 5** (*continued*)

ID	R.A.	Decl.	$f_{336}$	$\sigma_{f_{336}}$	$f_{435}$	$\sigma_{f_{435}}$	$f_{814}$	$\sigma_{f_{814}}$
60	16.946422010	-17.506539383	3.00E-19	5.70E-20	2.17E-19	5.67E-20	1.81E-19	1.80E-20
61	16.946094439	-17.506846826	8.83E-18	2.01E-19	6.99E-18	1.35E-19	1.91E-18	8.39E-20
62	16.948518639	-17.511750047	2.11E-18	5.57E-20	2.70E-18	3.67E-20	8.52E-19	1.39E-20
63	16.946953432	-17.507883215	3.54E-19	4.94E-20	5.92E-19	5.96E-20	5.30E-19	2.47E-20
64	16.945965265	-17.505289185	1.18E-19	3.55E-20	1.45E-19	2.23E-20	7.38E-20	7.93E-21
65	16.945540057	-17.505167563	2.84E-19	4.05E-20	4.43E-19	3.79E-20	3.11E-19	1.39E-20
66	16.948142799	-17.510880461	3.97E-18	4.30E-20	2.83E-18	1.98E-20	6.71E-19	6.79E-21
67	16.946493149	-17.506889534	3.13E-19	4.56E-20	2.77E-19	3.28E-20	5.85E-20	1.54E-20
68	16.948062477	-17.511049327	1.57E-18	4.18E-20	1.33E-18	1.56E-20	2.74E-19	6.72E-21
69	16.946682984	-17.508136495	2.66E-19	3.92E-20	2.49E-19	5.35E-20	2.31E-19	1.84E-20
70	16.945234499	-17.505439446	1.40E-18	6.33E-20	1.17E-18	6.85E-20	3.77E-19	2.94E-20
71	16.945969821	-17.506759715	2.21E-17	2.94E-19	1.82E-17	4.66E-19	4.82E-18	1.06E-19
72	16.947901658	-17.510545063	5.81E-19	4.05E-20	5.22E-19	1.72E-20	9.63E-20	4.95E-21
73	16.946530267	-17.508011460	7.77E-19	4.05E-20	8.43E-19	6.69E-20	6.93E-19	3.45E-20
74	16.946643097	-17.507983442	6.77E-19	5.57E-20	5.45E-19	6.73E-20	2.42E-19	2.82E-20
75	16.944692419	-17.504623460	1.39E-18	4.43E-20	1.52E-18	2.49E-20	4.09E-19	1.19E-20
76	16.946320608	-17.508471490	1.10E-18	4.94E-20	8.78E-19	6.12E-20	4.81E-19	3.23E-20
77	16.947062861	-17.509181492	4.76E-19	3.42E-20	5.96E-19	3.41E-20	1.61E-19	1.02E-20
78	16.945398036	-17.506120962	7.76E-18	2.91E-19	9.69E-18	2.75E-19	4.06E-18	7.40E-20
79	16.944434232	-17.506128945	2.58E-17	1.32E-18	2.87E-17	1.18E-18	9.34E-18	3.96E-19
80	16.944936624	-17.505436674	3.53E-18	8.23E-20	8.74E-18	7.55E-20	3.13E-18	2.61E-20
81	16.945624964	-17.506315582	2.28E-17	5.71E-19	1.60E-17	1.43E-19	2.01E-18	4.76E-20
82	16.946032944	-17.507331770	2.78E-18	1.52E-19	1.79E-18	2.19E-19	9.89E-19	8.41E-20
83	16.946058840	-17.507798293	6.52E-19	1.48E-19	8.68E-19	1.60E-19	4.64E-19	4.84E-20
84	16.945808445	-17.506932406	3.30E-18	2.39E-19	2.45E-18	3.72E-19	1.08E-18	6.77E-20
85	16.945360563	-17.506399314	3.16E-18	1.82E-19	2.21E-18	2.96E-19	6.01E-19	6.01E-20
86	16.945514157	-17.506409280	2.17E-17	3.58E-19	1.85E-17	2.53E-19	3.40E-18	7.11E-20
87	16.945939568	-17.507243124	8.37E-18	2.70E-19	8.71E-18	3.25E-19	2.27E-18	1.37E-19
88	16.946139734	-17.508346754	2.43E-17	3.22E-19	1.61E-17	2.06E-19	4.37E-18	9.12E-20
89	16.945122304	-17.506508861	3.72E-17	3.15E-19	2.40E-17	3.95E-19	5.08E-18	1.15E-19
90	16.945855697	-17.507263000	6.89E-18	2.81E-19	5.78E-18	2.57E-19	1.71E-18	1.73E-19
91	16.944892946	-17.506046744	5.72E-18	1.54E-19	4.84E-18	1.82E-19	1.43E-18	5.72E-20
92	16.945022553	-17.505606732	3.93E-18	9.75E-20	3.09E-18	7.49E-20	4.51E-19	3.32E-20
93	16.947831523	-17.512134698	3.73E-19	4.56E-20	6.10E-19	3.06E-20	1.28E-19	1.19E-20
94	16.944425198	-17.504560418	2.53E-19	4.68E-20	3.11E-19	3.86E-20	1.95E-19	9.84E-21
95	16.944753197	-17.506384457	1.83E-17	6.13E-19	2.07E-17	4.58E-19	3.09E-18	9.70E-20
96	16.947549999	-17.511920170	7.24E-19	3.80E-20	9.07E-19	1.69E-20	2.85E-19	6.58E-21
97	16.944749356	-17.506748533	1.84E-18	2.06E-19	3.74E-18	3.26E-19	1.26E-18	9.86E-20
98	16.944415486	-17.504935321	2.67E-18	7.22E-20	1.77E-18	1.01E-19	3.45E-19	2.09E-20
99	16.945682285	-17.508713991	1.22E-17	3.01E-19	1.10E-17	3.26E-19	3.52E-18	6.46E-20
100	16.946192902	-17.508672591	2.76E-19	4.94E-20	3.95E-19	7.59E-20	1.53E-19	2.41E-20
101	16.944848869	-17.506457859	4.10E-17	6.23E-19	2.62E-17	6.23E-19	4.83E-18	1.28E-19
102	16.943471002	-17.505395744	1.01E-18	5.06E-20	4.65E-19	6.63E-20	5.59E-19	1.83E-20
103	16.944580305	-17.506042845	6.04E-18	4.33E-19	5.49E-18	1.07E-18	2.89E-18	3.10E-19
104	16.945235468	-17.507243388	2.52E-17	9.66E-19	1.70E-17	8.34E-19	5.22E-18	2.50E-19
105	16.944710276	-17.506542753	3.69E-17	2.81E-19	2.25E-17	2.47E-19	5.74E-18	1.14E-19
106	16.944844406	-17.507312092	1.35E-17	3.27E-19	1.24E-17	3.60E-19	2.23E-18	1.19E-19

*Table 5 continued*

**Table 5** (*continued*)

ID	R.A.	Decl.	$f_{336}$	$\sigma_{f_{336}}$	$f_{435}$	$\sigma_{f_{435}}$	$f_{814}$	$\sigma_{f_{814}}$
107	16.945296523	-17.506960602	3.31E-18	2.30E-19	1.12E-18	2.80E-19	8.98E-19	1.02E-19
108	16.946047398	-17.508618200	3.40E-19	5.70E-20	1.00E-18	7.81E-20	1.24E-19	3.22E-20
109	16.944501877	-17.505892939	8.06E-18	4.68E-19	7.47E-18	1.16E-18	2.52E-18	3.95E-19
110	16.945074374	-17.507305903	8.40E-18	4.34E-19	4.37E-18	5.90E-19	1.53E-18	2.02E-19
111	16.944467245	-17.506601687	8.97E-18	3.62E-19	9.96E-18	5.98E-19	3.89E-18	1.93E-19
112	16.946774065	-17.510866373	1.18E-18	4.56E-20	9.14E-19	1.78E-20	2.06E-19	6.09E-21
113	16.943929110	-17.504871749	3.92E-18	9.12E-20	2.48E-18	1.09E-19	8.29E-19	1.73E-20
114	16.944291472	-17.506016274	8.94E-18	5.84E-19	7.14E-18	7.96E-19	2.28E-18	2.26E-19
115	16.944198148	-17.507259813	1.39E-17	3.36E-19	1.70E-17	3.98E-19	9.72E-18	1.40E-19
116	16.944767385	-17.507737361	1.51E-16	3.42E-18	7.60E-17	1.86E-18	3.46E-17	6.25E-19
117	16.946010694	-17.509611770	3.57E-19	6.20E-20	6.78E-19	2.49E-20	2.31E-19	1.05E-20
118	16.945032031	-17.507254109	5.03E-18	2.99E-19	2.43E-18	5.40E-19	1.32E-18	1.01E-19
119	16.943871004	-17.505334561	1.51E-18	1.23E-19	2.45E-18	1.35E-19	5.04E-19	4.45E-20
120	16.945326160	-17.508278668	1.91E-18	6.46E-20	1.20E-18	6.60E-20	2.29E-19	1.95E-20
121	16.943687458	-17.505791646	9.33E-18	4.52E-19	8.70E-18	5.16E-19	2.83E-18	1.66E-19
122	16.944623235	-17.506899815	2.66E-17	3.96E-19	2.51E-17	5.21E-19	8.22E-18	1.57E-19
123	16.944737164	-17.507514185	8.44E-18	5.18E-19	2.82E-18	5.93E-19	3.02E-18	2.13E-19
124	16.943009665	-17.506280105	3.31E-19	5.95E-20	1.00E-18	5.29E-20	5.04E-19	2.72E-20
125	16.944699230	-17.507424096	1.02E-17	3.77E-19	6.80E-18	4.55E-19	2.70E-18	2.12E-19
126	16.945240974	-17.508384781	1.06E-18	5.57E-20	1.94E-18	5.32E-20	6.76E-19	2.55E-20
127	16.945078484	-17.509080892	1.53E-18	6.33E-20	1.70E-18	9.40E-20	2.79E-19	2.72E-20
128	16.944550912	-17.506899307	2.37E-17	4.61E-19	2.40E-17	5.84E-19	8.00E-18	2.18E-19
129	16.943699249	-17.504821909	2.55E-19	5.06E-20	3.35E-19	5.64E-20	6.20E-20	1.50E-20
130	16.943485251	-17.504766311	5.01E-19	6.33E-20	4.38E-19	4.05E-20	1.41E-19	1.14E-20
131	16.943702074	-17.505030635	1.32E-18	4.81E-20	1.08E-18	3.89E-20	3.54E-19	1.34E-20
132	16.943916325	-17.506141272	6.32E-17	1.71E-18	6.10E-17	3.14E-18	1.10E-17	9.70E-19
133	16.944482053	-17.506867448	6.00E-18	4.56E-19	9.35E-18	4.69E-19	4.36E-18	2.14E-19
134	16.943252755	-17.504826992	2.73E-19	5.06E-20	7.09E-19	4.53E-20	4.09E-19	1.73E-20
135	16.944059029	-17.506634288	3.78E-18	2.05E-19	6.98E-18	8.91E-19	3.64E-18	2.61E-19
136	16.945999240	-17.510729997	2.62E-18	4.43E-20	1.80E-18	2.29E-20	3.69E-19	7.29E-21
137	16.943626127	-17.505234155	6.10E-19	6.46E-20	7.06E-19	5.35E-20	1.54E-19	2.55E-20
138	16.943578710	-17.504686369	4.16E-19	4.68E-20	4.13E-19	3.38E-20	7.98E-20	1.66E-20
139	16.944882397	-17.508939808	2.11E-17	1.62E-19	2.12E-17	1.76E-19	5.45E-18	3.79E-20
140	16.946261540	-17.511191572	3.84E-19	4.30E-20	3.95E-19	1.78E-20	5.86E-20	7.08E-21
141	16.945888173	-17.510898407	4.72E-18	8.23E-20	3.33E-18	3.28E-20	6.30E-19	8.92E-21
142	16.945148530	-17.510137217	1.93E-18	8.48E-20	1.86E-18	3.86E-20	7.78E-19	2.00E-20
143	16.944775647	-17.509316346	1.06E-18	5.32E-20	1.44E-19	2.01E-20	3.14E-19	1.08E-20
144	16.945398735	-17.509884292	6.76E-19	4.30E-20	9.27E-19	1.78E-20	2.63E-19	7.64E-21
145	16.943802331	-17.507003457	1.04E-17	8.23E-20	9.48E-18	1.14E-19	4.35E-18	3.72E-20
146	16.943217574	-17.506867444	4.89E-19	5.19E-20	1.41E-18	7.68E-20	5.87E-19	2.34E-20
147	16.943650953	-17.506660386	2.50E-18	1.08E-19	2.57E-18	1.40E-19	7.02E-19	7.93E-20
148	16.945681364	-17.510859147	3.24E-18	6.20E-20	2.89E-18	4.59E-20	5.69E-19	1.35E-20
149	16.944146393	-17.507657768	1.49E-18	1.22E-19	5.42E-19	1.48E-19	3.68E-19	7.33E-20
150	16.944736845	-17.509010897	1.45E-18	6.46E-20	1.14E-18	7.49E-20	2.71E-19	3.81E-20
151	16.945048246	-17.509489327	2.28E-19	4.43E-20	1.74E-19	1.98E-20	2.49E-20	6.79E-21
152	16.944838317	-17.509998763	2.80E-19	4.30E-20	3.16E-19	1.88E-20	9.27E-20	1.13E-20
153	16.944691762	-17.509672621	8.65E-19	4.30E-20	6.77E-19	2.52E-20	1.58E-19	9.91E-21

*Table 5 continued*

**Table 5** (*continued*)

ID	R.A.	Decl.	$f_{336}$	$\sigma_{f_{336}}$	$f_{435}$	$\sigma_{f_{435}}$	$f_{814}$	$\sigma_{f_{814}}$
154	16.942905487	-17.507047512	1.39E-16	6.90E-19	9.22E-17	4.14E-19	1.33E-17	8.12E-20
155	16.943705718	-17.508325068	2.61E-18	7.47E-20	2.59E-18	1.29E-19	7.45E-19	4.85E-20
156	16.944097663	-17.509111084	6.71E-19	4.81E-20	6.34E-19	3.70E-20	2.42E-19	1.68E-20
157	16.944035899	-17.508439526	2.10E-18	7.34E-20	1.40E-18	7.97E-20	2.40E-19	2.39E-20
158	16.942886937	-17.508040845	3.09E-16	8.90E-19	2.14E-16	6.53E-19	3.37E-17	1.32E-19
159	16.943567475	-17.507738466	1.53E-18	1.19E-19	1.38E-18	1.37E-19	2.43E-19	6.77E-20
160	16.943638596	-17.508676774	5.31E-19	6.71E-20	8.09E-19	7.90E-20	3.70E-19	2.47E-20
161	16.943309351	-17.508043026	2.33E-17	6.08E-19	1.87E-17	5.50E-19	3.30E-18	1.41E-19
162	16.943509235	-17.508245022	1.20E-17	5.20E-19	1.17E-17	2.12E-19	5.03E-19	8.85E-20
163	16.943487445	-17.508182486	9.87E-18	5.96E-19	1.06E-17	8.58E-19	5.68E-19	1.40E-19
164	16.942628052	-17.506668043	2.41E-19	3.92E-20	7.71E-19	2.61E-20	2.93E-19	1.01E-20
165	16.943070594	-17.507890030	4.06E-17	9.22E-19	3.52E-17	1.01E-18	5.89E-18	2.66E-19
166	16.943507240	-17.509586501	2.00E-18	4.43E-20	1.44E-18	3.06E-20	4.36E-19	1.27E-20
167	16.943218679	-17.508114808	4.33E-18	3.01E-19	4.56E-18	3.58E-19	4.91E-19	8.22E-20
168	16.943625620	-17.509217601	3.93E-19	5.19E-20	4.00E-19	4.40E-20	8.89E-20	1.98E-20
169	16.942244586	-17.506579230	7.61E-19	4.05E-20	9.63E-19	2.74E-20	2.66E-19	8.99E-21
170	16.942573217	-17.507897826	2.83E-18	1.01E-19	2.25E-18	1.69E-19	7.09E-19	5.29E-20
171	16.943492065	-17.509226702	2.69E-19	5.32E-20	4.17E-19	5.45E-20	2.10E-19	2.41E-20
172	16.942853625	-17.509161495	1.59E-18	6.20E-20	1.97E-18	6.50E-20	8.71E-19	2.70E-20
173	16.941825546	-17.506694949	3.36E-19	3.67E-20	5.51E-19	2.04E-20	1.20E-19	7.29E-21
174	16.942144905	-17.507960677	2.33E-19	5.19E-20	2.84E-19	6.12E-20	1.81E-19	1.81E-20
175	16.942311938	-17.508462330	2.45E-19	5.06E-20	2.37E-19	4.65E-20	6.54E-20	1.59E-20
176	16.941812747	-17.507915887	1.91E-19	4.05E-20	2.71E-19	2.42E-20	7.27E-20	1.09E-20
177	16.941798439	-17.508212173	3.74E-19	4.18E-20	6.22E-19	3.92E-20	1.61E-19	1.36E-20
178	16.937643223	-17.502271807	6.21E-19	3.42E-20	5.30E-19	2.49E-20	1.23E-19	6.79E-21
179	16.937748789	-17.502161950	2.39E-19	3.04E-20	2.38E-19	1.27E-20	4.96E-20	7.01E-21
180	16.939126424	-17.507439554	2.18E-18	3.42E-20	1.79E-18	1.40E-20	9.58E-19	1.15E-20

IRAS14378-3651								
1	220.245188574	-37.079012817	3.27E-19	2.79E-20	2.83E-18	1.34E-20	1.04E-17	1.62E-20
2	220.245601058	-37.076101935	1.31E-18	3.17E-20	1.96E-18	5.65E-20	5.23E-19	2.53E-20
3	220.245991264	-37.075613240	2.83E-18	5.19E-20	8.56E-18	1.44E-19	3.96E-17	4.59E-19
4	220.253339337	-37.068994414	7.58E-18	3.42E-20	4.60E-17	4.51E-20	7.21E-17	1.04E-19
5	220.252564206	-37.065958219	3.22E-18	3.17E-20	1.29E-17	1.51E-20	1.43E-17	2.08E-20
6	220.251577818	-37.065198208	9.14E-19	4.56E-20	1.02E-18	4.69E-20	3.67E-19	1.69E-20
7	220.251021993	-37.064251976	8.68E-19	3.04E-20	8.42E-19	1.73E-20	3.66E-19	7.66E-21
8	220.251849954	-37.063106953	7.93E-18	1.71E-19	6.33E-18	1.60E-19	1.30E-18	3.18E-20
9	220.252769577	-37.062017270	1.97E-17	4.05E-20	3.30E-17	2.05E-20	1.96E-17	2.92E-20
10	220.247466409	-37.064321421	1.34E-16	1.38E-19	2.43E-16	1.56E-19	1.04E-16	1.45E-19
11	220.234749361	-37.069964277	1.54E-18	3.17E-20	4.75E-18	1.21E-20	5.26E-18	8.34E-21

IRASF08572+3915								
1	135.104376272	39.065192661	2.75E-19	3.17E-20	4.11E-19	1.84E-20	1.34E-19	9.47E-21
2	135.105338178	39.064726566	4.73E-19	4.43E-20	3.69E-19	5.18E-20	1.80E-19	2.35E-20
3	135.107809889	39.062810319	1.10E-18	3.04E-20	8.77E-19	1.53E-20	1.83E-19	7.07E-21
4	135.107890839	39.062914247	3.69E-19	4.94E-20	6.46E-19	2.63E-20	1.00E-19	1.13E-20

*Table 5 continued*

**Table 5** (*continued*)

ID	R.A.	Decl.	$f_{336}$	$\sigma_{f_{336}}$	$f_{435}$	$\sigma_{f_{435}}$	$f_{814}$	$\sigma_{f_{814}}$
5	135.107963073	39.062689830	5.23E-19	3.04E-20	3.53E-19	1.44E-20	9.84E-20	5.97E-21
6	135.109960161	39.063250810	7.30E-19	3.04E-20	8.07E-19	2.58E-20	2.24E-19	9.51E-21
7	135.109564681	39.063170540	1.08E-18	3.67E-20	8.11E-19	1.86E-20	2.18E-19	8.03E-21
8	135.110918073	39.063011108	3.31E-19	3.42E-20	2.27E-19	1.96E-20	5.21E-20	6.22E-21
IRASF12112+0305								
1	183.444389005	2.808148590	4.54E-18	2.66E-20	6.95E-18	1.66E-20	3.24E-18	1.03E-20
2	183.442171690	2.809289987	1.63E-18	3.80E-20	1.46E-18	3.00E-20	7.19E-19	1.23E-20
3	183.443025620	2.809631292	3.39E-19	2.79E-20	1.84E-19	1.63E-20	8.56E-20	7.08E-21
4	183.441938663	2.809256343	4.44E-19	3.55E-20	4.76E-19	3.86E-20	1.38E-19	8.78E-21
5	183.441748544	2.809609326	1.83E-18	3.92E-20	1.12E-18	4.33E-20	4.41E-19	1.79E-20
6	183.441794866	2.809499470	5.16E-19	4.43E-20	7.01E-19	5.64E-20	2.33E-19	2.96E-20
7	183.442343064	2.810497195	1.42E-18	3.80E-20	1.10E-18	3.60E-20	3.04E-19	1.28E-20
8	183.440951228	2.809444908	6.39E-19	3.29E-20	3.81E-19	1.88E-20	7.85E-20	1.05E-20
9	183.442252824	2.810559867	4.89E-19	3.67E-20	4.69E-19	2.17E-20	2.03E-19	1.08E-20
10	183.442462829	2.811423844	1.98E-18	6.46E-20	3.79E-18	9.85E-20	1.14E-18	3.30E-20
11	183.442227065	2.811234192	1.63E-18	5.70E-20	1.76E-18	8.83E-20	1.21E-18	6.41E-20
12	183.440905977	2.810949464	4.60E-19	3.80E-20	6.14E-19	2.87E-20	3.19E-19	1.38E-20
13	183.442451914	2.811659334	8.75E-19	6.84E-20	1.34E-18	8.22E-20	5.85E-19	3.02E-20
14	183.439770379	2.810306124	7.24E-19	2.91E-20	6.06E-19	1.50E-20	1.75E-19	9.34E-21
15	183.442932505	2.811755486	4.94E-19	3.29E-20	5.19E-19	1.50E-20	2.81E-19	7.86E-21
16	183.442623709	2.812045792	1.11E-18	3.29E-20	1.61E-18	3.57E-20	4.83E-19	1.05E-20
17	183.442276125	2.811961758	6.07E-19	3.04E-20	5.82E-19	2.17E-20	1.38E-19	8.28E-21
18	183.441649964	2.811871181	7.83E-19	3.92E-20	7.71E-19	3.06E-20	1.90E-19	1.22E-20
19	183.442957512	2.812775989	9.41E-19	3.04E-20	1.00E-18	1.69E-20	2.92E-19	5.73E-21
20	183.439372320	2.811241919	3.56E-19	2.79E-20	1.63E-19	1.47E-20	7.43E-20	5.24E-21
21	183.443162665	2.813415484	3.33E-19	2.79E-20	5.38E-19	2.77E-20	1.40E-19	6.23E-21
22	183.443092592	2.813436515	5.50E-19	3.17E-20	6.47E-19	2.77E-20	1.47E-19	9.41E-21
23	183.443106795	2.813654752	1.94E-18	2.79E-20	1.93E-18	1.91E-20	5.51E-19	7.36E-21
24	183.443220359	2.813746669	6.25E-19	2.66E-20	4.82E-19	1.50E-20	2.10E-19	6.16E-21
25	183.439802170	2.813516804	2.34E-19	3.80E-20	2.97E-19	1.24E-20	5.03E-20	5.45E-21
IRASF17207-0014								
1	260.837198269	-0.287979491	2.78E-17	3.17E-20	5.51E-17	1.77E-20	3.83E-17	3.97E-20
2	260.842028703	-0.283223436	9.60E-19	2.66E-20	2.40E-18	4.01E-20	9.46E-19	9.24E-20
3	260.842545441	-0.284283076	1.43E-18	3.92E-20	2.70E-18	4.23E-20	1.13E-18	2.04E-20
4	260.842200429	-0.282861509	7.46E-18	2.91E-20	1.40E-17	2.79E-20	6.36E-18	2.36E-20
5	260.841597178	-0.283210990	1.29E-18	3.17E-20	4.34E-18	6.79E-20	8.34E-18	1.76E-19
6	260.841699543	-0.283259702	8.80E-18	4.18E-20	1.29E-17	8.38E-20	5.51E-18	3.52E-19
7	260.841837898	-0.283231376	4.00E-18	3.80E-20	8.64E-18	8.76E-20	5.61E-18	2.80E-19
8	260.841058401	-0.283173502	1.11E-18	3.29E-20	3.10E-18	2.98E-20	2.55E-18	5.44E-20
9	260.836341192	-0.281360948	6.92E-17	3.80E-20	1.37E-16	4.28E-20	8.27E-17	8.68E-20
Mrk 231 - Center								
1	194.059834915	56.874131763	5.86E-18	1.73E-19	1.34E-17	3.66E-19	4.63E-18	1.48E-19

Table 5 continued

**Table 5** (*continued*)

ID	R.A.	Decl.	$f_{336}$	$\sigma_{f_{336}}$	$f_{435}$	$\sigma_{f_{435}}$	$f_{814}$	$\sigma_{f_{814}}$
2	194.059833841	56.873642959	1.10E-17	2.95E-19	1.31E-17	6.12E-19	7.36E-18	7.87E-19
Mrk 231 - Extended Galaxy								
1	194.062618168	56.875447094	2.19E-19	3.67E-20	7.84E-19	1.42E-20	2.66E-19	5.09E-21
2	194.059362818	56.875227717	3.33E-19	2.91E-20	2.72E-18	1.96E-20	2.42E-18	9.83E-21
3	194.062816723	56.874502731	3.74E-19	2.79E-20	6.58E-19	1.59E-20	2.28E-19	7.57E-21
4	194.050987104	56.876546488	3.26E-19	2.66E-20	4.73E-19	1.71E-20	2.79E-19	4.91E-21
5	194.058132336	56.874168111	7.04E-19	5.95E-20	3.34E-18	8.01E-20	2.96E-18	3.24E-20
6	194.060359373	56.873286213	1.23E-18	7.60E-20	1.66E-18	1.67E-19	8.06E-19	1.07E-19
7	194.055163293	56.873972517	1.14E-18	3.42E-20	2.53E-18	2.92E-20	9.81E-19	1.09E-20
8	194.060152531	56.872853822	1.15E-17	1.19E-19	1.70E-17	1.64E-19	6.42E-18	1.13E-19
9	194.054717691	56.873982656	2.85E-19	3.67E-20	7.69E-19	3.91E-20	2.75E-19	1.50E-20
10	194.060334669	56.872920241	1.99E-18	1.22E-19	1.76E-18	1.87E-19	6.63E-19	1.24E-19
11	194.059504658	56.872859932	4.51E-19	7.34E-20	1.28E-18	8.88E-20	7.72E-19	3.25E-20
12	194.059790383	56.872658683	3.11E-18	1.11E-19	4.31E-18	1.74E-19	1.38E-18	4.67E-20
13	194.060201324	56.872544918	5.78E-19	7.85E-20	8.33E-19	1.30E-19	2.81E-19	4.26E-20
14	194.058896215	56.872460715	1.14E-18	8.99E-20	2.78E-18	1.61E-19	6.66E-19	6.86E-20
15	194.058929716	56.872678827	1.33E-17	3.05E-19	1.79E-17	4.76E-19	5.81E-18	2.46E-19
16	194.059507661	56.872436584	1.97E-18	1.01E-19	1.33E-18	1.86E-19	1.08E-18	6.24E-20
17	194.059782501	56.872528884	1.09E-18	8.10E-20	8.14E-19	2.23E-19	1.74E-19	4.29E-20
18	194.056184871	56.872672378	6.97E-19	2.79E-20	1.66E-18	1.82E-20	6.49E-19	6.98E-21
19	194.051681795	56.873287796	1.48E-19	3.04E-20	7.23E-20	1.69E-20	4.68E-20	5.16E-21
20	194.058323461	56.872196389	1.69E-19	3.67E-20	1.93E-19	1.67E-20	3.12E-20	6.55E-21
21	194.056634064	56.872152713	2.10E-19	2.79E-20	7.66E-19	1.52E-20	3.11E-19	6.11E-21
22	194.058427778	56.870652081	3.48E-18	4.05E-20	6.51E-18	1.63E-20	2.27E-18	5.57E-21
23	194.057168387	56.870623558	9.60E-19	3.29E-20	1.88E-18	1.90E-20	5.30E-19	4.97E-21
24	194.053721360	56.871088503	8.87E-19	3.55E-20	1.91E-18	1.86E-20	6.29E-19	7.20E-21
25	194.053865501	56.870639610	1.45E-18	3.04E-20	2.82E-18	1.90E-20	1.11E-18	5.27E-21
26	194.054559180	56.870334239	2.37E-19	3.29E-20	1.99E-19	1.60E-20	6.73E-20	5.72E-21
27	194.053851480	56.869025517	4.71E-18	2.79E-20	9.05E-18	1.67E-20	3.04E-18	6.92E-21
28	194.050822057	56.867598372	2.40E-19	2.79E-20	2.27E-19	1.17E-20	1.22E-19	4.51E-21
NGC 3256								
1	156.938847659	-43.920972207	6.34E-18	3.04E-20	1.16E-17	1.33E-20	5.06E-18	9.35E-21
2	156.937446200	-43.917401271	8.74E-17	2.18E-19	3.95E-16	1.07E-19	2.69E-16	6.92E-19
3	156.957457643	-43.926641923	3.56E-18	2.91E-20	2.47E-17	1.43E-20	6.60E-17	5.69E-20
4	156.953743483	-43.924400772	1.02E-17	3.29E-20	3.65E-17	3.13E-20	3.61E-17	5.21E-20
5	156.960454492	-43.926141908	5.17E-17	4.81E-20	8.11E-17	7.43E-20	3.73E-17	4.45E-20
6	156.957522591	-43.922692436	2.47E-18	3.04E-20	1.82E-17	1.30E-20	5.47E-17	1.36E-19
7	156.975540763	-43.929940669	2.04E-16	1.38E-19	3.81E-16	1.92E-19	1.15E-16	2.31E-19
8	156.976180843	-43.930211531	2.64E-18	3.42E-20	5.54E-18	1.31E-20	3.46E-18	6.55E-21
9	156.951006734	-43.918937971	1.17E-18	3.29E-20	8.45E-18	1.32E-20	3.90E-17	5.27E-20
10	156.941274253	-43.913136873	2.76E-17	4.30E-20	9.33E-17	3.31E-20	6.24E-17	1.10E-19
11	156.947146751	-43.916398824	3.24E-19	2.53E-20	4.15E-18	1.02E-20	2.35E-17	3.61E-20
12	156.969133450	-43.926195523	4.24E-19	2.79E-20	3.68E-19	1.40E-20	8.50E-20	5.32E-21
13	156.934232358	-43.910484466	9.96E-18	2.79E-20	3.97E-17	2.04E-20	4.16E-17	6.97E-20

*Table 5 continued*

**Table 5** (*continued*)

ID	R.A.	Decl.	$f_{336}$	$\sigma_{f_{336}}$	$f_{435}$	$\sigma_{f_{435}}$	$f_{814}$	$\sigma_{f_{814}}$
14	156.978953832	-43.929530068	1.30E-17	4.56E-20	5.64E-17	2.45E-20	6.88E-17	8.28E-20
15	156.972192682	-43.926971948	8.83E-18	3.67E-20	4.70E-19	1.97E-20	1.59E-19	7.46E-21
16	156.938411006	-43.911223207	1.84E-17	3.29E-20	3.53E-17	2.64E-20	2.12E-17	3.01E-20
17	156.953085895	-43.917519337	4.26E-18	2.91E-20	9.60E-18	1.37E-20	6.81E-18	1.34E-20
18	156.961177901	-43.919181476	5.95E-17	5.06E-20	1.93E-16	1.43E-19	5.01E-17	1.76E-19
19	156.934842777	-43.908153361	5.96E-19	2.79E-20	5.46E-18	1.17E-20	3.08E-17	4.42E-20
20	156.933409124	-43.906790552	4.51E-17	9.37E-20	1.21E-16	7.01E-20	6.90E-17	1.13E-19
21	156.954905210	-43.916107035	1.93E-17	3.17E-20	3.59E-17	1.92E-20	1.95E-17	2.68E-20
22	156.967620549	-43.921105889	7.61E-18	3.17E-20	5.35E-17	3.58E-20	5.79E-17	1.64E-19
23	156.943175045	-43.910562994	8.48E-18	2.91E-20	2.95E-17	2.20E-20	3.19E-17	3.95E-20
24	156.947636840	-43.911595838	4.49E-19	3.04E-20	1.22E-18	1.05E-20	1.89E-18	5.59E-21
25	156.947663413	-43.908459000	1.41E-16	9.50E-20	3.37E-16	2.78E-19	2.62E-16	4.81E-19
26	156.936365470	-43.905141536	5.23E-19	3.29E-20	1.46E-18	1.16E-20	4.51E-19	4.22E-21
27	156.946899705	-43.907988212	3.20E-18	3.92E-20	2.01E-17	1.51E-20	7.21E-17	9.68E-20
28	156.931227420	-43.902400664	3.65E-19	3.29E-20	3.96E-19	1.44E-20	1.68E-19	5.84E-21
29	156.953425523	-43.911555290	3.47E-19	3.80E-20	1.14E-18	1.26E-20	4.26E-19	6.23E-21
30	156.961788530	-43.915101580	5.79E-19	2.66E-20	8.55E-19	1.59E-20	4.31E-19	7.57E-21
31	156.933535569	-43.902180171	4.21E-19	2.41E-20	3.61E-19	1.19E-20	4.33E-19	1.31E-20
32	156.946148173	-43.907201601	2.04E-18	3.04E-20	1.12E-17	1.45E-20	1.62E-17	2.23E-20
33	156.973924613	-43.919265812	1.86E-18	3.17E-20	4.24E-18	1.48E-20	3.72E-18	6.00E-21
34	156.933574505	-43.901973654	5.21E-19	2.91E-20	5.70E-19	1.38E-20	2.18E-19	8.52E-21
35	156.960374620	-43.913018658	4.43E-19	3.04E-20	9.31E-19	1.79E-20	3.17E-19	8.46E-21
36	156.954365756	-43.910045670	1.71E-16	1.30E-19	3.91E-16	1.62E-19	2.16E-16	2.82E-19
37	156.971677577	-43.917552504	7.45E-19	2.66E-20	3.95E-19	1.87E-20	1.53E-19	2.67E-20
38	156.957924474	-43.911597032	4.30E-19	3.17E-20	8.00E-19	1.93E-20	2.65E-19	9.89E-21
39	156.959465854	-43.911976787	3.57E-19	2.91E-20	6.36E-19	2.25E-20	2.50E-19	1.07E-20
40	156.959654875	-43.911901799	2.28E-18	3.67E-20	2.67E-18	1.75E-20	7.71E-19	9.61E-21
41	156.954943420	-43.909491213	5.92E-19	3.29E-20	8.62E-19	1.88E-20	2.64E-19	1.19E-20
42	156.964932400	-43.912538428	1.25E-15	8.76E-19	2.33E-16	1.00E-18	4.08E-16	1.90E-18
43	156.957011995	-43.910484188	6.42E-19	3.55E-20	4.08E-19	1.76E-20	7.90E-20	8.35E-21
44	156.955339665	-43.909379987	5.33E-19	3.80E-20	6.63E-19	2.32E-20	2.27E-19	1.35E-20
45	156.959063971	-43.910986676	4.83E-19	3.29E-20	8.78E-19	1.78E-20	2.92E-19	7.89E-21
46	156.955491309	-43.909190278	1.06E-18	3.92E-20	1.15E-18	2.74E-20	1.67E-19	1.05E-20
47	156.954115513	-43.908614519	2.64E-19	3.04E-20	9.64E-19	2.25E-20	2.98E-19	9.27E-21
48	156.959160782	-43.910773809	4.12E-19	3.29E-20	2.60E-19	1.41E-20	4.39E-20	8.92E-21
49	156.956716871	-43.909719000	5.93E-19	2.53E-20	4.32E-19	1.41E-20	1.52E-19	6.73E-21
50	156.953817730	-43.908000671	9.29E-19	2.79E-20	1.96E-18	2.01E-20	6.28E-19	9.17E-21
51	156.955823530	-43.909210608	3.21E-19	3.92E-20	3.62E-19	3.24E-20	1.11E-19	1.33E-20
52	156.956035377	-43.908950528	1.18E-18	6.08E-20	1.37E-18	5.58E-20	3.04E-19	2.42E-20
53	156.956535206	-43.909240475	6.60E-19	3.55E-20	1.47E-18	1.85E-20	5.53E-19	9.30E-21
54	156.960319423	-43.910703313	1.63E-18	3.55E-20	1.59E-18	1.54E-20	5.06E-19	9.82E-21
55	156.956062448	-43.909092456	8.06E-19	5.06E-20	1.14E-18	4.26E-20	3.58E-19	2.08E-20
56	156.959449515	-43.910429753	1.04E-18	2.91E-20	1.69E-18	1.84E-20	6.60E-19	1.03E-20
57	156.948292671	-43.902586623	7.75E-16	7.65E-19	9.41E-16	6.07E-19	4.49E-16	1.35E-18
58	156.956851859	-43.908911927	4.60E-18	8.48E-20	2.93E-18	7.40E-20	9.54E-19	3.26E-20
59	156.953347549	-43.907089812	1.08E-18	3.80E-20	3.02E-18	2.19E-20	1.02E-18	1.22E-20
60	156.954447709	-43.907854424	1.09E-18	3.67E-20	7.89E-19	2.62E-20	2.34E-19	1.15E-20

*Table 5 continued*

**Table 5** (*continued*)

ID	R.A.	Decl.	$f_{336}$	$\sigma_{f_{336}}$	$f_{435}$	$\sigma_{f_{435}}$	$f_{814}$	$\sigma_{f_{814}}$
61	156.953338961	-43.906846003	1.83E-18	3.80E-20	1.45E-18	2.87E-20	4.14E-19	1.21E-20
62	156.957056386	-43.908914571	2.59E-18	7.72E-20	2.15E-18	6.31E-20	8.15E-19	1.48E-20
63	156.957391037	-43.909029071	2.48E-19	4.30E-20	2.62E-19	2.26E-20	1.23E-19	9.75E-21
64	156.957346182	-43.909126978	5.16E-19	4.18E-20	4.26E-19	1.51E-20	1.06E-19	7.52E-21
65	156.953383491	-43.907231309	5.23E-19	4.18E-20	6.23E-19	2.73E-20	2.01E-19	1.46E-20
66	156.956105199	-43.908521181	4.73E-19	3.55E-20	2.07E-19	1.84E-20	5.34E-20	7.87E-21
67	156.954563902	-43.907847881	5.58E-19	3.17E-20	7.37E-19	2.29E-20	1.41E-19	1.44E-20
68	156.953639889	-43.907192274	5.49E-19	3.29E-20	3.59E-19	1.70E-20	1.18E-19	9.00E-21
69	156.959136393	-43.909518476	8.39E-19	4.43E-20	7.56E-19	2.93E-20	1.84E-19	1.19E-20
70	156.956899657	-43.908688492	6.84E-19	4.05E-20	4.66E-19	3.55E-20	6.35E-20	1.00E-20
71	156.982535296	-43.919045697	2.57E-18	2.66E-20	1.40E-17	1.74E-20	1.83E-17	2.69E-20
72	156.969226509	-43.913679510	6.04E-19	3.42E-20	2.00E-18	1.85E-20	6.26E-19	1.38E-20
73	156.955628696	-43.907702577	3.06E-18	5.44E-20	1.96E-18	3.25E-20	3.55E-19	1.60E-20
74	156.955333103	-43.907783859	7.73E-19	3.17E-20	6.22E-19	2.28E-20	6.19E-20	9.79E-21
75	156.957373231	-43.908570241	8.65E-19	4.43E-20	3.40E-19	2.41E-20	1.73E-19	1.47E-20
76	156.958162043	-43.908640587	3.27E-19	3.42E-20	3.20E-19	1.38E-20	5.05E-20	1.03E-20
77	156.957883889	-43.908559297	6.33E-19	3.67E-20	1.88E-19	1.71E-20	3.72E-20	6.78E-21
78	156.956115962	-43.907569839	1.05E-17	6.20E-20	5.76E-18	5.06E-20	9.23E-19	2.69E-20
79	156.959644004	-43.906493783	7.31E-19	6.20E-20	6.91E-19	8.70E-20	2.34E-19	5.77E-20
80	156.955295936	-43.907206344	3.74E-19	3.67E-20	2.80E-19	3.17E-20	8.67E-20	1.38E-20
81	156.955403649	-43.907105855	2.55E-19	4.18E-20	2.79E-19	3.57E-20	3.91E-19	1.47E-20
82	156.954701206	-43.906423978	5.25E-19	3.29E-20	1.62E-18	3.27E-20	6.01E-19	1.71E-20
83	156.971288772	-43.913761250	6.75E-19	3.42E-20	1.46E-18	2.02E-20	5.07E-19	8.54E-21
84	156.975543511	-43.914545708	3.94E-19	3.42E-20	3.15E-18	1.32E-20	1.13E-17	1.39E-20
85	156.954092990	-43.906425732	3.06E-19	3.80E-20	1.57E-18	2.89E-20	5.11E-19	1.83E-20
86	156.955336689	-43.906626282	6.64E-18	4.94E-20	1.68E-17	4.85E-20	5.60E-18	2.42E-20
87	156.953335297	-43.905446708	6.79E-18	4.56E-20	1.64E-17	3.88E-20	5.25E-18	1.88E-20
88	156.971535450	-43.913706378	7.94E-19	3.42E-20	1.71E-18	1.95E-20	5.14E-19	8.05E-21
89	156.955922001	-43.907021449	7.86E-19	4.43E-20	1.63E-18	3.19E-20	5.28E-19	1.42E-20
90	156.954955769	-43.906597173	7.81E-19	4.18E-20	2.45E-18	2.37E-20	7.23E-19	1.14E-20
91	156.953187609	-43.905728299	3.75E-19	3.29E-20	1.07E-18	1.87E-20	2.90E-19	1.12E-20
92	156.954805451	-43.906565986	4.72E-19	3.55E-20	9.44E-19	3.07E-20	2.38E-19	1.26E-20
93	156.956833784	-43.907178870	1.86E-18	5.06E-20	1.43E-18	6.13E-20	7.59E-19	3.94E-20
94	156.966131608	-43.911108813	1.64E-18	3.42E-20	2.25E-18	1.71E-20	6.55E-19	9.56E-21
95	156.955662848	-43.906724758	1.31E-18	4.18E-20	3.22E-18	3.58E-20	9.08E-19	1.92E-20
96	156.954028963	-43.905665047	2.35E-18	3.55E-20	6.12E-18	3.37E-20	1.98E-18	1.93E-20
97	156.955905677	-43.906883727	7.22E-19	4.68E-20	7.31E-19	2.76E-20	1.88E-19	1.09E-20
98	156.976986592	-43.915783221	4.83E-19	2.66E-20	1.38E-18	1.32E-20	4.25E-19	5.56E-21
99	156.955634213	-43.906573079	5.68E-19	4.18E-20	1.64E-18	3.89E-20	4.95E-19	1.34E-20
100	156.956218953	-43.906627049	1.47E-18	5.06E-20	2.51E-18	4.46E-20	6.87E-19	2.67E-20
101	156.960624256	-43.907893973	3.39E-19	2.79E-20	8.55E-19	3.17E-20	8.67E-19	2.77E-20
102	156.956042937	-43.905923459	7.48E-19	4.18E-20	1.27E-18	5.08E-20	6.63E-19	2.61E-20
103	156.956132700	-43.906569362	1.50E-18	4.18E-20	4.16E-18	3.32E-20	1.29E-18	2.03E-20
104	156.974551450	-43.913649026	1.12E-18	3.04E-20	2.63E-18	2.93E-20	7.93E-19	1.25E-20
105	156.955738702	-43.906380890	6.00E-19	3.55E-20	1.58E-18	3.78E-20	6.67E-19	1.62E-20
106	156.960009465	-43.907527710	6.93E-18	3.80E-20	3.36E-17	1.24E-19	3.48E-17	1.53E-19
107	156.956508610	-43.905418934	5.42E-17	2.11E-19	8.23E-17	2.88E-19	3.58E-17	1.23E-19

*Table 5 continued*

**Table 5** (*continued*)

ID	R.A.	Decl.	$f_{336}$	$\sigma_{f_{336}}$	$f_{435}$	$\sigma_{f_{435}}$	$f_{814}$	$\sigma_{f_{814}}$
108	156.956044894	-43.905489184	1.78E-17	1.22E-19	2.49E-17	2.23E-19	7.31E-18	1.35E-19
109	156.955320072	-43.906290132	2.73E-19	3.67E-20	1.99E-19	2.49E-20	8.67E-20	1.19E-20
110	156.941110968	-43.898787718	6.66E-17	5.32E-20	1.72E-16	7.67E-20	1.07E-16	1.59E-19
111	156.954814721	-43.905996785	5.99E-19	4.18E-20	1.11E-18	5.50E-20	4.31E-19	2.15E-20
112	156.956795271	-43.906805867	3.24E-19	4.81E-20	4.98E-19	3.58E-20	1.37E-19	2.15E-20
113	156.957092814	-43.906491680	8.58E-19	6.20E-20	8.08E-19	4.81E-20	4.23E-19	2.54E-20
114	156.957169965	-43.905641362	2.30E-18	5.44E-20	3.72E-18	1.11E-19	1.27E-18	5.17E-20
115	156.946530829	-43.901753391	8.34E-18	3.29E-20	1.32E-17	1.70E-20	5.57E-18	8.77E-21
116	156.964895560	-43.909789517	3.46E-19	3.17E-20	1.26E-18	1.91E-20	3.61E-19	7.65E-21
117	156.955639274	-43.905946176	1.50E-18	3.92E-20	2.73E-18	6.21E-20	7.45E-19	1.91E-20
118	156.959756948	-43.906127892	5.96E-19	4.56E-20	1.43E-18	1.13E-19	3.09E-18	1.06E-19
119	156.955092282	-43.905735605	2.56E-19	3.42E-20	5.81E-19	2.87E-20	1.54E-19	1.47E-20
120	156.954631107	-43.905205758	4.61E-19	3.80E-20	8.06E-19	2.10E-20	2.76E-19	1.18E-20
121	156.955145926	-43.905321609	8.42E-19	3.17E-20	1.97E-18	2.70E-20	6.71E-19	1.22E-20
122	156.966289721	-43.910192938	3.86E-19	2.91E-20	1.24E-18	1.68E-20	4.63E-19	8.76E-21
123	156.961885408	-43.908296720	1.62E-18	1.30E-19	2.04E-18	1.69E-19	8.85E-19	4.00E-20
124	156.958297710	-43.905470611	1.74E-17	1.10E-19	3.77E-17	1.61E-19	1.43E-17	8.75E-20
125	156.957783123	-43.905464132	1.32E-18	4.68E-20	3.12E-18	6.97E-20	2.22E-18	5.90E-20
126	156.963048646	-43.908203490	3.34E-19	3.42E-20	1.03E-18	3.27E-20	1.08E-18	2.25E-20
127	156.958372436	-43.906358656	4.70E-19	4.81E-20	1.29E-18	1.50E-19	1.80E-18	9.56E-20
128	156.959692386	-43.906287106	5.54E-19	4.68E-20	2.21E-18	6.55E-20	1.42E-18	6.97E-20
129	156.959772153	-43.906646244	2.06E-18	7.09E-20	7.25E-18	1.01E-19	6.54E-18	8.17E-20
130	156.960885889	-43.907119374	3.37E-19	3.80E-20	4.35E-19	2.88E-20	3.86E-19	2.19E-20
131	156.955999268	-43.905367222	2.93E-18	7.34E-20	4.06E-18	1.35E-19	1.05E-18	5.44E-20
132	156.958478216	-43.905744839	1.51E-18	7.22E-20	1.88E-18	1.75E-19	2.81E-18	6.18E-20
133	156.956221772	-43.905330086	2.25E-18	8.74E-20	2.36E-18	1.10E-19	6.68E-19	5.74E-20
134	156.956596865	-43.905207405	1.81E-18	8.86E-20	4.41E-18	1.40E-19	1.73E-18	7.22E-20
135	156.960330325	-43.906203856	1.70E-17	1.05E-19	2.39E-17	1.96E-19	1.06E-17	1.37E-19
136	156.963180474	-43.907763024	7.00E-19	3.29E-20	8.33E-19	2.13E-20	4.65E-19	1.06E-20
137	156.960229603	-43.906665413	9.64E-19	7.60E-20	1.39E-18	7.48E-20	3.67E-19	2.56E-20
138	156.957695841	-43.905679019	7.35E-19	5.19E-20	1.60E-18	8.46E-20	2.89E-19	4.20E-20
139	156.958611067	-43.905987202	4.44E-18	7.47E-20	5.21E-18	1.80E-19	2.93E-18	1.03E-19
140	156.956506836	-43.904561391	1.48E-18	4.18E-20	4.52E-18	7.38E-20	3.10E-18	3.26E-20
141	156.978723906	-43.914256634	3.63E-19	3.17E-20	9.03E-19	1.44E-20	3.20E-19	5.34E-21
142	156.958103096	-43.905632499	5.01E-18	8.61E-20	5.73E-18	1.52E-19	3.56E-18	1.50E-19
143	156.964428285	-43.908290784	5.04E-19	3.80E-20	8.03E-19	1.72E-20	2.65E-19	1.04E-20
144	156.960661928	-43.906632018	9.12E-19	6.20E-20	9.50E-19	1.02E-19	5.71E-19	4.06E-20
145	156.975940296	-43.913124252	5.32E-19	3.92E-20	1.37E-18	1.48E-20	5.76E-19	7.73E-21
146	156.967323010	-43.909442925	3.56E-19	3.42E-20	9.44E-19	1.49E-20	2.54E-19	7.46E-21
147	156.956592839	-43.904751258	1.22E-18	5.57E-20	3.21E-18	8.68E-20	2.92E-18	3.29E-20
148	156.960562349	-43.906039006	3.63E-18	9.75E-20	4.28E-18	2.16E-19	4.01E-18	1.10E-19
149	156.963326585	-43.906356648	1.14E-17	9.88E-20	1.31E-17	1.63E-19	2.83E-18	2.37E-19
150	156.956630759	-43.904886688	6.68E-19	4.43E-20	1.23E-18	7.62E-20	3.44E-19	2.61E-20
151	156.964737894	-43.908397509	4.21E-19	4.05E-20	1.05E-19	2.15E-20	8.88E-20	9.39E-21
152	156.962515338	-43.907087314	3.50E-19	3.29E-20	9.40E-19	3.25E-20	7.65E-19	3.22E-20
153	156.966133873	-43.908434700	9.27E-19	4.43E-20	1.09E-18	2.34E-20	3.76E-19	8.40E-21
154	156.956464734	-43.904750923	5.77E-19	5.06E-20	4.07E-19	8.66E-20	1.88E-19	3.22E-20

Table 5 continued

**Table 5** (*continued*)

ID	R.A.	Decl.	$f_{336}$	$\sigma_{f_{336}}$	$f_{435}$	$\sigma_{f_{435}}$	$f_{814}$	$\sigma_{f_{814}}$
155	156.956662367	-43.904839417	4.76E-19	5.32E-20	1.31E-18	6.03E-20	6.12E-19	3.27E-20
156	156.954943887	-43.903590564	3.61E-19	2.66E-20	2.51E-18	1.74E-20	2.13E-18	8.73E-21
157	156.962336473	-43.906602974	7.84E-19	4.30E-20	1.91E-18	7.93E-20	7.56E-19	5.67E-20
158	156.965336301	-43.908167373	3.91E-18	4.81E-20	4.12E-18	4.25E-20	1.63E-18	1.54E-20
159	156.965164203	-43.908298456	1.90E-18	4.30E-20	1.28E-18	3.10E-20	2.77E-19	2.05E-20
160	156.957317496	-43.904789884	1.69E-18	4.30E-20	5.55E-18	3.09E-20	5.72E-18	1.79E-20
161	156.959716307	-43.905780983	1.13E-17	2.79E-19	1.91E-17	6.48E-19	8.96E-18	2.69E-19
162	156.961666630	-43.906652272	1.21E-18	4.94E-20	1.51E-18	6.31E-20	8.88E-19	3.13E-20
163	156.965149016	-43.908175302	6.20E-19	3.42E-20	6.39E-19	3.86E-20	5.87E-20	1.55E-20
164	156.962530532	-43.906871971	1.17E-18	3.29E-20	2.83E-18	2.65E-20	3.35E-18	2.44E-20
165	156.960804770	-43.906267765	2.11E-18	8.23E-20	2.59E-18	1.67E-19	9.45E-19	7.12E-20
166	156.964957259	-43.907963076	5.85E-19	4.18E-20	1.02E-18	1.96E-20	4.93E-19	1.47E-20
167	156.959945266	-43.905483439	5.38E-18	4.18E-20	1.91E-17	8.74E-20	2.01E-17	1.33E-19
168	156.968239503	-43.909333595	1.21E-18	3.29E-20	2.86E-18	1.75E-20	9.34E-19	8.80E-21
169	156.978514428	-43.913711736	9.76E-19	4.05E-20	2.46E-18	1.69E-20	7.43E-19	6.27E-21
170	156.954868923	-43.903323399	1.65E-18	3.29E-20	6.14E-18	2.90E-20	2.62E-18	1.92E-20
171	156.960697711	-43.905296591	6.39E-18	7.85E-20	1.14E-17	1.51E-19	7.93E-18	1.42E-19
172	156.942411381	-43.896880334	9.91E-18	3.67E-20	6.66E-17	4.19E-20	9.93E-17	2.39E-19
173	156.960737774	-43.905482312	3.85E-18	6.71E-20	1.07E-17	1.47E-19	1.92E-17	2.50E-19
174	156.965481687	-43.907755087	9.44E-19	3.80E-20	1.36E-18	2.21E-20	7.59E-19	1.66E-20
175	156.965892608	-43.908082753	5.80E-19	4.05E-20	6.36E-19	2.66E-20	2.30E-19	1.61E-20
176	156.980321801	-43.913768834	5.22E-17	5.06E-20	1.25E-16	7.74E-20	8.07E-17	8.56E-20
177	156.960956691	-43.906079841	2.92E-18	7.72E-20	3.28E-18	1.22E-19	9.64E-19	6.41E-20
178	156.961869188	-43.906551086	2.87E-19	3.67E-20	8.26E-19	4.46E-20	1.50E-19	4.03E-20
179	156.962197285	-43.906644609	5.81E-19	4.18E-20	1.08E-18	4.31E-20	6.39E-19	4.81E-20
180	156.968340121	-43.909167646	1.12E-18	3.42E-20	2.89E-18	1.55E-20	1.01E-18	9.70E-21
181	156.9655525340	-43.907986978	5.82E-19	4.94E-20	6.32E-19	4.63E-20	1.18E-19	3.04E-20
182	156.972460379	-43.910930236	3.72E-19	4.18E-20	4.83E-19	1.29E-20	1.68E-19	6.18E-21
183	156.965727561	-43.907972761	2.74E-19	4.56E-20	9.87E-19	4.26E-20	3.40E-19	2.17E-20
184	156.962632847	-43.906158693	4.14E-19	4.18E-20	2.61E-18	8.27E-20	5.57E-18	8.52E-20
185	156.952392158	-43.902052926	1.01E-18	3.04E-20	2.84E-18	1.53E-20	9.88E-19	7.61E-21
186	156.964814126	-43.907405478	4.78E-19	2.79E-20	1.08E-18	2.02E-20	3.67E-19	1.27E-20
187	156.958250904	-43.904217082	3.56E-19	4.81E-20	1.68E-18	4.74E-20	1.46E-18	2.69E-20
188	156.967184477	-43.907623013	1.76E-17	6.08E-20	2.00E-17	3.52E-20	7.40E-18	3.32E-20
189	156.963919733	-43.906901193	1.38E-18	4.94E-20	1.47E-18	4.22E-20	4.56E-19	2.40E-20
190	156.967223793	-43.908388036	2.82E-19	3.92E-20	8.73E-19	1.94E-20	3.16E-19	1.55E-20
191	156.966317623	-43.907618042	2.77E-18	4.05E-20	4.66E-18	2.19E-20	2.28E-18	1.47E-20
192	156.963363633	-43.905993411	4.57E-18	4.18E-20	7.59E-18	1.20E-19	8.45E-18	1.83E-19
193	156.965741622	-43.907634000	7.60E-19	4.18E-20	7.61E-19	2.37E-20	8.53E-20	1.25E-20
194	156.966787202	-43.907618564	1.40E-18	3.55E-20	3.56E-18	2.58E-20	1.13E-18	1.54E-20
195	156.964211095	-43.906747729	6.72E-19	4.43E-20	9.69E-19	6.56E-20	2.45E-19	5.22E-20
196	156.977776898	-43.912650484	6.93E-19	4.05E-20	1.68E-19	1.26E-20	6.44E-20	6.00E-21
197	156.971777619	-43.909556212	2.46E-18	3.67E-20	4.04E-18	2.29E-20	1.30E-18	9.18E-21
198	156.964268892	-43.906229732	2.10E-18	4.18E-20	2.44E-18	4.01E-20	1.65E-18	4.28E-20
199	156.961669535	-43.904245082	3.60E-19	6.58E-20	1.42E-18	1.17E-19	1.56E-18	1.38E-19
200	156.960935624	-43.904295665	1.68E-18	1.01E-19	6.53E-18	1.75E-19	2.04E-17	2.65E-19
201	156.955560579	-43.902378190	1.26E-18	4.43E-20	2.83E-18	2.26E-20	1.28E-18	1.14E-20

*Table 5 continued*

**Table 5** (*continued*)

ID	R.A.	Decl.	$f_{336}$	$\sigma_{f_{336}}$	$f_{435}$	$\sigma_{f_{435}}$	$f_{814}$	$\sigma_{f_{814}}$
202	156.965676035	-43.905381342	2.90E-18	1.09E-19	8.13E-18	3.10E-19	1.12E-17	2.25E-19
203	156.939733126	-43.895635221	9.55E-19	3.17E-20	1.34E-18	1.02E-20	5.73E-19	6.89E-21
204	156.983800121	-43.914476692	7.82E-19	3.55E-20	1.90E-18	1.46E-20	5.36E-19	5.44E-21
205	156.945598559	-43.898077791	1.27E-18	3.29E-20	3.44E-18	1.35E-20	2.63E-18	6.19E-21
206	156.958444148	-43.903389226	2.94E-19	3.80E-20	5.67E-19	2.45E-20	3.53E-19	1.70E-20
207	156.943113703	-43.896557439	7.10E-18	4.30E-20	1.03E-17	1.28E-20	5.34E-18	8.39E-21
208	156.979711983	-43.912606178	3.58E-19	2.91E-20	5.08E-19	1.24E-20	2.25E-19	5.83E-21
209	156.964007615	-43.905785563	1.41E-18	4.56E-20	5.62E-18	9.37E-20	4.57E-18	2.05E-19
210	156.965086626	-43.906054358	9.39E-19	5.57E-20	1.41E-18	5.32E-20	7.01E-19	3.93E-20
211	156.961302557	-43.904525012	7.08E-18	1.16E-19	1.03E-17	3.29E-19	6.22E-18	3.20E-19
212	156.970570186	-43.908447767	5.98E-19	3.55E-20	1.49E-18	1.91E-20	4.64E-19	8.75E-21
213	156.984143540	-43.914099167	2.02E-18	3.29E-20	4.50E-18	1.82E-20	1.40E-18	8.32E-21
214	156.970855793	-43.908514803	5.40E-19	3.80E-20	8.49E-19	1.80E-20	4.27E-19	7.53E-21
215	156.962128386	-43.904428089	7.17E-18	7.34E-20	1.65E-17	8.23E-20	1.12E-17	2.47E-19
216	156.960319232	-43.903540686	4.48E-18	5.57E-20	8.91E-18	1.90E-19	8.97E-18	1.96E-19
217	156.965858010	-43.905934029	9.18E-18	8.61E-20	9.83E-18	1.72E-19	3.96E-18	1.23E-19
218	156.960559918	-43.903658432	2.04E-18	1.13E-19	6.74E-18	2.22E-19	4.17E-18	1.53E-19
219	156.958740618	-43.902987593	4.00E-19	3.42E-20	2.46E-18	3.38E-20	6.28E-18	4.32E-20
220	156.964175023	-43.904942605	6.66E-19	5.19E-20	2.75E-18	1.22E-19	8.76E-18	4.14E-19
221	156.962363552	-43.903771538	1.24E-18	4.05E-20	4.28E-18	7.56E-20	3.15E-18	1.40E-19
222	156.960091881	-43.903321683	1.95E-18	4.43E-20	2.85E-18	8.72E-20	1.99E-18	5.94E-20
223	156.960725535	-43.901721133	1.46E-18	8.23E-20	2.91E-18	1.04E-19	1.72E-18	5.14E-20
224	156.959877956	-43.901899575	1.13E-18	4.68E-20	2.80E-18	6.91E-20	4.08E-18	4.12E-20
225	156.959711173	-43.902679106	1.30E-18	3.67E-20	3.66E-18	5.40E-20	2.43E-18	3.20E-20
226	156.964308979	-43.904878395	2.35E-18	4.43E-20	6.21E-18	1.13E-19	6.26E-18	5.29E-19
227	156.960011434	-43.902560800	1.79E-18	6.58E-20	2.86E-18	8.56E-20	9.23E-19	3.28E-20
228	156.952100713	-43.899999877	2.17E-19	3.55E-20	2.16E-19	1.35E-20	8.41E-20	6.49E-21
229	156.965973202	-43.904301350	2.75E-17	4.32E-19	3.45E-17	4.44E-19	1.45E-17	1.66E-19
230	156.965556020	-43.905549498	2.69E-18	9.50E-20	2.69E-18	1.46E-19	1.16E-18	4.45E-20
231	156.965781411	-43.905631015	1.90E-18	9.62E-20	1.36E-18	1.47E-19	3.68E-19	6.62E-20
232	156.966269997	-43.905879780	4.57E-19	3.42E-20	1.02E-18	2.40E-20	4.56E-19	2.61E-20
233	156.959216467	-43.902728576	6.99E-19	4.05E-20	2.21E-18	6.48E-20	1.65E-18	2.79E-20
234	156.964071037	-43.904235535	1.25E-16	7.48E-19	1.33E-16	1.24E-18	5.09E-17	7.25E-19
235	156.966168527	-43.905672200	9.32E-19	4.30E-20	1.63E-18	4.33E-20	7.87E-19	6.62E-20
236	156.964359273	-43.904476808	1.15E-17	3.46E-19	1.64E-17	6.54E-19	3.67E-18	3.60E-19
237	156.966103836	-43.905567569	1.57E-18	5.32E-20	1.54E-18	4.61E-20	5.35E-19	3.51E-20
238	156.960198593	-43.902496671	7.27E-19	5.06E-20	4.75E-18	1.20E-19	1.17E-17	6.74E-20
239	156.962823509	-43.904011048	3.79E-19	6.33E-20	3.01E-18	1.60E-19	4.02E-18	3.10E-19
240	156.964455320	-43.904170491	1.36E-17	5.53E-19	1.97E-17	8.53E-19	7.98E-18	3.68E-19
241	156.962345091	-43.903067586	1.75E-18	1.27E-19	4.73E-18	3.35E-19	5.12E-18	3.27E-19
242	156.964227026	-43.904555564	3.39E-18	3.94E-19	6.77E-18	6.07E-19	1.50E-18	3.34E-19
243	156.962176002	-43.903711156	7.52E-19	4.18E-20	9.46E-19	5.94E-20	1.16E-18	1.45E-19
244	156.964792451	-43.904572082	4.90E-18	1.15E-19	8.86E-18	3.03E-19	6.75E-18	3.85E-19
245	156.961085475	-43.902938332	1.79E-18	5.32E-20	3.15E-18	1.23E-19	1.27E-18	1.48E-19
246	156.964886233	-43.904471658	7.15E-18	2.58E-19	7.44E-18	3.38E-19	6.07E-18	4.08E-19
247	156.984785876	-43.912853017	1.30E-18	3.67E-20	3.12E-18	1.60E-20	9.51E-19	6.79E-21
248	156.966869989	-43.904995471	4.99E-19	3.29E-20	1.12E-18	4.50E-20	9.56E-19	8.79E-20

*Table 5 continued*

**Table 5** (*continued*)

ID	R.A.	Decl.	$f_{336}$	$\sigma_{f_{336}}$	$f_{435}$	$\sigma_{f_{435}}$	$f_{814}$	$\sigma_{f_{814}}$
249	156.964327737	-43.904131753	1.50E-17	1.40E-18	1.68E-17	1.60E-18	8.39E-18	6.35E-19
250	156.965495850	-43.904536336	2.87E-17	4.32E-19	3.55E-17	6.54E-19	1.68E-17	3.21E-19
251	156.960047616	-43.901978679	5.52E-19	3.92E-20	1.88E-18	4.36E-20	2.55E-18	4.58E-20
252	156.966951796	-43.903856930	6.25E-17	2.77E-19	8.58E-17	5.66E-19	3.98E-17	2.83E-19
253	156.958198260	-43.900580331	1.06E-16	1.30E-19	2.39E-16	1.29E-19	1.01E-16	1.56E-19
254	156.961308552	-43.902206257	3.47E-17	3.47E-19	2.43E-17	5.69E-19	8.22E-18	2.66E-19
255	156.963973746	-43.903498956	3.48E-17	5.31E-19	7.40E-17	8.54E-19	5.56E-17	1.18E-18
256	156.966445872	-43.904236555	2.24E-17	1.73E-19	1.68E-17	3.03E-19	5.32E-18	1.70E-19
257	156.965075204	-43.903627934	9.72E-17	1.31E-18	8.85E-17	1.69E-18	1.96E-17	5.75E-19
258	156.965409584	-43.903818930	3.76E-17	8.50E-19	3.68E-17	1.36E-18	9.42E-18	3.27E-19
259	156.966787911	-43.904720055	1.58E-18	3.55E-20	2.61E-18	5.72E-20	1.82E-18	8.63E-20
260	156.964054635	-43.903398018	9.23E-17	7.52E-19	1.07E-16	1.27E-18	5.91E-17	1.09E-18
261	156.965646656	-43.903642290	7.55E-16	1.84E-18	6.94E-16	2.93E-18	1.55E-16	7.02E-19
262	156.988913485	-43.913755236	6.17E-18	3.29E-20	1.10E-17	1.55E-20	6.43E-18	1.01E-20
263	156.974162624	-43.907391806	2.83E-19	3.42E-20	1.11E-18	1.64E-20	3.74E-19	8.22E-21
264	156.963202140	-43.902709459	2.56E-17	3.53E-19	2.53E-17	6.38E-19	1.00E-17	2.53E-19
265	156.962344503	-43.902694418	5.09E-18	2.71E-19	5.65E-18	5.20E-19	1.97E-18	3.21E-19
266	156.964489138	-43.903679485	3.70E-17	7.41E-19	4.64E-17	1.35E-18	1.35E-17	5.37E-19
267	156.963497594	-43.902846745	3.33E-17	1.87E-19	5.54E-17	4.05E-19	2.10E-17	2.43E-19
268	156.953220835	-43.898608110	9.96E-19	3.55E-20	3.56E-18	1.67E-20	1.34E-18	6.73E-21
269	156.958990724	-43.901057953	3.84E-19	3.55E-20	1.86E-18	2.07E-20	5.71E-19	9.62E-21
270	156.963717343	-43.903115581	1.02E-17	1.89E-19	1.08E-17	6.29E-19	6.21E-18	2.52E-19
271	156.966192919	-43.903975046	7.79E-17	5.93E-19	5.79E-17	7.70E-19	1.12E-17	2.07E-19
272	156.963779668	-43.902887614	7.27E-18	1.94E-19	9.38E-18	2.65E-19	2.14E-18	1.77E-19
273	156.965318553	-43.903353424	5.62E-18	2.63E-19	2.49E-18	4.80E-19	6.36E-18	2.48E-19
274	156.964494786	-43.903014622	4.29E-18	9.24E-20	7.94E-18	3.25E-19	3.96E-18	1.43E-19
275	156.965667952	-43.903859265	1.33E-16	1.45E-18	8.50E-17	1.16E-18	1.52E-17	4.71E-19
276	156.965227530	-43.903720348	1.48E-17	1.10E-18	1.64E-17	8.68E-19	1.28E-18	3.38E-19
277	156.962507246	-43.902297092	3.72E-18	1.46E-19	5.21E-18	3.58E-19	1.41E-18	2.17E-19
278	156.962134167	-43.901908149	8.58E-18	1.49E-19	2.79E-17	2.56E-19	2.05E-17	1.39E-19
279	156.964225614	-43.902996278	5.48E-18	1.10E-19	7.61E-18	2.93E-19	4.54E-18	1.59E-19
280	156.963120801	-43.901988256	1.34E-18	1.09E-19	1.34E-18	2.55E-19	2.63E-18	1.10E-19
281	156.965766303	-43.903843305	9.47E-17	1.43E-18	6.72E-17	9.86E-19	1.31E-17	4.10E-19
282	156.962309195	-43.902184506	4.37E-18	1.11E-19	3.49E-18	2.36E-19	1.49E-18	1.48E-19
283	156.963898925	-43.902584811	3.08E-17	5.18E-19	4.80E-17	6.82E-19	2.45E-17	3.35E-19
284	156.963920687	-43.902756957	9.89E-18	5.36E-19	8.69E-18	4.96E-19	2.67E-18	2.61E-19
285	156.961582456	-43.901844756	1.17E-17	3.00E-19	1.78E-17	3.19E-19	1.05E-17	2.23E-19
286	156.963400720	-43.902607473	7.09E-18	2.47E-19	8.91E-18	3.20E-19	3.38E-18	1.72E-19
287	156.964425668	-43.902836585	6.77E-18	4.30E-19	1.20E-17	6.08E-19	7.84E-18	2.61E-19
288	156.961811235	-43.901929911	1.44E-17	2.63E-19	8.78E-18	2.97E-19	2.21E-18	9.17E-20
289	156.959409722	-43.900873428	5.17E-19	3.42E-20	1.74E-18	2.52E-20	7.06E-19	1.15E-20
290	156.968532510	-43.904794794	8.70E-19	3.55E-20	1.32E-18	3.32E-20	4.31E-19	2.28E-20
291	156.963064609	-43.902306987	2.53E-18	1.85E-19	1.84E-18	3.87E-19	8.29E-19	1.16E-19
292	156.967011449	-43.903709698	6.39E-18	1.28E-19	5.57E-18	3.50E-19	8.04E-19	1.11E-19
293	156.959946260	-43.900483616	7.43E-19	3.55E-20	2.86E-18	4.40E-20	1.94E-18	2.51E-20
294	156.965319088	-43.902775291	1.55E-17	4.36E-19	1.64E-17	6.75E-19	3.23E-18	1.74E-19
295	156.964537155	-43.902411108	5.15E-17	4.18E-19	6.76E-17	6.54E-19	2.86E-17	3.33E-19

*Table 5 continued*

**Table 5** (*continued*)

ID	R.A.	Decl.	$f_{336}$	$\sigma_{f_{336}}$	$f_{435}$	$\sigma_{f_{435}}$	$f_{814}$	$\sigma_{f_{814}}$
296	156.965952481	-43.903212799	5.33E-17	3.86E-19	6.63E-17	6.57E-19	3.14E-17	2.78E-19
297	156.962842232	-43.902227000	3.69E-17	2.37E-19	2.05E-17	4.63E-19	4.01E-18	1.41E-19
298	156.963763810	-43.902408656	8.63E-18	3.27E-19	8.17E-18	3.53E-19	2.61E-18	1.57E-19
299	156.962730898	-43.901678486	1.72E-18	8.99E-20	3.35E-18	1.67E-19	1.11E-18	7.60E-20
300	156.963937473	-43.902427415	1.53E-17	4.80E-19	1.80E-17	6.38E-19	6.47E-18	2.31E-19
301	156.986753720	-43.912399448	3.63E-19	3.55E-20	8.19E-19	1.38E-20	2.48E-19	4.86E-21
302	156.961730128	-43.901480653	6.38E-17	1.56E-19	4.55E-17	2.15E-19	7.93E-18	1.28E-19
303	156.963318796	-43.902228490	6.98E-18	1.79E-19	7.12E-18	2.63E-19	1.74E-18	1.25E-19
304	156.976821808	-43.908159650	4.58E-19	3.04E-20	6.49E-19	1.92E-20	1.54E-19	8.30E-21
305	156.966796135	-43.903533468	3.47E-18	4.98E-19	6.29E-18	3.75E-19	1.76E-18	2.09E-19
306	156.964897705	-43.902803641	1.84E-17	4.57E-19	1.08E-17	5.51E-19	5.93E-18	2.77E-19
307	156.964076677	-43.902589964	5.10E-18	4.77E-19	9.06E-18	5.51E-19	1.92E-18	4.37E-19
308	156.966844903	-43.903724815	2.75E-18	1.13E-19	2.36E-18	4.01E-19	2.60E-18	2.46E-19
309	156.962074947	-43.901707725	1.61E-17	2.33E-19	7.31E-18	2.24E-19	7.30E-19	1.78E-19
310	156.965994623	-43.902963808	9.16E-18	3.37E-19	1.62E-17	5.99E-19	7.55E-18	2.21E-19
311	156.962151416	-43.901225329	3.27E-18	3.85E-19	6.04E-18	4.15E-19	1.24E-18	1.96E-19
312	156.961643853	-43.900776267	9.39E-18	1.35E-19	1.15E-17	1.62E-19	7.08E-18	8.06E-20
313	156.958807786	-43.899767657	2.33E-18	2.79E-20	7.20E-18	1.83E-20	3.07E-18	1.86E-20
314	156.960614259	-43.900557152	1.54E-18	4.18E-20	4.04E-18	2.97E-20	1.59E-18	2.13E-20
315	156.967494475	-43.902362645	1.81E-17	2.86E-19	3.95E-17	3.39E-19	7.60E-18	1.94E-19
316	156.965954530	-43.902765801	1.30E-17	3.47E-19	9.59E-18	5.48E-19	3.81E-18	1.83E-19
317	156.965127829	-43.902626596	1.38E-17	8.88E-19	1.69E-17	1.44E-18	6.01E-18	3.46E-19
318	156.964660918	-43.902599556	9.52E-18	3.42E-19	1.06E-17	7.86E-19	2.30E-18	2.64E-19
319	156.963512523	-43.902077355	3.70E-18	8.61E-20	4.92E-18	1.26E-19	1.16E-18	5.49E-20
320	156.977419079	-43.907037664	9.58E-17	5.82E-20	2.17E-16	6.07E-20	1.13E-16	2.01E-19
321	156.961476046	-43.901016122	2.99E-18	8.10E-20	4.48E-18	9.55E-20	3.13E-18	7.10E-20
322	156.965422715	-43.902485006	1.86E-16	8.82E-19	2.43E-16	1.58E-18	7.58E-17	4.19E-19
323	156.962012838	-43.901492249	3.22E-18	1.87E-19	1.49E-18	2.30E-19	8.63E-19	8.41E-20
324	156.968059119	-43.903750564	3.44E-18	1.35E-19	2.60E-18	9.57E-20	7.41E-19	3.58E-20
325	156.966970031	-43.903176728	7.54E-18	4.14E-19	9.86E-18	4.42E-19	3.08E-18	2.57E-19
326	156.965334496	-43.902658548	3.30E-17	7.41E-19	1.75E-17	1.45E-18	2.03E-18	3.26E-19
327	156.970291745	-43.904461794	8.38E-19	3.29E-20	4.79E-18	2.21E-20	1.63E-17	1.90E-20
328	156.961895460	-43.901312022	4.05E-18	1.99E-19	2.55E-18	2.30E-19	6.69E-19	1.10E-19
329	156.965768213	-43.901926746	3.95E-17	1.98E-19	3.30E-17	2.00E-19	9.64E-18	7.43E-20
330	156.965281210	-43.902254444	5.12E-18	1.35E-19	2.58E-18	2.04E-19	1.94E-18	8.20E-20
331	156.956648633	-43.898626881	1.02E-18	3.92E-20	1.02E-18	1.91E-20	2.78E-19	6.99E-21
332	156.980057560	-43.908446006	7.83E-19	2.66E-20	8.28E-18	1.32E-20	2.40E-17	3.06E-20
333	156.963641798	-43.901408987	8.20E-18	1.00E-19	8.40E-18	1.59E-19	3.05E-18	9.84E-20
334	156.968806685	-43.903866828	5.34E-19	5.82E-20	1.55E-18	5.72E-20	3.55E-19	3.20E-20
335	156.965699926	-43.902499616	4.25E-17	3.49E-19	4.48E-17	2.60E-19	1.24E-17	1.13E-19
336	156.964899471	-43.902404491	3.44E-18	1.91E-19	3.95E-18	3.90E-19	1.02E-18	1.57E-19
337	156.966709515	-43.903146351	2.89E-17	7.32E-19	1.62E-17	7.37E-19	3.94E-18	3.27E-19
338	156.969149739	-43.904289087	2.82E-18	4.81E-20	1.78E-18	3.87E-20	3.29E-19	1.62E-20
339	156.968462533	-43.903865609	6.52E-19	5.95E-20	3.36E-19	4.34E-20	1.20E-19	2.72E-20
340	156.961362776	-43.900535601	3.45E-19	3.92E-20	1.01E-18	4.20E-20	2.01E-18	5.31E-20
341	156.957993346	-43.898628430	1.06E-18	4.43E-20	3.76E-18	2.06E-20	1.69E-18	9.89E-21
342	156.957489900	-43.898818713	3.19E-19	4.30E-20	1.25E-18	2.08E-20	7.12E-19	1.21E-20

*Table 5 continued*

**Table 5** (*continued*)

ID	R.A.	Decl.	$f_{336}$	$\sigma_{f_{336}}$	$f_{435}$	$\sigma_{f_{435}}$	$f_{814}$	$\sigma_{f_{814}}$
343	156.967839036	-43.903382588	1.63E-18	6.84E-20	1.96E-18	8.29E-20	1.41E-18	4.42E-20
344	156.962307412	-43.901038256	5.35E-18	1.57E-19	3.47E-18	1.49E-19	1.62E-18	9.74E-20
345	156.963817206	-43.901644948	2.31E-18	8.61E-20	3.74E-18	1.12E-19	9.36E-19	6.86E-20
346	156.963557111	-43.901170442	9.57E-18	8.99E-20	1.61E-17	1.40E-19	8.02E-18	9.16E-20
347	156.965517980	-43.902556127	1.55E-17	4.96E-19	3.92E-17	1.01E-18	1.27E-17	3.82E-19
348	156.969019446	-43.903831782	2.83E-18	6.20E-20	2.27E-18	7.83E-20	7.73E-19	2.60E-20
349	156.964590467	-43.902193878	2.04E-18	1.18E-19	3.24E-18	1.49E-19	8.23E-19	9.04E-20
350	156.960189543	-43.899616246	8.37E-18	3.80E-20	1.37E-17	3.88E-20	4.51E-18	2.35E-20
351	156.961898356	-43.900809850	2.11E-18	7.34E-20	2.63E-18	9.46E-20	9.94E-19	6.87E-20
352	156.963327706	-43.901449366	1.06E-18	6.58E-20	1.91E-18	1.57E-19	7.82E-19	7.82E-20
353	156.968707950	-43.903003912	8.40E-18	6.96E-20	7.92E-18	7.94E-20	3.76E-18	4.99E-20
354	156.965906089	-43.902410205	8.16E-18	1.86E-19	4.95E-18	2.01E-19	2.24E-18	1.02E-19
355	156.968899972	-43.903760948	6.85E-19	6.08E-20	8.36E-19	7.54E-20	1.67E-19	3.21E-20
356	156.966055015	-43.902224589	3.87E-18	8.74E-20	4.55E-18	1.19E-19	1.15E-18	4.59E-20
357	156.968322474	-43.903582969	1.26E-18	1.18E-19	2.17E-18	1.75E-19	4.39E-19	6.94E-20
358	156.968377429	-43.902739356	1.03E-17	9.12E-20	1.28E-17	1.67E-19	6.14E-18	6.78E-20
359	156.967935531	-43.903164864	5.81E-19	7.85E-20	5.76E-19	5.70E-20	5.02E-19	4.29E-20
360	156.964545850	-43.901650576	1.02E-18	5.82E-20	1.44E-18	6.79E-20	7.12E-19	3.24E-20
361	156.969317382	-43.903777578	9.78E-19	4.30E-20	9.54E-19	3.35E-20	3.44E-19	2.11E-20
362	156.963866174	-43.901421129	3.06E-18	1.01E-19	3.91E-18	1.33E-19	1.54E-18	4.88E-20
363	156.962953416	-43.900893088	4.15E-18	1.20E-19	2.41E-18	1.82E-19	6.73E-19	5.91E-20
364	156.965837751	-43.902283675	2.54E-18	2.13E-19	6.31E-18	2.08E-19	1.32E-18	5.99E-20
365	156.962126462	-43.900396301	1.27E-18	4.30E-20	2.14E-18	7.12E-20	1.33E-18	4.31E-20
366	156.963031972	-43.900972431	2.91E-18	7.85E-20	3.45E-18	1.08E-19	5.86E-19	5.62E-20
367	156.963848596	-43.901061051	1.32E-18	6.58E-20	1.60E-18	7.48E-20	1.04E-18	5.61E-20
368	156.969636235	-43.903472107	2.53E-19	3.29E-20	5.53E-19	3.30E-20	2.41E-19	2.26E-20
369	156.967128254	-43.902430799	1.57E-16	7.10E-19	1.10E-16	7.78E-19	2.09E-17	3.21E-19
370	156.987238721	-43.910352254	9.81E-17	1.23E-19	2.79E-16	8.41E-20	1.27E-16	2.40E-19
371	156.968011028	-43.902671067	3.93E-17	1.75E-19	3.80E-17	2.23E-19	1.38E-17	1.01E-19
372	156.969937094	-43.903765184	2.51E-19	3.42E-20	2.09E-19	1.95E-20	1.06E-19	1.33E-20
373	156.965104155	-43.901505818	4.31E-19	4.94E-20	6.47E-19	7.47E-20	4.01E-19	3.58E-20
374	156.966248328	-43.902161162	6.92E-19	6.58E-20	1.44E-18	6.54E-20	5.64E-19	2.96E-20
375	156.964497184	-43.901309080	1.83E-18	6.20E-20	2.27E-18	1.02E-19	7.95E-19	3.15E-20
376	156.970487854	-43.903223684	3.45E-16	1.33E-18	2.69E-16	7.86E-19	5.34E-17	5.33E-19
377	156.966483297	-43.902122427	4.09E-18	7.34E-20	4.34E-18	8.98E-20	1.34E-18	3.32E-20
378	156.966351435	-43.901927199	2.22E-18	6.84E-20	3.19E-18	6.36E-20	1.57E-18	3.37E-20
379	156.941834804	-43.889899748	3.95E-16	4.24E-19	4.94E-16	3.96E-19	2.08E-16	5.59E-19
380	156.963484856	-43.900677380	2.27E-18	1.30E-19	2.34E-18	1.05E-19	6.68E-19	4.30E-20
381	156.970886290	-43.903863380	3.97E-19	3.92E-20	3.52E-19	1.98E-20	7.77E-20	1.05E-20
382	156.969024235	-43.903009865	1.51E-18	4.68E-20	1.87E-18	5.77E-20	8.45E-19	3.69E-20
383	156.963744326	-43.900803142	8.24E-18	1.66E-19	1.05E-17	2.22E-19	4.87E-18	1.09E-19
384	156.962876934	-43.900644356	3.37E-19	4.94E-20	2.93E-19	5.58E-20	9.55E-20	2.51E-20
385	156.966201215	-43.901880587	1.34E-18	6.58E-20	1.01E-18	7.48E-20	4.07E-19	3.45E-20
386	156.964645581	-43.900804826	3.78E-19	3.80E-20	1.32E-18	5.75E-20	9.04E-19	3.55E-20
387	156.968537698	-43.902489631	7.69E-19	4.81E-20	5.98E-19	5.99E-20	1.60E-18	2.38E-20
388	156.966919585	-43.902063852	5.25E-18	7.34E-20	3.78E-18	1.02E-19	9.77E-19	5.17E-20
389	156.968394122	-43.902568795	1.45E-18	6.33E-20	1.71E-18	6.69E-20	1.18E-18	5.13E-20

*Table 5 continued*

**Table 5** (*continued*)

ID	R.A.	Decl.	$f_{336}$	$\sigma_{f_{336}}$	$f_{435}$	$\sigma_{f_{435}}$	$f_{814}$	$\sigma_{f_{814}}$
390	156.963976657	-43.900835184	1.43E-18	6.33E-20	1.44E-18	6.97E-20	3.75E-19	7.18E-20
391	156.966616570	-43.901666983	1.22E-18	5.57E-20	1.77E-18	4.28E-20	5.82E-19	2.94E-20
392	156.968046699	-43.902172805	1.22E-18	5.32E-20	1.32E-18	7.23E-20	7.36E-19	3.62E-20
393	156.963340656	-43.900449242	7.75E-19	4.05E-20	6.30E-19	3.78E-20	1.94E-19	2.26E-20
394	156.969147835	-43.902815739	9.79E-19	5.32E-20	1.61E-18	6.66E-20	4.55E-19	3.81E-20
395	156.969923411	-43.903285897	9.84E-19	5.44E-20	1.75E-18	5.35E-20	7.86E-19	3.28E-20
396	156.965533027	-43.900574814	8.91E-18	7.09E-20	9.83E-18	8.98E-20	2.93E-18	4.30E-20
397	156.962911178	-43.900260349	4.73E-19	4.18E-20	4.48E-19	5.71E-20	1.99E-19	3.37E-20
398	156.963764148	-43.900268930	1.39E-18	4.30E-20	9.94E-19	5.79E-20	2.44E-19	3.16E-20
399	156.969311747	-43.902826488	4.83E-19	5.19E-20	8.50E-19	1.34E-19	1.93E-19	4.79E-20
400	156.973873636	-43.904626017	2.65E-18	3.17E-20	6.21E-18	1.67E-20	4.23E-18	9.18E-21
401	156.967621022	-43.902138819	3.13E-18	1.20E-19	1.65E-18	1.67E-19	6.61E-19	8.20E-20
402	156.989028758	-43.910869355	9.83E-18	3.17E-20	1.92E-17	1.88E-20	1.13E-17	1.53E-20
403	156.968878499	-43.902488655	4.21E-18	5.95E-20	3.80E-18	3.70E-20	7.02E-19	5.96E-20
404	156.963368049	-43.899699886	3.52E-18	8.74E-20	4.28E-18	1.02E-19	1.07E-18	6.23E-20
405	156.967004864	-43.901639344	8.00E-19	4.18E-20	9.55E-19	3.97E-20	2.51E-19	2.52E-20
406	156.963347122	-43.900129876	3.15E-19	4.68E-20	3.10E-19	4.40E-20	2.82E-19	2.83E-20
407	156.969888700	-43.902722287	2.63E-18	4.81E-20	2.47E-18	6.39E-20	7.51E-19	3.25E-20
408	156.968099052	-43.902010049	1.12E-18	4.81E-20	2.48E-18	5.81E-20	1.08E-18	3.79E-20
409	156.965728370	-43.901127203	6.19E-19	3.80E-20	3.81E-19	4.98E-20	7.82E-20	1.96E-20
410	156.966245326	-43.900637422	3.71E-18	8.23E-20	3.10E-18	8.69E-20	1.46E-18	3.54E-20
411	156.964642774	-43.900531268	3.57E-18	1.23E-19	2.53E-18	2.06E-19	7.70E-19	7.69E-20
412	156.965408750	-43.900967067	1.60E-18	5.57E-20	1.64E-18	5.91E-20	3.49E-19	3.70E-20
413	156.963052323	-43.899519268	2.80E-18	4.18E-20	3.34E-18	5.11E-20	2.03E-18	3.33E-20
414	156.967693049	-43.901704945	4.45E-19	4.30E-20	8.45E-19	3.79E-20	6.76E-19	2.58E-20
415	156.963610244	-43.899509452	6.31E-17	3.11E-19	7.57E-17	5.61E-19	2.44E-17	2.48E-19
416	156.965857470	-43.900876963	5.15E-19	3.55E-20	2.82E-19	4.05E-20	3.95E-19	1.77E-20
417	156.968489549	-43.902143377	6.39E-19	4.18E-20	5.16E-19	5.53E-20	1.84E-19	2.38E-20
418	156.964198395	-43.900277812	3.71E-19	3.80E-20	3.35E-19	5.71E-20	1.85E-19	3.96E-20
419	156.970297697	-43.902729057	3.69E-19	5.19E-20	1.00E-18	7.39E-20	1.60E-19	2.82E-20
420	156.968499770	-43.901613016	9.31E-18	5.44E-20	1.01E-17	3.88E-20	4.86E-18	2.15E-20
421	156.963435124	-43.899321073	2.54E-18	4.30E-20	5.00E-18	1.43E-19	5.35E-18	5.12E-20
422	156.967497374	-43.901585583	4.13E-19	4.05E-20	3.48E-19	4.45E-20	1.33E-19	1.75E-20
423	156.968963655	-43.901817077	1.42E-18	5.95E-20	1.28E-18	8.53E-20	4.64E-19	6.72E-20
424	156.965891221	-43.900630403	1.02E-18	5.44E-20	9.45E-19	7.54E-20	3.68E-19	2.96E-20
425	156.970092985	-43.902382107	1.19E-18	7.60E-20	2.03E-18	1.07E-19	3.29E-19	4.57E-20
426	156.968532281	-43.901325633	3.12E-19	6.08E-20	7.64E-19	7.61E-20	3.02E-19	3.35E-20
427	156.969271799	-43.901978438	1.15E-18	6.33E-20	1.60E-18	8.03E-20	9.07E-19	4.14E-20
428	156.968074521	-43.901614137	9.07E-19	4.18E-20	1.15E-18	6.13E-20	5.89E-19	2.47E-20
429	156.969928238	-43.902433046	2.03E-18	6.33E-20	2.79E-18	9.17E-20	1.27E-19	3.33E-20
430	156.969695215	-43.902035246	9.31E-19	7.34E-20	1.18E-18	8.17E-20	5.02E-19	5.48E-20
431	156.975275381	-43.904103647	2.45E-18	3.17E-20	1.95E-17	1.90E-20	4.72E-17	6.92E-20
432	156.959630255	-43.897959136	3.09E-19	4.05E-20	6.81E-19	1.81E-20	4.15E-19	8.99E-21
433	156.970694807	-43.902709260	1.50E-18	7.98E-20	8.37E-19	1.28E-19	3.13E-19	7.64E-20
434	156.969409681	-43.901997519	4.46E-18	9.12E-20	3.18E-18	1.04E-19	9.84E-19	4.76E-20
435	156.969215012	-43.901582447	1.64E-17	1.68E-19	1.58E-17	1.01E-19	5.31E-18	4.90E-20
436	156.967823960	-43.901130165	1.19E-18	4.81E-20	2.15E-18	6.03E-20	9.44E-19	3.41E-20

*Table 5 continued*

**Table 5** (*continued*)

ID	R.A.	Decl.	$f_{336}$	$\sigma_{f_{336}}$	$f_{435}$	$\sigma_{f_{435}}$	$f_{814}$	$\sigma_{f_{814}}$
437	156.965121647	-43.899917258	3.08E-19	3.42E-20	7.57E-19	3.31E-20	2.92E-19	4.15E-20
438	156.966556718	-43.900862612	8.19E-19	3.92E-20	1.21E-18	4.90E-20	3.71E-19	2.07E-20
439	156.968817206	-43.901489749	1.18E-18	5.95E-20	1.50E-18	4.42E-20	4.52E-19	2.90E-20
440	156.964241026	-43.899767670	4.37E-19	5.32E-20	9.63E-19	5.82E-20	4.70E-19	2.60E-20
441	156.969543200	-43.902270841	4.79E-19	4.68E-20	2.54E-19	5.15E-20	1.96E-19	2.90E-20
442	156.965791794	-43.900617885	1.04E-18	5.70E-20	8.46E-19	8.93E-20	2.03E-19	4.94E-20
443	156.966707191	-43.900822343	1.16E-18	3.80E-20	1.17E-18	5.21E-20	4.78E-19	2.77E-20
444	156.969552029	-43.902035136	1.13E-18	8.23E-20	1.10E-18	8.18E-20	3.64E-19	4.16E-20
445	156.964868504	-43.899896927	1.37E-18	4.81E-20	2.76E-18	6.25E-20	1.85E-18	2.99E-20
446	156.968182136	-43.901367773	4.81E-19	4.56E-20	1.25E-18	5.76E-20	7.06E-19	2.77E-20
447	156.966040994	-43.900684246	3.81E-19	5.06E-20	4.47E-19	6.90E-20	1.91E-19	4.31E-20
448	156.970905938	-43.902776366	6.48E-18	1.48E-19	4.96E-18	1.00E-19	1.35E-18	3.15E-20
449	156.964346993	-43.899004793	3.86E-18	6.33E-20	4.22E-18	9.95E-20	3.86E-18	4.04E-20
450	156.963576429	-43.899139113	1.26E-18	4.94E-20	1.38E-18	8.12E-20	4.11E-19	3.47E-20
451	156.970465814	-43.901824008	8.17E-19	5.44E-20	8.00E-19	6.15E-20	3.42E-19	2.25E-20
452	156.966095465	-43.900606569	1.88E-18	5.19E-20	9.50E-19	7.08E-20	3.92E-19	2.94E-20
453	156.965469584	-43.900133624	7.65E-19	4.05E-20	1.28E-18	5.05E-20	5.98E-19	4.68E-20
454	156.967234574	-43.901004020	2.64E-19	4.05E-20	8.02E-19	4.63E-20	1.49E-19	1.92E-20
455	156.968115890	-43.901296123	7.41E-19	4.81E-20	1.61E-18	7.20E-20	6.11E-19	3.58E-20
456	156.964409558	-43.899694434	3.71E-19	4.30E-20	9.39E-19	5.26E-20	8.09E-19	3.01E-20
457	156.963922503	-43.899321687	9.90E-18	1.06E-19	1.24E-17	1.06E-19	4.99E-18	1.07E-19
458	156.956027971	-43.894742990	2.83E-17	4.30E-20	4.11E-17	2.23E-20	1.01E-16	2.26E-19
459	156.970516303	-43.902282291	1.87E-18	1.00E-19	1.19E-18	1.68E-19	8.13E-19	5.65E-20
460	156.970465210	-43.902120531	7.69E-18	8.74E-20	6.24E-18	7.96E-20	2.35E-18	3.51E-20
461	156.966993464	-43.900535335	7.86E-18	7.34E-20	6.17E-18	5.44E-20	1.48E-18	2.37E-20
462	156.969583573	-43.901881919	5.73E-19	5.57E-20	4.26E-19	5.62E-20	1.20E-19	3.13E-20
463	156.967472227	-43.900397674	1.16E-17	1.42E-19	1.18E-17	1.93E-19	4.93E-18	8.79E-20
464	156.968870536	-43.900787570	6.76E-18	8.74E-20	6.36E-18	1.03E-19	2.24E-18	7.27E-20
465	156.967488344	-43.900892976	4.31E-19	3.67E-20	4.18E-19	4.16E-20	2.07E-19	1.84E-20
466	156.993626556	-43.911548923	2.94E-17	6.08E-20	5.03E-17	1.90E-20	2.06E-17	2.95E-20
467	156.963392614	-43.899151707	3.88E-19	4.18E-20	6.17E-19	6.23E-20	2.47E-19	2.09E-20
468	156.966279121	-43.900293657	1.52E-18	6.46E-20	1.34E-18	6.82E-20	1.72E-19	4.59E-20
469	156.968260159	-43.901026776	5.05E-18	4.81E-20	4.75E-18	7.34E-20	1.92E-18	2.82E-20
470	156.967106469	-43.900174476	5.12E-18	6.46E-20	7.63E-18	7.93E-20	3.65E-18	3.74E-20
471	156.971965293	-43.901880815	1.26E-17	4.43E-20	2.67E-17	3.40E-20	1.71E-17	2.87E-20
472	156.968215128	-43.900872333	6.09E-19	5.44E-20	8.30E-19	4.22E-20	3.75E-19	2.44E-20
473	156.968666504	-43.900554882	5.71E-17	2.76E-19	3.46E-17	2.92E-19	7.74E-18	9.70E-20
474	156.971166021	-43.902028269	4.66E-19	3.80E-20	4.37E-19	4.03E-20	5.60E-19	1.17E-20
475	156.971506772	-43.902218636	4.65E-18	4.94E-20	3.73E-18	2.63E-20	7.40E-19	1.30E-20
476	156.967016449	-43.900399441	1.05E-18	6.96E-20	1.16E-18	4.15E-20	1.34E-19	3.56E-20
477	156.976861967	-43.904273910	8.85E-19	3.29E-20	3.13E-18	1.58E-20	1.24E-18	8.99E-21
478	156.967852761	-43.900555412	2.86E-19	5.32E-20	4.66E-19	6.23E-20	3.79E-19	3.75E-20
479	156.959465954	-43.897017232	3.59E-19	4.05E-20	4.71E-19	1.64E-20	1.73E-19	8.44E-21
480	156.970472609	-43.901624022	1.32E-17	6.08E-20	1.20E-17	4.24E-20	3.76E-18	2.30E-20
481	156.967813644	-43.900214804	1.08E-18	7.34E-20	8.95E-19	1.41E-19	7.30E-19	4.63E-20
482	156.970220600	-43.901540997	1.63E-18	6.58E-20	1.91E-18	7.21E-20	7.22E-19	3.02E-20
483	156.970296038	-43.901472144	2.84E-18	4.43E-20	2.72E-18	3.76E-20	8.79E-19	2.48E-20

*Table 5 continued*

**Table 5** (*continued*)

ID	R.A.	Decl.	$f_{336}$	$\sigma_{f_{336}}$	$f_{435}$	$\sigma_{f_{435}}$	$f_{814}$	$\sigma_{f_{814}}$
484	156.968013132	-43.900467046	1.50E-18	5.06E-20	1.45E-18	7.43E-20	3.86E-19	5.68E-20
485	156.968482623	-43.900429171	6.61E-18	2.24E-19	4.65E-18	1.54E-19	1.73E-18	7.56E-20
486	156.969291387	-43.901016753	2.59E-18	6.58E-20	1.33E-18	8.12E-20	3.32E-19	4.50E-20
487	156.968124723	-43.900518528	5.86E-19	5.82E-20	7.23E-19	1.02E-19	3.24E-19	4.15E-20
488	156.973390704	-43.902559274	7.90E-19	3.29E-20	8.49E-19	3.23E-20	2.80E-19	2.00E-20
489	156.973220843	-43.902429456	3.51E-18	3.92E-20	3.23E-18	2.66E-20	9.06E-19	1.01E-20
490	156.969297794	-43.900854594	5.49E-19	6.08E-20	7.05E-19	5.47E-20	3.45E-19	2.95E-20
491	156.970629111	-43.901543596	2.94E-19	5.06E-20	2.49E-19	4.25E-20	5.86E-20	1.50E-20
492	156.970357571	-43.901298214	2.46E-19	3.42E-20	4.12E-19	3.01E-20	2.38E-19	1.83E-20
493	156.964556089	-43.898992758	3.22E-19	4.30E-20	9.00E-19	3.94E-20	3.64E-19	2.01E-20
494	156.969490692	-43.900618290	3.78E-18	4.68E-20	3.07E-18	4.18E-20	8.74E-19	2.88E-20
495	156.967418706	-43.900132659	5.81E-19	4.30E-20	6.95E-19	4.11E-20	1.32E-19	1.67E-20
496	156.968641361	-43.900445773	2.76E-18	1.20E-19	2.77E-18	1.14E-19	9.91E-19	5.66E-20
497	156.972850431	-43.901991444	1.59E-18	3.29E-20	4.31E-18	2.61E-20	1.51E-18	1.27E-20
498	156.960317420	-43.896402698	3.47E-19	3.29E-20	1.63E-18	1.73E-20	4.17E-18	1.01E-20
499	156.954690490	-43.894217751	6.29E-19	3.55E-20	1.62E-18	1.48E-20	5.34E-19	5.77E-21
500	156.960929567	-43.896933933	5.20E-19	3.55E-20	1.64E-18	1.95E-20	6.67E-19	1.19E-20
501	156.961631310	-43.897298605	3.52E-19	3.55E-20	8.30E-20	1.80E-20	7.44E-20	8.92E-21
502	156.969311798	-43.900504432	6.99E-19	3.67E-20	5.01E-19	2.67E-20	1.07E-19	2.19E-20
503	156.963715929	-43.897503492	4.07E-19	3.92E-20	1.25E-18	2.08E-20	4.02E-19	9.03E-21
504	156.967013699	-43.898457627	6.39E-19	3.42E-20	1.50E-18	3.35E-20	6.80E-19	1.81E-20
505	156.966749670	-43.898417298	9.16E-19	3.67E-20	1.83E-18	3.27E-20	8.66E-19	1.96E-20
506	156.964082305	-43.896075544	2.96E-19	3.29E-20	1.35E-18	1.65E-20	7.14E-19	7.88E-21
507	156.971558399	-43.898971630	2.97E-17	4.05E-20	4.96E-17	2.33E-20	2.34E-17	2.37E-20
508	156.989172961	-43.906342383	2.17E-17	4.30E-20	3.75E-17	1.84E-20	1.73E-17	2.44E-20
509	156.973274279	-43.899903453	1.11E-18	3.42E-20	1.14E-18	1.61E-20	1.93E-19	9.41E-21
510	156.977963284	-43.901446161	3.01E-18	2.91E-20	7.50E-18	2.47E-20	2.75E-18	1.02E-20
511	156.962992887	-43.895257491	2.86E-19	2.53E-20	5.43E-19	1.42E-20	2.23E-19	7.71E-21
512	156.965555865	-43.895691851	1.71E-18	3.04E-20	1.01E-17	2.30E-20	2.17E-17	3.24E-20
513	156.967927133	-43.896800192	2.60E-19	3.17E-20	2.36E-19	2.29E-20	5.59E-20	9.31E-21
514	156.958004687	-43.891758846	2.14E-17	3.92E-20	3.74E-17	2.63E-20	1.99E-17	2.85E-20
515	156.969328860	-43.895926920	1.47E-18	3.80E-20	3.95E-18	3.18E-20	1.49E-18	2.12E-20
516	156.966656515	-43.894426130	8.37E-19	4.30E-20	1.93E-18	1.74E-20	2.22E-18	8.38E-21
517	156.980355167	-43.899043040	2.80E-19	2.91E-20	5.11E-19	1.20E-20	1.70E-19	5.34E-21
518	156.956382439	-43.888116734	1.26E-17	4.18E-20	3.06E-17	1.98E-20	2.17E-17	3.11E-20
519	156.955733186	-43.887719892	2.00E-17	3.67E-20	7.19E-17	4.59E-20	6.86E-17	7.86E-20
520	156.986919376	-43.899697627	5.41E-17	5.44E-20	1.66E-16	8.39E-20	8.73E-17	1.75E-19
521	156.980811866	-43.897552193	1.46E-18	2.79E-20	1.28E-17	3.03E-20	7.02E-17	1.57E-19
522	156.980995524	-43.897223818	1.70E-16	8.36E-20	7.33E-16	3.58E-19	4.84E-16	2.60E-18
523	156.966657093	-43.891636812	1.28E-18	3.04E-20	3.49E-18	1.68E-20	2.55E-18	7.22E-21
524	156.956790109	-43.887206627	1.44E-18	2.91E-20	6.01E-18	1.17E-20	6.86E-18	8.56E-21
525	156.982832483	-43.897244471	2.11E-17	3.55E-20	6.61E-17	3.58E-20	5.64E-17	8.05E-20
526	156.962254569	-43.889634097	4.03E-19	2.66E-20	7.23E-19	1.23E-20	3.69E-19	6.31E-21
527	156.993567107	-43.901502715	1.89E-17	3.67E-20	7.86E-17	2.99E-20	7.68E-17	1.14E-19
528	156.980242847	-43.893242423	4.37E-17	4.05E-20	1.89E-16	1.44E-19	1.18E-16	2.56E-19
529	156.966727887	-43.888816715	1.63E-19	3.17E-20	3.56E-19	1.32E-20	6.26E-20	5.24E-21
530	156.966942801	-43.888393846	6.24E-18	3.29E-20	3.27E-17	2.62E-20	1.50E-19	2.79E-20

*Table 5 continued*

**Table 5** (*continued*)

ID	R.A.	Decl.	$f_{336}$	$\sigma_{f_{336}}$	$f_{435}$	$\sigma_{f_{435}}$	$f_{814}$	$\sigma_{f_{814}}$
531	156.981700499	-43.894324338	8.98E-18	3.29E-20	2.94E-17	2.14E-20	2.89E-17	3.78E-20
532	156.966699136	-43.887782177	3.98E-19	3.80E-20	1.10E-18	1.53E-20	1.21E-19	5.50E-21
533	156.986112495	-43.894668773	7.99E-18	3.92E-20	1.73E-17	1.83E-20	1.18E-17	1.87E-20
534	156.979114992	-43.890783923	2.26E-18	3.04E-20	8.44E-18	1.46E-20	9.11E-18	9.92E-21
535	156.948235816	-43.877326786	9.30E-18	4.68E-20	7.75E-17	5.04E-20	1.39E-16	2.47E-19
536	156.984591778	-43.893631793	4.24E-19	3.04E-20	3.54E-19	1.18E-20	1.36E-19	5.86E-21
537	156.948978535	-43.877024557	2.95E-16	1.38E-19	5.62E-16	2.46E-19	2.93E-16	6.41E-19
538	156.968247275	-43.885767497	4.62E-17	4.18E-20	1.14E-16	4.71E-20	8.01E-17	8.95E-20
539	156.979617821	-43.889977176	8.91E-17	6.71E-20	2.60E-16	1.00E-19	1.47E-16	2.81E-19
540	156.981021074	-43.890744019	1.77E-17	3.55E-20	6.67E-17	2.90E-20	6.57E-17	6.75E-20
541	156.998122997	-43.896622068	3.09E-18	3.04E-20	2.17E-17	1.68E-20	6.47E-17	1.16E-19
542	156.973281044	-43.886394621	4.77E-19	2.91E-20	1.29E-18	1.16E-20	4.48E-19	6.23E-21
543	156.975829175	-43.887633927	4.22E-19	2.53E-20	2.86E-19	1.35E-20	6.83E-20	5.58E-21
544	156.984006672	-43.890441016	1.25E-18	2.66E-20	4.18E-18	1.48E-20	4.32E-18	7.22E-21
545	156.981131422	-43.886561545	1.92E-18	3.29E-20	2.01E-19	1.30E-20	9.80E-20	4.74E-21
546	156.956147514	-43.876020451	4.42E-17	8.10E-20	1.23E-16	9.65E-20	6.62E-17	1.23E-19
547	156.973115601	-43.883928026	2.72E-17	5.19E-20	1.07E-16	4.20E-20	8.55E-17	1.01E-19
548	156.965032410	-43.879979577	2.46E-17	3.92E-20	8.31E-17	4.10E-20	7.57E-17	1.07E-19
549	157.002316135	-43.898129594	2.51E-18	4.43E-20	1.44E-19	1.02E-20	1.17E-19	4.44E-21

## NGC 6240

1	253.245151301	2.385341817	5.36E-19	2.53E-20	3.90E-19	1.48E-20	7.50E-20	7.31E-21
2	253.240476147	2.385195675	3.42E-19	2.91E-20	4.31E-19	1.41E-20	1.15E-19	5.62E-21
3	253.233335488	2.385569137	4.11E-19	2.91E-20	2.92E-19	1.20E-20	3.24E-19	8.01E-21
4	253.235648695	2.386861539	4.37E-19	2.91E-20	4.19E-19	1.36E-20	1.44E-19	5.07E-21
5	253.256689255	2.390426093	4.55E-18	3.17E-20	1.02E-17	1.48E-20	9.02E-18	1.28E-20
6	253.235597099	2.389104110	2.06E-17	3.80E-20	7.08E-17	5.58E-20	6.40E-17	1.15E-19
7	253.248123273	2.392081469	9.31E-18	3.17E-20	1.98E-17	1.81E-20	1.39E-17	1.95E-20
8	253.258165578	2.393571304	7.80E-19	3.17E-20	7.51E-18	1.35E-20	2.18E-17	3.48E-20
9	253.250820715	2.392368899	6.00E-19	2.66E-20	1.00E-18	1.22E-20	5.11E-19	4.95E-21
10	253.236703120	2.391623448	6.52E-18	3.42E-20	1.54E-17	1.33E-20	1.12E-17	1.63E-20
11	253.257281505	2.396666846	1.11E-16	9.12E-20	1.94E-16	7.90E-20	9.65E-17	1.75E-19
12	253.254707133	2.396941003	8.46E-17	6.96E-20	1.54E-16	1.02E-19	7.31E-17	1.60E-19
13	253.249015863	2.394923363	4.31E-19	3.29E-20	1.02E-18	2.58E-20	2.93E-19	9.62E-21
14	253.242341496	2.393931430	3.06E-19	3.80E-20	4.88E-19	1.31E-20	1.65E-19	6.41E-21
15	253.249637806	2.395750504	3.62E-19	3.04E-20	6.51E-19	1.27E-20	3.17E-19	5.98E-21
16	253.254921289	2.397132350	3.75E-19	3.67E-20	4.70E-19	2.47E-20	2.02E-19	9.97E-21
17	253.243147832	2.395653155	7.50E-19	3.29E-20	1.48E-18	2.10E-20	4.37E-19	1.15E-20
18	253.242519685	2.395423430	3.39E-19	2.79E-20	4.40E-19	1.69E-20	1.60E-19	1.31E-20
19	253.252436540	2.397291421	1.10E-18	3.42E-20	2.56E-18	1.25E-20	1.92E-18	7.01E-21
20	253.244368992	2.396311372	6.35E-19	3.29E-20	1.31E-18	1.79E-20	5.70E-19	1.34E-20
21	253.243075362	2.396399998	3.92E-19	3.04E-20	4.19E-19	2.37E-20	1.95E-19	1.90E-20
22	253.243227067	2.396379353	3.40E-19	3.29E-20	5.57E-19	2.38E-20	1.71E-19	2.28E-20
23	253.243124319	2.396963250	1.28E-18	4.43E-20	1.45E-18	4.48E-20	4.71E-19	2.34E-20
24	253.242997190	2.396703917	2.81E-19	3.29E-20	5.71E-19	2.55E-20	2.79E-19	2.04E-20
25	253.243299863	2.396913538	8.13E-19	3.80E-20	1.27E-18	4.06E-20	3.46E-19	1.78E-20

Table 5 continued

**Table 5** (*continued*)

ID	R.A.	Decl.	$f_{336}$	$\sigma_{f_{336}}$	$f_{435}$	$\sigma_{f_{435}}$	$f_{814}$	$\sigma_{f_{814}}$
26	253.242624709	2.396881557	5.20E-19	4.31E-20	3.92E-19	3.00E-20	3.46E-19	2.42E-20
27	253.241743351	2.396806099	6.24E-19	3.80E-20	1.02E-18	3.19E-20	3.73E-19	1.19E-20
28	253.243362265	2.397125081	2.15E-18	3.93E-20	2.11E-18	3.58E-20	5.51E-19	2.12E-20
29	253.243376376	2.397207908	4.35E-19	4.05E-20	4.28E-19	3.29E-20	1.81E-19	2.92E-20
30	253.247577063	2.397991952	4.86E-19	3.67E-20	1.53E-18	2.06E-20	5.16E-19	1.03E-20
31	253.248138049	2.398332174	4.88E-19	3.42E-20	1.41E-18	2.63E-20	5.17E-19	1.57E-20
32	253.246897177	2.397885485	2.90E-19	4.05E-20	8.23E-19	2.02E-20	2.11E-19	1.06E-20
33	253.242374464	2.397319279	2.59E-19	5.70E-20	6.67E-19	7.73E-20	1.05E-19	3.00E-20
34	253.242592456	2.397617117	2.67E-18	7.22E-20	2.16E-18	6.50E-20	3.13E-19	3.43E-20
35	253.242272341	2.397557089	3.24E-18	4.56E-20	3.17E-18	3.62E-20	1.18E-18	2.27E-20
36	253.242579131	2.397733169	1.08E-18	5.44E-20	1.34E-18	6.93E-20	5.22E-19	2.62E-20
37	253.243170864	2.398110564	1.20E-18	5.06E-20	1.46E-18	3.58E-20	5.90E-19	2.54E-20
38	253.249076438	2.398929117	2.40E-19	3.80E-20	1.26E-19	1.97E-20	1.22E-19	8.22E-21
39	253.242502516	2.398433398	1.27E-18	4.56E-20	2.49E-18	4.82E-20	9.89E-19	2.23E-20
40	253.241593692	2.398132362	3.85E-19	3.42E-20	2.88E-19	2.21E-20	9.54E-20	1.01E-20
41	253.242718514	2.398287283	6.28E-19	5.19E-20	9.02E-19	6.37E-20	2.68E-19	4.29E-20
42	253.246581717	2.399531760	3.20E-19	4.05E-20	8.01E-19	3.23E-20	3.65E-19	1.43E-20
43	253.242669533	2.398232841	3.76E-19	5.44E-20	7.65E-19	3.71E-20	2.21E-19	2.98E-20
44	253.241537262	2.398246390	1.94E-19	3.67E-20	5.25E-19	2.17E-20	1.75E-19	9.46E-21
45	253.242670302	2.398646382	4.16E-19	3.93E-20	9.51E-19	3.60E-20	4.18E-19	1.59E-20
46	253.245273324	2.399861965	6.00E-19	3.42E-20	1.96E-18	6.61E-20	6.54E-19	9.78E-20
47	253.247646124	2.399936318	4.86E-19	3.80E-20	9.94E-19	1.66E-20	3.32E-19	9.18E-21
48	253.242487672	2.399281715	3.19E-19	3.17E-20	4.27E-19	2.55E-20	1.08E-19	1.27E-20
49	253.245625048	2.401380005	7.00E-18	4.05E-20	2.29E-17	9.96E-20	5.40E-17	1.85E-18
50	253.242300520	2.400082154	4.71E-19	3.42E-20	7.30E-19	1.67E-20	2.11E-19	7.91E-21
51	253.247814584	2.401035511	1.70E-19	2.79E-20	1.75E-19	2.19E-20	7.25E-20	1.17E-20
52	253.242403649	2.400046367	4.29E-19	3.29E-20	3.41E-19	2.44E-20	4.88E-20	9.70E-21
53	253.246512681	2.401571412	2.69E-19	3.04E-20	5.65E-19	5.15E-20	5.34E-19	3.87E-20
54	253.241982293	2.400299091	2.11E-19	3.67E-20	2.79E-19	1.64E-20	9.61E-20	7.98E-21
55	253.241617320	2.400700246	1.03E-18	4.43E-20	1.69E-18	1.70E-20	5.21E-19	7.67E-21
56	253.245390286	2.401945551	5.67E-19	3.93E-20	1.22E-18	6.47E-20	1.25E-18	1.87E-19
57	253.245331882	2.401452436	4.40E-19	3.55E-20	1.61E-18	5.41E-20	2.14E-18	3.11E-19
58	253.241325120	2.401040504	3.46E-19	3.29E-20	4.84E-19	1.28E-20	1.67E-19	5.94E-21
59	253.243092395	2.401470764	3.34E-19	4.05E-20	5.74E-19	2.35E-20	2.40E-19	1.11E-20
60	253.246884584	2.402088261	3.94E-19	3.42E-20	1.25E-18	3.11E-20	6.65E-19	1.57E-20
61	253.244188945	2.402373150	3.09E-19	4.05E-20	6.45E-19	2.51E-20	1.77E-19	1.78E-20
62	253.249443823	2.403818420	1.22E-18	3.04E-20	8.29E-18	1.99E-20	4.11E-17	5.54E-20
63	253.245321888	2.403457249	4.22E-19	3.29E-20	1.23E-18	3.32E-20	9.47E-19	4.67E-20
64	253.246186138	2.403553613	2.85E-19	3.04E-20	7.93E-19	2.29E-20	2.35E-19	1.33E-20
65	253.245792981	2.403727200	2.34E-18	3.55E-20	1.80E-18	4.37E-20	1.52E-19	3.35E-20
66	253.245845333	2.404062263	4.74E-18	3.29E-20	9.68E-18	5.22E-20	3.19E-18	2.44E-20
67	253.247268748	2.404058367	3.28E-19	3.42E-20	8.67E-19	1.80E-20	3.89E-19	1.10E-20
68	253.242143023	2.403665666	3.83E-19	2.79E-20	3.35E-19	1.75E-20	6.97E-20	6.66E-21
69	253.242972001	2.404239477	2.80E-19	3.17E-20	4.77E-19	1.80E-20	1.65E-19	7.73E-21
70	253.247679536	2.406161662	7.01E-17	8.86E-20	9.38E-17	4.82E-20	6.16E-17	9.77E-20
71	253.246338598	2.405268175	2.14E-19	3.55E-20	6.78E-19	2.71E-20	5.79E-19	1.28E-20
72	253.246916849	2.405877434	1.72E-19	3.67E-20	3.93E-19	3.65E-20	5.02E-20	1.21E-20

*Table 5 continued*

**Table 5** (*continued*)

ID	R.A.	Decl.	$f_{336}$	$\sigma_{f_{336}}$	$f_{435}$	$\sigma_{f_{435}}$	$f_{814}$	$\sigma_{f_{814}}$
73	253.247315034	2.406354336	8.77E-19	3.42E-20	2.16E-18	4.72E-20	7.09E-19	1.68E-20
74	253.247733950	2.407170359	2.38E-19	3.42E-20	4.24E-19	2.30E-20	1.25E-19	1.08E-20
75	253.245061372	2.406528953	2.83E-19	3.42E-20	2.66E-19	1.41E-20	3.46E-20	6.79E-21
76	253.245497866	2.406880021	2.20E-19	3.93E-20	4.33E-19	2.35E-20	4.72E-20	1.14E-20
77	253.242154454	2.407563375	2.35E-18	3.04E-20	1.10E-17	1.84E-20	1.84E-17	2.38E-20
78	253.250073988	2.409126104	3.49E-19	3.29E-20	3.70E-19	1.75E-20	1.57E-19	6.75E-21
79	253.247921386	2.409238853	5.54E-19	3.04E-20	7.91E-19	1.89E-20	2.85E-19	7.95E-21
80	253.248968940	2.414310701	7.42E-17	6.20E-20	1.25E-16	9.94E-20	6.92E-17	9.98E-20
81	253.237699219	2.412622719	2.53E-19	2.53E-20	1.47E-18	1.28E-20	3.18E-18	5.95E-21
82	253.233434586	2.412364706	5.17E-19	3.55E-20	5.82E-19	1.40E-20	5.99E-19	8.40E-21
83	253.235273753	2.412667808	1.20E-18	2.66E-20	3.91E-18	1.37E-20	4.22E-18	7.66E-21
84	253.244029290	2.415295186	3.85E-19	2.66E-20	3.97E-18	1.50E-20	3.68E-17	5.10E-20
85	253.253047150	2.419620687	2.09E-17	4.18E-20	5.58E-17	4.75E-20	4.58E-17	6.25E-20
86	253.247310386	2.420393656	4.79E-19	3.42E-20	2.98E-19	1.36E-20	1.17E-19	5.32E-21
87	253.232192931	2.414740323	3.76E-19	2.91E-20	3.05E-19	1.24E-20	7.08E-20	5.34E-21
NGC 7469 - Center								
1	345.816394351	8.874674009	4.62E-19	3.93E-20	1.53E-18	3.33E-20	6.53E-19	3.33E-20
2	345.815126935	8.871716691	1.21E-17	3.44E-19	9.24E-18	3.68E-19	1.74E-18	8.24E-20
3	345.815894330	8.873206478	6.11E-18	1.75E-19	8.80E-18	2.30E-19	2.73E-18	1.02E-19
4	345.815266216	8.871845945	1.90E-18	8.23E-20	1.48E-18	1.52E-19	2.34E-19	4.77E-20
5	345.815802806	8.873600887	5.68E-18	9.88E-20	3.76E-18	2.78E-19	4.86E-18	1.93E-19
6	345.815557282	8.874816390	4.80E-19	5.19E-20	1.74E-18	7.54E-20	1.00E-18	6.20E-20
7	345.815625808	8.873844245	5.08E-17	8.56E-19	8.54E-17	1.86E-18	3.40E-17	1.83E-18
8	345.814496650	8.872920692	6.28E-18	1.03E-19	6.25E-18	1.99E-19	1.47E-18	6.96E-20
9	345.815297761	8.874815993	2.77E-18	6.33E-20	4.08E-18	9.87E-20	1.77E-18	1.13E-19
10	345.815420526	8.874223200	2.04E-16	3.81E-18	2.40E-16	1.99E-18	8.00E-17	3.38E-18
11	345.815290289	8.874120031	3.50E-17	1.26E-18	1.07E-17	2.08E-18	1.61E-17	1.47E-18
12	345.815217422	8.873600801	8.24E-17	5.24E-18	6.93E-17	6.17E-18	1.99E-17	3.56E-18
13	345.815013974	8.873415349	2.17E-16	2.32E-18	1.98E-16	1.51E-18	5.91E-17	6.57E-19
14	345.815406198	8.873808790	8.40E-17	1.62E-18	9.34E-17	1.68E-18	1.40E-17	2.11E-18
15	345.814258264	8.872610553	7.63E-19	4.69E-20	1.05E-18	3.76E-20	1.55E-19	2.17E-20
16	345.814659356	8.873876872	1.71E-16	3.71E-18	1.56E-16	4.52E-18	5.72E-17	2.39E-18
17	345.814031500	8.872533496	7.54E-19	5.95E-20	8.49E-19	4.47E-20	1.29E-19	2.72E-20
18	345.814978168	8.874293404	2.53E-17	1.03E-18	4.92E-17	1.17E-19	2.95E-17	9.36E-20
19	345.813232223	8.872904107	6.14E-19	4.18E-20	7.01E-19	3.93E-20	1.91E-19	1.65E-20
NGC 7469 - Extended Galaxy and Companion								
1	345.821279745	8.861853007	5.04E-19	3.04E-20	3.14E-19	1.45E-20	8.85E-20	4.70E-21
2	345.824580588	8.872132633	4.86E-19	3.42E-20	1.09E-18	1.44E-20	9.70E-19	6.67E-21
3	345.821362773	8.871531687	2.70E-19	3.42E-20	3.55E-19	1.39E-20	1.05E-19	6.31E-21
4	345.820713131	8.871284929	1.90E-18	5.95E-20	2.16E-18	4.00E-20	3.04E-19	1.09E-20
5	345.819853475	8.870399206	5.17E-19	3.29E-20	6.83E-19	1.46E-20	1.90E-19	6.09E-21
6	345.818999800	8.868943264	9.95E-19	3.80E-20	9.04E-19	2.08E-20	2.59E-19	8.05E-21
7	345.816058885	8.864634713	4.48E-19	3.29E-20	1.17E-18	1.29E-20	8.56E-19	6.03E-21
8	345.822632550	8.875992178	4.53E-19	3.04E-20	6.88E-19	1.76E-20	1.50E-19	6.74E-21

*Table 5 continued*

**Table 5** (*continued*)

ID	R.A.	Decl.	$f_{336}$	$\sigma_{f_{336}}$	$f_{435}$	$\sigma_{f_{435}}$	$f_{814}$	$\sigma_{f_{814}}$
9	345.820590021	8.873419106	2.97E-19	3.80E-20	7.26E-19	2.47E-20	3.09E-19	1.04E-20
10	345.830947575	8.891575037	6.27E-19	2.66E-20	7.08E-19	1.17E-20	3.04E-19	5.05E-21
11	345.817918795	8.872921049	3.42E-19	5.44E-20	2.89E-19	5.07E-20	2.94E-19	1.80E-20
12	345.818340830	8.872728189	2.42E-19	3.80E-20	4.18E-19	4.48E-20	1.47E-19	2.41E-20
13	345.817468958	8.871884290	1.33E-18	3.42E-20	1.20E-18	3.43E-20	3.72E-19	1.90E-20
14	345.817970838	8.871952126	3.85E-19	3.67E-20	6.13E-19	3.35E-20	1.31E-19	1.34E-20
15	345.817901920	8.872136632	1.87E-18	4.56E-20	1.31E-18	4.86E-20	3.69E-19	1.42E-20
16	345.817824211	8.872401317	3.12E-18	6.46E-20	3.05E-18	6.75E-20	9.94E-19	2.75E-20
17	345.816584385	8.871434483	4.34E-18	4.05E-20	3.78E-18	4.03E-20	8.17E-19	1.68E-20
18	345.817632093	8.872447694	4.66E-18	1.24E-19	3.79E-18	1.11E-19	6.93E-19	3.03E-20
19	345.817840460	8.872167802	4.11E-19	4.43E-20	4.18E-19	6.27E-20	1.14E-19	2.05E-20
20	345.817487316	8.872574582	3.36E-18	5.82E-20	2.50E-18	8.55E-20	7.10E-19	2.85E-20
21	345.817992000	8.873158709	9.94E-19	4.31E-20	1.25E-18	4.73E-20	4.22E-19	1.82E-20
22	345.818242512	8.873434953	4.10E-19	3.04E-20	3.82E-19	2.04E-20	1.29E-19	1.13E-20
23	345.817562577	8.872561983	2.66E-18	8.86E-20	2.35E-18	6.68E-20	4.92E-19	2.45E-20
24	345.816161871	8.870666403	4.10E-19	3.93E-20	5.11E-19	2.09E-20	1.55E-19	9.49E-21
25	345.815616679	8.870362327	5.90E-18	4.43E-20	4.58E-18	3.46E-20	1.01E-18	1.10E-20
26	345.821511705	8.879199906	4.20E-19	3.67E-20	6.09E-19	1.10E-20	3.24E-19	5.81E-21
27	345.816632482	8.871927746	1.73E-18	5.44E-20	2.12E-18	6.01E-20	5.26E-19	1.83E-20
28	345.816052909	8.871531562	7.70E-18	8.86E-20	7.49E-18	7.05E-20	1.73E-18	3.27E-20
29	345.816244524	8.871155863	2.83E-19	3.93E-20	3.29E-19	1.36E-20	5.75E-20	1.13E-20
30	345.815916478	8.871236707	3.53E-19	3.29E-20	6.83E-19	2.09E-20	2.82E-19	1.21E-20
31	345.817797861	8.874785980	4.57E-17	5.32E-20	7.42E-17	3.66E-20	3.08E-17	5.00E-20
32	345.813895424	8.868027321	6.35E-19	3.04E-20	5.34E-19	1.39E-20	1.50E-19	5.27E-21
33	345.818189304	8.874801984	5.20E-19	3.17E-20	4.13E-19	1.93E-20	9.98E-20	9.65E-21
34	345.815424890	8.871463171	5.19E-19	3.04E-20	1.22E-18	2.47E-20	2.93E-19	1.28E-20
35	345.817205489	8.874397613	8.87E-19	4.69E-20	8.92E-19	3.20E-20	2.00E-19	2.87E-20
36	345.814515730	8.870599498	1.00E-18	4.69E-20	1.46E-18	1.83E-20	4.70E-19	7.98E-21
37	345.820321235	8.879466834	1.31E-18	3.93E-20	1.49E-18	1.82E-20	2.67E-19	6.45E-21
38	345.814900598	8.871774657	1.03E-17	1.23E-19	1.10E-17	7.56E-20	2.86E-18	2.73E-20
39	345.828044433	8.891748297	1.94E-19	4.43E-20	2.58E-19	2.33E-20	1.47E-19	1.19E-20
40	345.816688659	8.874715204	3.60E-19	4.69E-20	5.32E-19	3.34E-20	2.49E-19	1.91E-20
41	345.827884238	8.892363744	1.71E-18	4.43E-20	2.18E-18	5.72E-20	1.02E-18	3.99E-20
42	345.816633147	8.875438197	3.99E-19	5.57E-20	1.29E-18	6.09E-20	1.45E-19	2.68E-20
43	345.816370169	8.875790398	6.19E-19	4.94E-20	1.36E-18	1.99E-20	5.91E-19	1.24E-20
44	345.828688234	8.895161365	3.20E-18	3.04E-20	1.80E-17	1.50E-20	2.85E-17	3.94E-20
45	345.816273615	8.875295552	5.17E-18	4.43E-20	2.40E-19	3.38E-20	9.14E-20	1.53E-20
46	345.819663503	8.880677173	2.26E-19	4.56E-20	1.95E-19	1.96E-20	6.12E-20	7.33E-21
47	345.813375781	8.871220466	4.46E-19	4.05E-20	6.35E-19	1.68E-20	1.75E-19	9.74E-21
48	345.819220024	8.880455326	5.99E-19	6.96E-20	7.65E-19	7.10E-20	2.34E-19	1.68E-20
49	345.826915516	8.892704187	3.59E-19	3.67E-20	8.35E-19	4.82E-20	7.64E-19	4.15E-20
50	345.816061959	8.875700775	3.61E-19	4.69E-20	2.45E-19	2.98E-20	6.23E-20	1.83E-20
51	345.813978448	8.872394185	8.54E-19	4.31E-20	1.59E-19	2.66E-20	6.87E-20	1.46E-20
52	345.813583375	8.872585223	9.81E-19	4.94E-20	1.06E-18	2.57E-20	4.02E-19	1.54E-20
53	345.812175092	8.870176943	4.48E-19	3.80E-20	4.95E-19	1.29E-20	9.91E-20	7.86E-21
54	345.818414310	8.880360929	2.62E-19	3.93E-20	4.39E-19	2.30E-20	1.09E-19	7.30E-21
55	345.812772686	8.872609104	1.08E-18	3.67E-20	1.37E-18	4.17E-20	4.30E-19	1.65E-20

*Table 5 continued*

**Table 5** (*continued*)

ID	R.A.	Decl.	$f_{336}$	$\sigma_{f_{336}}$	$f_{435}$	$\sigma_{f_{435}}$	$f_{814}$	$\sigma_{f_{814}}$
56	345.813041485	8.872814169	4.07E-19	3.17E-20	3.06E-19	2.41E-20	1.83E-19	1.18E-20
57	345.825839661	8.893197068	4.26E-19	4.31E-20	9.14E-19	6.74E-20	5.71E-19	5.30E-20
58	345.826065281	8.893383888	5.32E-19	6.71E-20	7.59E-19	1.31E-19	4.93E-19	7.39E-20
59	345.812675682	8.872818978	3.71E-19	4.05E-20	2.45E-19	2.02E-20	8.97E-20	1.07E-20
60	345.825899875	8.893346655	1.18E-18	7.09E-20	1.43E-18	7.85E-20	5.40E-19	8.01E-20
61	345.825763804	8.893671677	1.06E-17	6.84E-20	8.74E-18	1.42E-19	2.80E-18	1.22E-19
62	345.812542696	8.874103463	4.20E-18	6.96E-20	7.56E-18	1.02E-19	3.25E-18	4.55E-20
63	345.812669399	8.873872696	9.44E-19	5.57E-20	1.79E-18	5.82E-20	4.85E-19	2.51E-20
64	345.812977571	8.874416916	2.82E-19	3.42E-20	4.45E-19	3.90E-20	1.84E-19	2.23E-20
65	345.816862094	8.880460632	3.16E-19	3.42E-20	4.88E-19	2.81E-20	1.66E-19	9.38E-21
66	345.816648700	8.880378669	7.31E-19	4.69E-20	1.70E-18	3.49E-20	4.33E-19	1.40E-20
67	345.824982315	8.893791396	3.52E-18	4.81E-20	4.83E-18	6.98E-20	2.62E-18	8.85E-20
68	345.812126463	8.873938802	5.84E-19	4.31E-20	1.45E-18	1.86E-20	4.69E-19	9.89E-21
69	345.820139390	8.886027517	5.12E-19	3.80E-20	4.51E-19	1.30E-20	9.68E-20	4.98E-21
70	345.825321669	8.893927349	5.72E-19	3.80E-20	1.99E-18	5.94E-20	3.02E-19	4.34E-20
71	345.812625928	8.874697270	1.47E-18	4.18E-20	1.54E-18	3.74E-20	5.06E-19	2.20E-20
72	345.812391872	8.874693785	2.86E-19	3.93E-20	3.44E-19	3.09E-20	8.93E-20	1.31E-20
73	345.812628753	8.875279681	9.33E-19	3.80E-20	1.07E-18	7.03E-20	2.12E-19	2.91E-20
74	345.812114655	8.875357333	1.05E-18	3.42E-20	1.70E-18	2.39E-20	5.71E-19	1.39E-20
75	345.812653056	8.875595305	5.82E-19	5.32E-20	6.29E-19	3.68E-20	2.60E-19	1.65E-20
76	345.812225254	8.874827859	3.71E-19	3.93E-20	4.96E-19	2.44E-20	1.31E-19	1.36E-20
77	345.824792319	8.895227735	1.32E-18	3.42E-20	1.85E-18	2.57E-20	8.64E-19	1.31E-20
78	345.823867904	8.893648148	2.05E-19	4.05E-20	7.68E-19	3.62E-20	8.15E-19	8.71E-20
79	345.812040797	8.875680825	4.31E-19	3.93E-20	5.71E-19	3.95E-20	2.03E-19	1.18E-20
80	345.812123434	8.875742494	1.15E-18	5.44E-20	1.11E-18	3.46E-20	3.66E-19	1.25E-20
81	345.824073457	8.894508613	7.92E-18	5.95E-20	8.85E-18	3.51E-20	3.77E-18	3.00E-20
82	345.813710169	8.878434560	1.13E-18	6.20E-20	1.70E-18	4.31E-20	4.42E-19	1.47E-20
83	345.811873738	8.875716630	4.21E-19	4.05E-20	4.45E-19	4.55E-20	3.79E-19	1.88E-20
84	345.812071080	8.876111634	5.34E-19	3.93E-20	1.34E-18	3.55E-20	4.66E-19	1.88E-20
85	345.813318836	8.878553905	1.35E-18	4.69E-20	1.57E-18	2.07E-20	5.82E-19	1.18E-20
86	345.813102141	8.877583682	1.26E-18	4.69E-20	1.10E-18	3.56E-20	1.77E-19	1.14E-20
87	345.812207394	8.876098969	2.52E-19	4.56E-20	2.40E-19	5.53E-20	1.01E-19	1.90E-20
88	345.824438800	8.895189044	2.81E-19	3.29E-20	4.59E-19	3.57E-20	2.63E-19	1.29E-20
89	345.813847762	8.878931023	2.61E-19	2.91E-20	3.17E-19	1.45E-20	7.09E-20	8.54E-21
90	345.813319734	8.878330373	1.24E-18	4.18E-20	1.10E-18	2.20E-20	1.53E-19	7.93E-21
91	345.812754059	8.877622128	9.04E-19	4.18E-20	8.79E-19	3.88E-20	2.96E-19	1.04E-20
92	345.812005991	8.876460995	5.68E-19	4.18E-20	9.19E-19	3.85E-20	2.57E-19	1.57E-20
93	345.811884951	8.876475277	5.09E-19	3.67E-20	5.29E-19	2.57E-20	1.63E-19	1.04E-20
94	345.823286878	8.894006939	1.13E-18	4.56E-20	1.98E-18	6.12E-20	2.40E-18	1.05E-19
95	345.813919361	8.879569565	2.51E-19	3.67E-20	3.85E-19	1.38E-20	8.01E-20	5.74E-21
96	345.823118866	8.894084550	1.79E-18	5.70E-20	1.90E-18	8.60E-20	5.85E-19	5.60E-20
97	345.823539862	8.894830448	2.97E-19	3.67E-20	4.82E-19	2.78E-20	8.55E-19	2.88E-20
98	345.823518656	8.895777361	3.78E-19	3.29E-20	1.21E-18	1.99E-20	4.68E-19	1.14E-20
99	345.814510405	8.881625777	1.90E-19	4.05E-20	2.90E-19	2.67E-20	8.83E-20	9.99E-21
100	345.814860227	8.882064016	3.88E-19	3.04E-20	1.59E-19	1.69E-20	7.03E-20	5.47E-21
101	345.822464193	8.894955265	1.23E-18	4.31E-20	2.68E-18	5.68E-20	2.21E-18	8.32E-20
102	345.814400536	8.881610582	3.76E-19	3.80E-20	2.85E-19	1.76E-20	8.86E-20	6.99E-21

*Table 5 continued*

**Table 5** (*continued*)

ID	R.A.	Decl.	$f_{336}$	$\sigma_{f_{336}}$	$f_{435}$	$\sigma_{f_{435}}$	$f_{814}$	$\sigma_{f_{814}}$
103	345.821439578	8.893413569	8.16E-19	3.67E-20	6.87E-19	2.00E-20	2.30E-19	1.08E-20
104	345.813527100	8.881678257	2.68E-19	3.29E-20	4.59E-19	1.31E-20	1.52E-19	5.82E-21
105	345.811418574	8.878806049	6.03E-19	4.31E-20	8.63E-19	2.15E-20	1.97E-19	9.53E-21
106	345.821118295	8.893793074	9.58E-19	3.42E-20	1.08E-18	2.09E-20	2.69E-19	1.04E-20
107	345.811648863	8.879540132	4.71E-19	3.80E-20	5.15E-19	1.78E-20	9.72E-20	6.80E-21
108	345.811179714	8.878872044	6.35E-19	3.80E-20	6.95E-19	1.86E-20	1.89E-19	7.76E-21
109	345.821890550	8.895707386	8.12E-18	7.34E-20	9.84E-18	1.41E-19	5.19E-18	9.45E-20
110	345.821013494	8.893886827	4.90E-19	3.42E-20	5.32E-19	1.93E-20	1.27E-19	9.81E-21
111	345.811730934	8.879924852	5.21E-19	4.31E-20	4.85E-19	1.43E-20	9.87E-20	7.92E-21
112	345.821820915	8.895663487	3.58E-18	5.32E-20	5.22E-18	9.43E-20	2.81E-18	7.40E-20
113	345.821926794	8.895869006	5.92E-19	7.72E-20	4.28E-19	1.01E-19	3.19E-19	3.92E-20
114	345.812280676	8.881538161	2.78E-18	7.60E-20	1.81E-18	7.90E-20	3.18E-19	2.05E-20
115	345.821546440	8.895766050	8.74E-19	5.95E-20	1.96E-18	1.21E-19	6.84E-19	5.53E-20
116	345.811722467	8.880493117	3.85E-19	3.29E-20	5.47E-19	1.31E-20	1.64E-19	4.61E-21
117	345.812042129	8.881347406	8.62E-19	5.32E-20	9.02E-19	4.15E-20	2.41E-19	1.54E-20
118	345.814753053	8.885228576	3.94E-19	3.67E-20	3.59E-19	1.78E-20	8.76E-20	6.60E-21
119	345.821716861	8.896196039	3.18E-18	6.20E-20	1.95E-18	7.12E-20	5.76E-19	6.04E-20
120	345.821526733	8.896178380	5.00E-18	4.69E-20	3.75E-18	6.51E-20	1.15E-18	4.11E-20
121	345.812009314	8.881905706	2.95E-19	3.93E-20	2.68E-19	1.42E-20	1.54E-19	1.10E-20
122	345.821564176	8.896252514	7.18E-19	5.57E-20	5.99E-19	5.49E-20	4.13E-19	3.43E-20
123	345.820270368	8.894469422	1.34E-18	3.67E-20	1.19E-18	2.61E-20	2.55E-19	9.75E-21
124	345.817422923	8.891120147	7.41E-17	6.46E-20	3.45E-17	2.67E-20	1.13E-17	2.20E-20
125	345.811370076	8.882297753	7.13E-18	1.27E-19	6.06E-18	5.95E-20	1.07E-18	3.44E-20
126	345.811839504	8.882471595	7.52E-19	3.80E-20	9.28E-19	1.67E-20	2.51E-19	6.57E-21
127	345.810932394	8.881775344	1.41E-18	3.93E-20	1.21E-18	2.41E-20	2.28E-19	8.37E-21
128	345.807364165	8.877017305	1.47E-18	3.80E-20	1.33E-18	3.85E-20	5.78E-19	1.21E-20
129	345.807313254	8.876636741	4.02E-19	3.42E-20	5.26E-19	2.67E-20	2.05E-19	8.82E-21
130	345.809750427	8.880250516	1.37E-18	3.42E-20	9.36E-19	1.39E-20	1.19E-19	5.20E-21
131	345.807491967	8.877112328	8.58E-19	4.56E-20	5.08E-19	2.48E-20	5.66E-20	1.39E-20
132	345.807330301	8.876905970	3.34E-19	4.18E-20	2.89E-19	2.84E-20	6.43E-20	1.17E-20
133	345.807068383	8.876848577	3.25E-19	3.80E-20	4.79E-19	2.08E-20	2.33E-19	7.73E-21
134	345.807108992	8.877506472	2.98E-19	3.80E-20	2.95E-19	2.28E-20	1.49E-19	8.30E-21
135	345.818437165	8.895120763	4.27E-19	3.29E-20	3.49E-19	1.62E-20	3.11E-20	7.21E-21
136	345.807814589	8.879177506	2.42E-19	3.29E-20	2.12E-19	1.15E-20	6.41E-20	4.72E-21
137	345.810870779	8.884172499	5.65E-19	2.91E-20	5.83E-19	2.05E-20	1.24E-19	6.48E-21
138	345.817836540	8.895893269	7.58E-19	3.42E-20	5.77E-19	1.72E-20	1.65E-19	5.99E-21
139	345.809769976	8.884208889	2.24E-19	2.53E-20	1.88E-18	1.28E-20	3.83E-18	6.75E-21
140	345.804864030	8.877937757	8.34E-19	3.55E-20	7.47E-19	1.32E-20	1.70E-19	4.70E-21
141	345.816828787	8.897096150	1.61E-18	3.42E-20	9.50E-19	1.96E-20	1.58E-19	7.20E-21
142	345.816135162	8.897500268	2.86E-18	3.80E-20	1.88E-18	2.10E-20	2.90E-19	8.43E-21
143	345.816230835	8.897514875	5.86E-19	3.67E-20	5.10E-19	2.30E-20	1.32E-19	6.90E-21
144	345.815796879	8.897830279	3.54E-19	3.04E-20	4.67E-19	1.78E-20	1.06E-19	6.16E-21
145	345.811433488	8.892652604	4.55E-19	2.79E-20	5.02E-19	1.29E-20	2.76E-19	5.07E-21
146	345.814247888	8.899668916	7.37E-19	2.91E-20	4.23E-19	1.17E-20	8.69E-20	4.76E-21

NOTE—All flux values and  $1\sigma$  uncertainties are given in ergs/s/cm<sup>2</sup>/Å

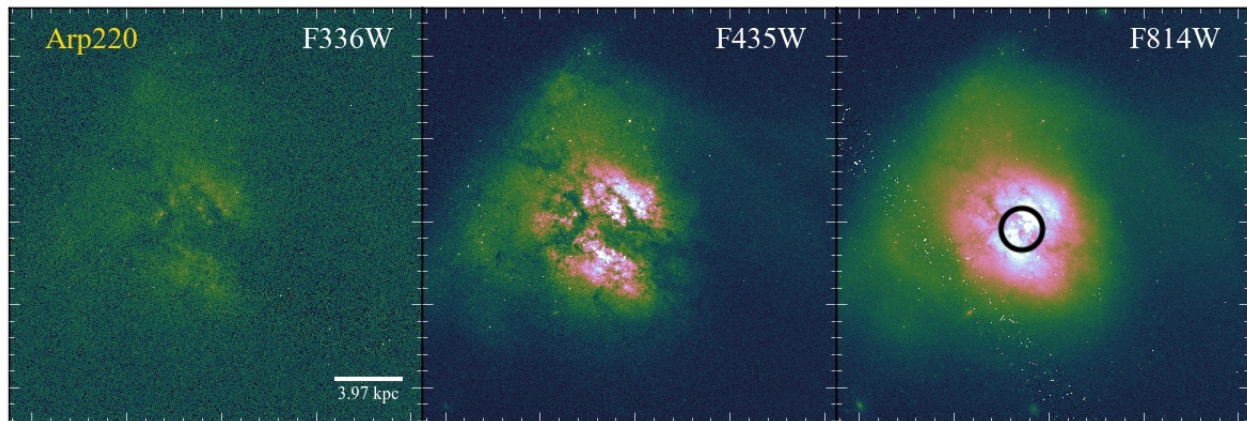


**Figure 12.** Same as Figure 1

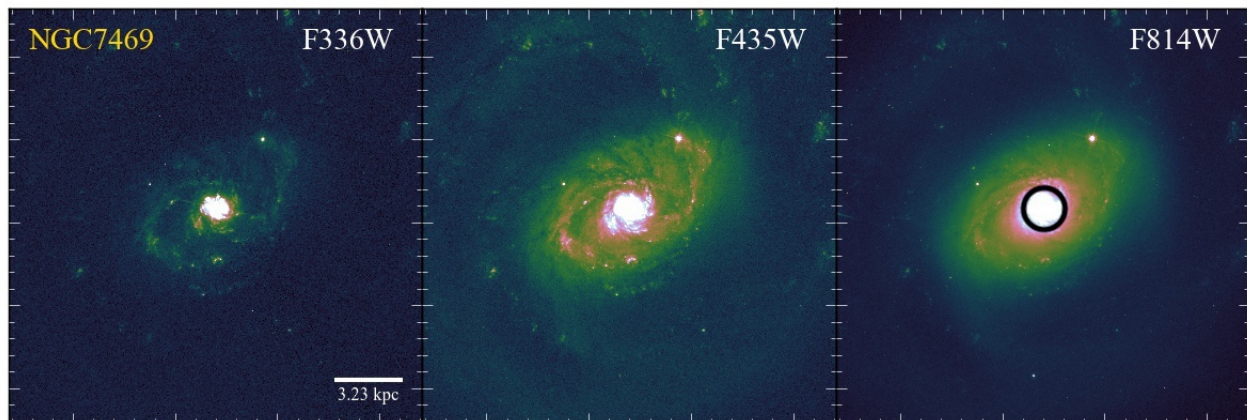


**Figure 13.** Same as Figure 1

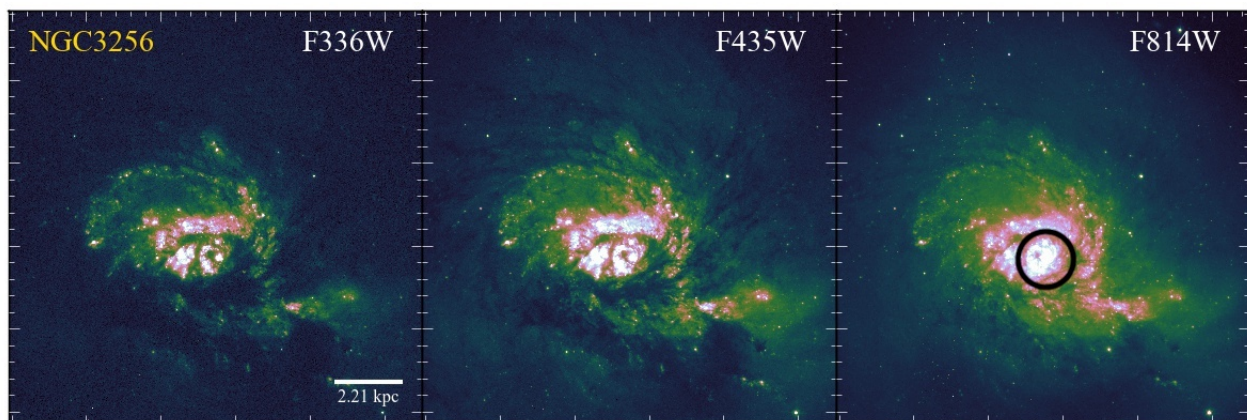


**Figure 14.** Same as Figure 1

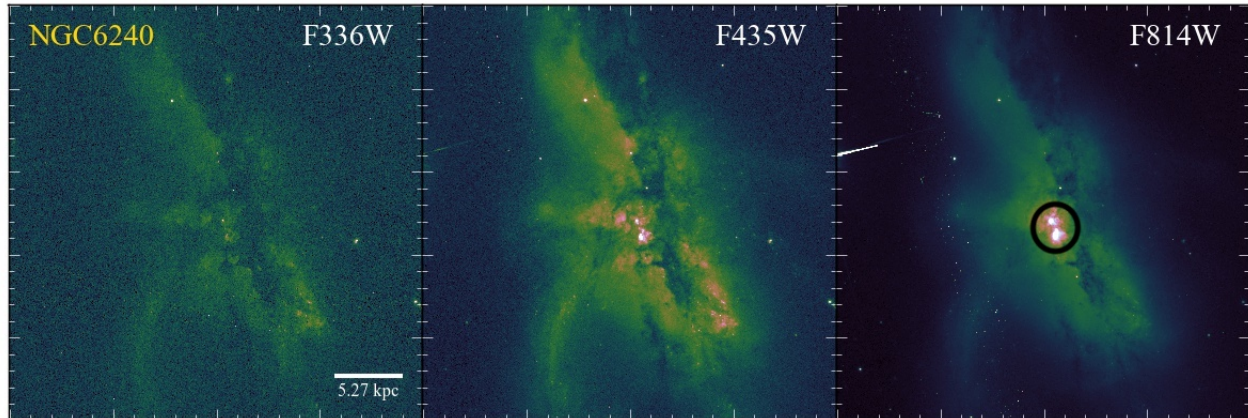


**Figure 15.** Same as Figure 1

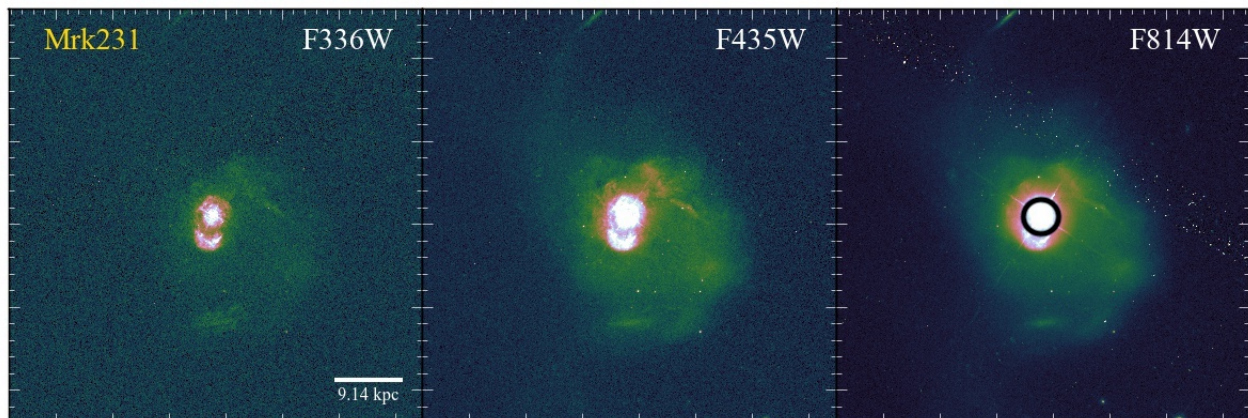


**Figure 16.** Same as Figure 1

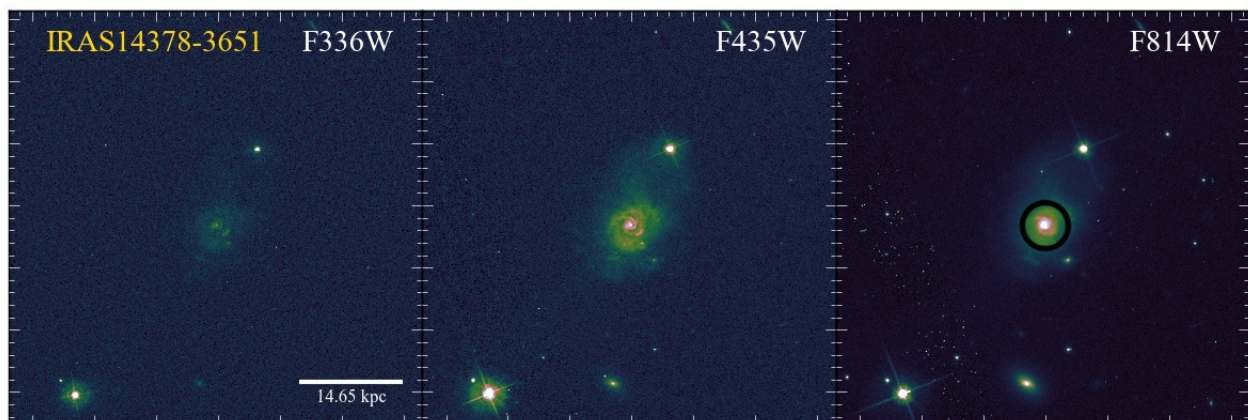


**Figure 17.** Same as Figure 1

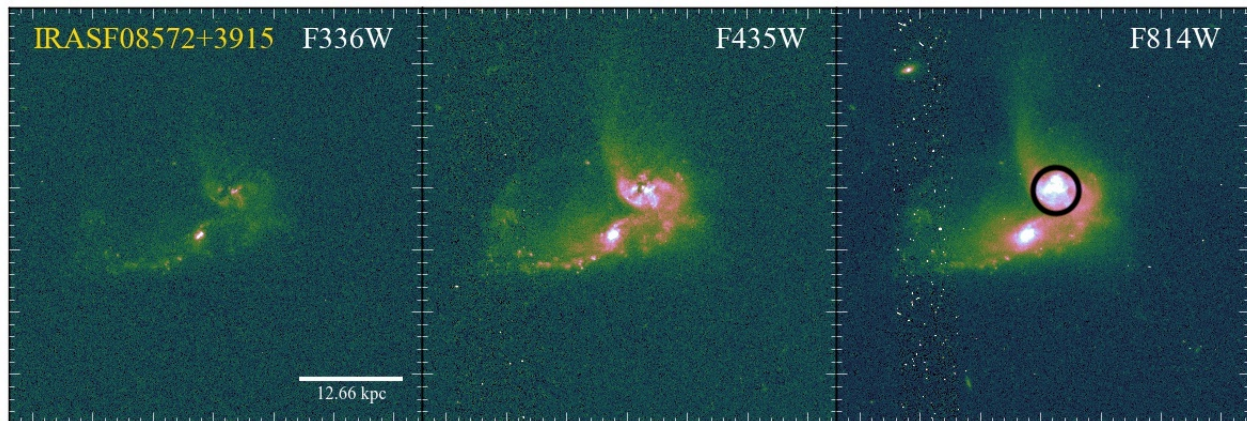


**Figure 18.** Same as Figure 1

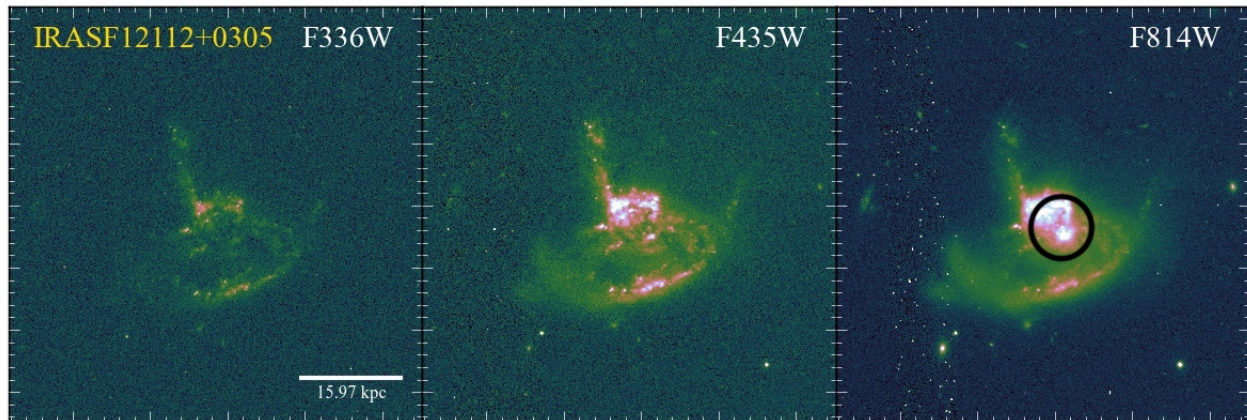


**Figure 19.** Same as Figure 1

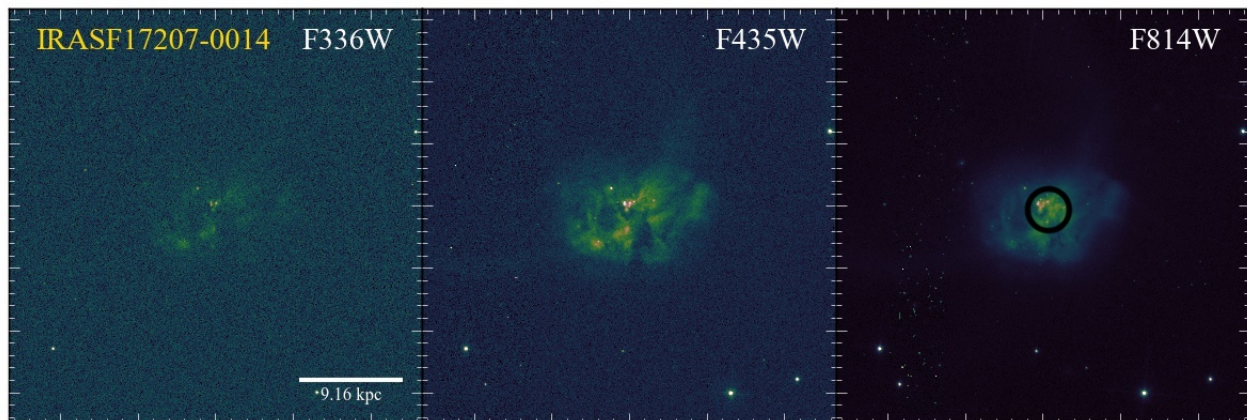


**Figure 20.** Same as Figure 1

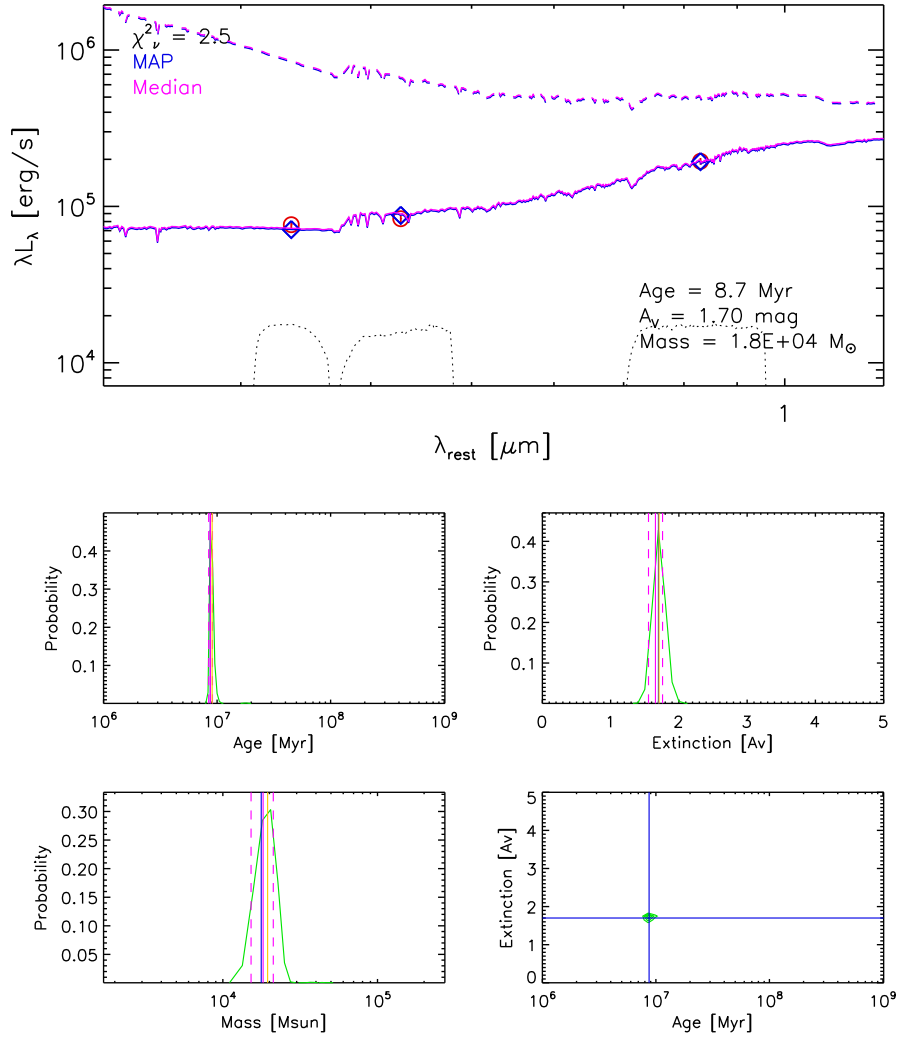


**Figure 21.** Example SED and resulting model fit for cluster 33 in NGC 3256 with an age of 8.7 Myr (blue) with an extinction of  $A_V = 1.7$  mags. The dashed lines correspond to the un-extincted SEDs for each model. In the example SEDs provided, this combination of filters can be used to uniquely solve for cluster age relative to the F140LP observations used in our previous study. Finally, in the lower Panels the resulting  $1\sigma$  errors for the age, mass, and extinction are shown as dashed pink lines superimposed over the marginalized posterior distribution for each parameter (green curves).